

Aus dem Zentralinstitut für Seelische Gesundheit  
der Medizinischen Fakultät Mannheim  
(Direktor: Prof. Dr. med. Andreas Meyer-Lindenberg)

Multi-neuroimaging model of identifying neuroplasticity under motor  
cognitive learning condition: MRI based study.

Inauguraldissertation  
zur Erlangung des Doctor scientiarum humanarum (Dr. sc. hum.)  
der  
Medizinischen Fakultät Mannheim  
der Ruprecht-Karls-Universität  
zu  
Heidelberg

vorgelegt von  
Zhenxiang Zang

aus  
HEBEI, CHINA  
2019

Dekan: Prof. Dr. med. Sergij Goerd  
Referentin: Prof. Dr. med. Dr. phil. Heike Tost

## TABLE OF CONTENTS

<b>ABBREVIATIONS</b> .....	1
<b>1 INTRODUCTION</b> .....	2
1.1 A brief introduction to motor learning.....	2
1.1.1 Short-term learning phase .....	3
1.1.2 Long-term learning phase.....	4
1.2 Basic neuro-biological background of motor learning.....	5
1.2.1 Cellular bases of motor learning-induced structural plasticity .....	5
1.2.2 Contributions of brain areas.....	7
1.3 Major brain neurotransmitters involved in motor learning .....	11
1.3.1 Glutamate is highly involved in learning.....	11
1.3.2 Role of GABA and dopamine during learning .....	12
1.4 Motor learning and schizophrenia.....	12
1.5 Imaging method and modeling .....	13
1.5.1 Brief introduction of MRI, fMRI and MRS.....	13
1.5.2 Functional Activation.....	14
1.5.3 Functional Connectivity.....	16
1.5.4 Graph theory.....	16
1.6 Hypotheses .....	18
<b>2 STUDY 1: RESTING-STATE BRAIN NETWORK FEATURES ASSOCIATED WITH SHORT-TERM SKILL LEARNING ABILITY IN HUMANS AND THE INFLUENCE OF N-METHYL-D-ASPARTATE RECEPTOR ANTAGONISM</b> .....	20
2.1 Abstract.....	20
2.2 Introduction.....	20
2.3 Materials and Methods .....	22
2.3.1 Participants and motor learning task description .....	22
2.3.2 Data acquisition and analyses .....	24
2.4 Results .....	29
2.4.1 Main results .....	29
2.4.2 Supplemental results .....	31

2.5	Discussion .....	35
2.6	Supplemental Information.....	39
2.6.1	S-Method .....	39
2.6.2	S-Results .....	40
<b>3</b>	<b>STUDY 2: MULTI-IMAGING MODALITY IDENTIFIES DYNAMIC GLUTAMATERGIC DEPENDENT NEURAL PLASTICITY IN HUMAN BRAIN DURING LONG-TERM MOTOR LEARNING .....</b>	<b>43</b>
3.1	Abstract .....	43
3.2	Introduction.....	43
3.3	Materials and Method .....	45
3.3.1	Motor learning task description .....	46
3.3.2	Data analysis .....	47
3.4	Results .....	50
3.4.1	Subjects and study protocol.....	50
3.4.2	Behavioral data.....	52
3.4.3	Brain imaging results .....	53
3.5	Discussion .....	58
3.6	Supplements .....	63
3.6.1	Data acquisition parameters .....	63
3.6.2	S-Results .....	64
<b>4</b>	<b>GENERAL DISCUSSION.....</b>	<b>73</b>
4.1	Result summary.....	73
4.2	Behavioral improvements .....	74
4.3	Short-term learning phase .....	75
4.4	Long-term learning phase.....	76
4.5	A neurobiological model to interpret the transition from short-term to long-term motor learning .....	76
4.6	Glutamatergic modulation during short-term and long-term motor learning..	79
4.7	Limitations and Future directions.....	80
4.7.1	Limitations of the current project.....	80
4.7.2	Future directions.....	80

<b>5 SUMMARY</b> .....	82
<b>6 REFERENCES</b> .....	83
<b>7 PUBLICATIONS</b> .....	97
<b>8 CURRICULUM VITAE</b> .....	98
<b>9 ACKNOWLEDGMENT</b> .....	99

**ABBREVIATIONS**

AAL	Automated anatomical labeling
AMPA	$\alpha$ -amino-3-hydroxy-5-methyl-4-isoxazolepropionic acid
ANOVA	Analysis of variance
BG	Basal ganglia
BOLD	Blood oxygen level dependent
Cho	Choline
Cr	Creatine
CSF	Cerebral spinal fluid
DLPFC	Dorsolateral prefrontal cortex
fMRI	Functional magnetic resonance imaging
GABA	Gamma-Aminobutyric acid
GLM	General linear model
Glu	Glutamate
GM	Grey matter
HRF	Hemodynamic response function
Hz	Hertz
ICA	Independent Component Analysis
ICC	Intra-class correlation
LDP	Long-term depression
LTP	Long-term potentiation
M1	Primary motor area
MNI	Montreal Neurological Institute
MRS	magnetic resonance spectroscopy
NAA	N-acetyl aspartate
NBS	Network Based Statistics
NMDA	N-methyl-D-aspartate
ROI	Region of interest
rs-fMRI	Resting-state functional magnetic resonance imaging
SMA	Supplementary motor area
SPM8	Statistical Parametric Mapping Version 8
SPSS	Statistical Package for the Social Sciences
SVIPT	Sequential visual isometric pinch task
WM	White matter

# 1 INTRODUCTION

## 1.1 A brief introduction to motor learning

Learning a new motor skill is one of the most critical abilities for surviving in nature. The ability of humans to acquire new motor skills, such as learning to ride a bike, playing ball or instruments, is innate, resulting in quick acquisition of new skills from childhood. The human brain is exceptionally suited to support the acquisition of new motor skills. Conversely, a growing number of studies support the notion that motor learning changes brain function and structures to achieve better performance. Several theories of motor learning propose that the complex process of learning a new motor skill can be divided into different stages. According to a well-established model given by Fitts and Posner (Fitts & Posner, 1967), motor learning can be divided into three stages: 1) the cognitive stage where the individual attains an understanding of the task, 2) the associative stage when subjects find a strategy to perform the task, and 3) the autonomous stage when performance reaches plateau after long-term motor learning. While this model was developed on purely behavioral data, newer models of motor learning incorporate findings from neurobiology, especially neuroimaging. Dayan and Cohen propose a division of motor learning into two stages: 1) a “short-term learning phase” corresponding to the cognitive and the associative stages of Fitts and Posner, in which subjects learn the task and improve their performance at a high speed and 2) a “long-term learning phase” corresponding to the autonomous stage where learning has been carried out for a longer time (Dayan & Cohen, 2011) but behavioral improvements are little (Hikosaka, Nakamura, Sakai, & Nakahara, 2002). It is sometimes difficult to distinguish between the cognitive stage and associative stage in the human neuroimaging studies on motor learning and since the model by Dayan and Cohen is better aligned with the underlying neurobiological changes during learning, the projects presented here will refer to the “two-stage learning phase” model. The definition of short-term and long-term learning phases is always relative since it depends on the exact type and complexity of the motor task, the desired level of expertise. For example, learning to drive a car takes several days or weeks but learning to play the violin may take years of practice. Therefore, most human imaging studies have concentrated on relatively simple tasks that can be learned within a time frame ranging from several minutes to several months. In particular, some types of motor

learning tasks are frequently used, including finger sequential pinching (Bassett et al., 2011; Bassett, Yang, Wymbs, & Grafton, 2015), oculomotor sequential learning (Albouy et al., 2008), spatial rotation (Sami & Miall, 2013; Sami, Robertson, & Miall, 2014), juggling (Draganski et al., 2004), balancing (Taubert, Lohmann, Margulies, Villringer, & Ragert, 2011) and playing golf (Bezzola, Merillat, Gaser, & Jancke, 2011). In general, brain functional changes such as alteration of activation and connectivity could be reliably detected after a shorter learning period (several hours to few days) whereas brain morphological changes were found after more extended learning periods (several weeks to few months). In the following sections, the specific neural circuits associated with each type of learning, as well as the underlying neurobiological mechanisms on the molecular and cellular levels will be shortly introduced.

### **1.1.1 Short-term learning phase**

The short-term learning phase heavily relies on attention and behavioral improvements are usually significant within a short amount of time (Hikosaka et al., 2002). The pattern and amplitude of brain activity and connectivity can change dramatically within this phase.

The association between motor skill acquisition and regional brain activity changes in humans was mainly studied using functional magnetic resonance imaging (fMRI) during motor learning tasks. These studies commonly reported associations in motor associated areas (e.g. primary motor cortex, basal ganglia, cerebellum) (Coynel et al., 2010; Laforce & Doyon, 2001). Two short-term motor learning fMRI studies additionally reported an increase of activation in the hippocampus after sequential motor learning tasks (Albouy et al., 2008; Schendan, Searl, Melrose, & Stern, 2003). Specifically, Albouy and colleagues found a different mechanism of the increased activation of the hippocampus compared to the increased activation of the putamen and interpreted the hippocampus as an area that contributes to motor memory consolidation during sleeping. Both studies introduced the hippocampus - an area that is considered to be highly involved in declarative memory and spatial navigation (Maguire et al., 2000) - as a key area in motor learning.

Further evidence for brain network reorganization after motor skill training was provided by resting-state studies. During resting-state, subjects are instructed to stay still without performing any particular task. Previous studies have demonstrated that resting-state fMRI (rs-fMRI) allows assessing relevant intrinsic brain networks, even



those related to cognition and motor function (Raichle et al., 2001). In a study by Albert and colleagues (Albert, Robertson, & Miall, 2009), subjects performed a visuomotor adaptation task for 11 minutes in between two resting-state scans. They found significant changes in resting-state frontal-parietal and cerebellar networks and provided critical evidence of resting human brain functional alterations in such a short time. A similar observation was reported in another resting-state study by Sami and colleagues (Sami et al., 2014) who found functional connectivity changes subsequent to a motor learning task that were associated with different time intervals: after 30 minutes, increased functional connectivity could be detected between the cerebellum, thalamus and basal ganglia; after six hours of motor learning, enhanced functional connectivity was found in the sensorimotor area. Associations of resting-state connectivity and short-term motor learning were also reported in other aspects of motor learning. For example, in a 30 minutes implicit sequential motor learning task, the functional connectivity from dorsal caudate to parahippocampus and hippocampus was positively correlated with the training performance whereas the connectivity from caudate to the sensorimotor cortex was negatively correlated with the performance (Stillman et al., 2013). Those rs-fMRI studies therefore provided abundant neuroimaging evidence of neurofunctional plasticity in resting brain networks during the short-term motor learning phase.

### **1.1.2 Long-term learning phase**

In the long-term learning phase, behavioral improvements slow down and the kinetics of the performed movements gradually become automatized. During this period of learning, attentional demands sharply decrease in standard settings. Despite reduced behavioral changes, learning-induced neurofunctional plasticity can still be observed throughout the long-term learning phase (Bassett et al., 2015; Draganski et al., 2004; Xiong et al., 2009). For task fMRI, long-term learning was associated with increased activations in the sensorimotor cortex (Floyer-Lea & Matthews, 2005), premotor cortex / supplementary motor area (SMA) (Lehericy et al., 2005) and the basal ganglia (Floyer-Lea & Matthews, 2005; Lehericy et al., 2005) as well as with decreased activation in the cerebellum (Lehericy et al., 2005). From a network perspective, long-term learning was associated with re-organizations in the premotor-striatum-cerebellum network (Coynel et al., 2010) and in the motor-visual networks (Bassett et al., 2015). Brain structural changes have been reported as well. Using a three-month

juggling task, Draganski and colleagues found increased grey matter volume in the visual area (Draganski et al., 2004). Similar observations have also been reported in a golf-training study where subjects showed increased grey matter volume in the parietal area after three months of training (Bezzola et al., 2011).

While the studies reviewed above cover time intervals from a few minutes to several months, some studies aimed at studying the effect of motor expertise acquired throughout years, such as mastering the piano. These studies relied on cross-sectional comparisons between untrained subjects and specific populations of the profession. For example, musicians show significantly increased gray matter volume in the left primary motor cortex, right superior parietal cortex as well as left cerebellum than non-musicians (Gaser & Schlaug, 2003).

## **1.2 Basic neuro-biological background of motor learning**

Animal and cellular studies have unraveled several neurobiological mechanisms that underlie motor learning. Key brain areas that contribute to motor learning include the visual area, the sensorimotor-basal ganglia-thalamus-sensorimotor loop, cerebellum and areas linked to cognition, such as the frontal-parietal network and the hippocampus. Each of those brain areas plays specific neuro-biological roles and contributes differently to motor learning. In the following sections, the neurobiological mechanisms as well as the roles of the above-mentioned brain areas are briefly introduced.

### **1.2.1 Cellular bases of motor learning-induced structural plasticity**

#### **Long-term potentiation and long-term depression**

Decades of research have consistently observed the “long-term potentiation” (LTP) and the “long-term depression” (LTD) (Cooke & Bliss, 2006) phenomenon, which are suggested to reflect the primary underlying cellular and molecular mechanisms of neural plasticity. Long-term potentiation refers to the recurrent strengthening of synapses following stimulation at high frequency, resulting in an increased and long-lasting amplitude of the postsynaptic membrane potentials facilitating signal transmission. Its opposite phenomena is “long-term depression”, which reduces the

signal transmission after low-frequency stimulation. LTP was first discovered in the glutamatergic synaptic process in the dentate gyrus of the rabbit hippocampus (Bliss & Lomo, 1973). Since then, it has been observed across different species such as rats (Xu, Anwyl, & Rowan, 1998), cats (Kimura, Caria, Melis, & Asanuma, 1994) and in almost all brain areas including the cerebellum (Lev-Ram, Wong, Storm, & Tsien, 2002), visual area (Lev-Ram et al., 2002), sensorimotor cortex (Iriki, Pavlides, Keller, & Asanuma, 1989) and basal ganglia (Ding & Perkel, 2004). These findings suggest that LTP is a universal process of neuronal adaptation to learning in the brain. LTD on the other hand acts as an opposing process of LTP, which allows reducing the strength of the synaptic transmission. The antagonistic effect of LTD is critical for the formation of new memories since it prevents that synapses reach an efficiency plateau that impairs synaptic plasticity.

The glutamatergic N-methyl-D-aspartate (NMDA) receptor plays a critical role for LTP and LTD. NMDA receptors can be activated by binding to glutamate, and thus allow positively charged ions to flow into the neuron. The coincident activation of pre- and postsynaptic neurons, mediated via NMDA receptors, is the basis of LTP (Lüscher & Malenka, 2012). It is well demonstrated in rodent studies that blockage of the NMDA receptor could lead to impaired learning. For example, NMDA antagonists prevented the formation of fear memories in the amygdala of rats (Lee & Kim, 1998). In humans, it is obviously challenging to directly study LTP during learning. However, there is indirect evidence for NMDA-mediated LTP in humans as well. For instance, the infusion of ketamine, an NMDA antagonist, was shown to impair cognitive functions (Ke et al., 2018). However, such an effect on the motor learning domain is still unclear. While LTP and LTD provide a compelling cellular explanation for motor learning, recent studies have also identified other, complementary cellular or molecular processes that might contribute to motor skill acquisition and might underly the changes detected by neuroimaging methods. Therefore, the following sections shortly outline these mechanisms and introduce their potential contributions to neural substrates of imaging-associated changes during learning.

### **Neurogenesis**

Neurogenesis refers to the process of neuron growth from neural stem cells. There is evidence that learning can induce neurogenesis in the adult brain. For example, an animal study obtained maturation of the dendritic trees of the newborn neuron in the

hippocampus (Tronel, Fabre et al. 2010). Despite the fact that neurogenesis could produce granule cell growth in the dentate gyrus (Aimone, Wiles et al. 2009), it is in comparison to a very small ratio of total hippocampal neurons. Thus, neurogenesis in MRI studies is not a primary cellular mechanism (Zatorre, Fields et al. 2012).

### **Synaptogenesis and neural morphology changes**

Synaptic changes and changes in neural morphology are discussed as key mechanisms that underly structural fMRI findings in motor learning studies (Kleim et al., 2002; Kolb, Cioe, & Comeau, 2008). These changes may persist after motor training to provide a structural basis for long-term memory formation (Kleim et al., 2007; Yang, Pan, & Gan, 2009).

### **Non-neuronal cell growth and vascular changes**

Another possible candidate mechanism for structural plasticity is gliogenesis (W. K. Dong & Greenough, 2004) which may contribute to observations in motor learning MRI studies. For example, some juggling studies found decreased gray matter volume when training was absent, consistent with the observation of the trajectory of glial cell changes in animal studies (Zatorre, Fields, & Johansen-Berg, 2012). Another less-well studied candidate explanation for learning-induced structural plasticity is vascular changes. As an example, a study in monkeys showed an increase in histologically quantified vascular volume in the brain during cognitive training (Rhyu et al., 2010). However, it is far from clear to what extent vascular changes may participate in the process of neural plasticity during motor learning.

## **1.2.2 Contributions of brain areas**

In this section, a brief introduction to motor learning-related brain areas is given. These brain areas include the visual area, the motor-basal ganglia-thalamus-motor loop (which is also known as direct/indirect pathway), the cerebellum, frontal-parietal areas and the hippocampus. The following sections provide individual descriptions of the role of these systems or areas in motor learning.

### **Visual system**

The visual system is located in the occipital lobe of the brain. It receives signals from the thalamus and via the optic nerve from the eyeballs. The more posterior part of the

occipital lobe supports basic visual functions. Functions become more complex when moving in the anterior direction towards the temporal lobe. An example is face recognition in the fusiform cortex (Born & Bradley, 2005). Most motor learning tasks in human subjects rely on visual guidance (Albouy et al., 2008; Reis et al., 2009; Sami et al., 2014; Xiong et al., 2009). The continuous update of visual sensory input is therefore crucial (Glickstein, 2000). For example, in a 3-month longitudinal juggling study, Draganski and colleagues (Draganski et al., 2004) found that the gray matter volume of the visual cortex increased after training and decreased when the training was stopped. This study points to the learning-induced plasticity of the morphology in the visual area.

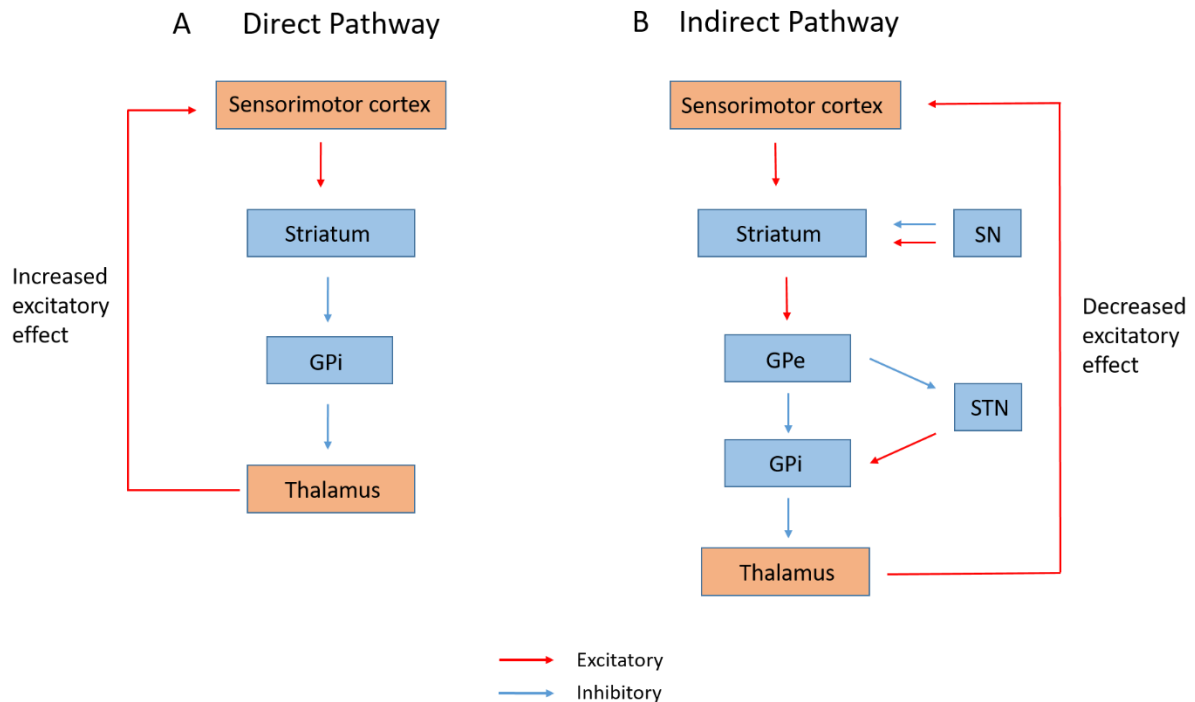
### **Cortical sensorimotor – Basal Ganglia – Thalamus – sensorimotor loop**

The cortical – basal ganglia – thalamus – cortical loop (Alexander, DeLong, & Strick, 1986) involves several functionally segregated yet anatomically overlapping circuits. In these loops, the cortex projects to the basal ganglia, the basal ganglia project to the thalamus, and the thalamus projects back to the cortex. The motor circuit primarily includes the sensorimotor cortex, putamen and thalamus and supports planned or wanted movements while inhibiting wrong or unwanted movements. The excitatory and inhibitory control of movement is also known as the functions of the direct and indirect pathways, respectively (Calabresi, Picconi, Tozzi, Ghiglieri, & Di Filippo, 2014) (Figure 1.1). Briefly, in the motor loop, the basal ganglia receive glutamatergic input from cortical motor areas and inhibit the internal Globus pallidum (GPi) through GABAergic release. This process reduces the inhibitory effect of the GPi to the thalamus and causes the increase of the excitatory effect of the thalamus to the sensorimotor cortex through glutamatergic release. In parallel, the more complex indirect pathway antagonizes the motor movements by the modulatory effect of the substantia nigra (SN) to striatum and participation of the external Globus pallidum (GPe) and the subthalamic nucleus (STN). The inhibitory effect of the GPi to the thalamus is strengthened through GABAergic release to reduce the excitatory effect of the thalamus to the sensorimotor cortex. In summary, the direct pathway is considered to excite movements while the indirect pathway inhibits movements.

The cortical – basal ganglia – thalamus – cortical loop has a direct effect on motor functions and is thus highly relevant during motor learning. In a neuroimaging study by

Lehericy and colleagues (Lehericy et al., 2005), the authors reported a shift in activation from the supplementary motor area (SMA) to the basal ganglia during motor learning in healthy subjects. There is also evidence of an interaction between the basal ganglia and the medial temporal lobe (specifically the hippocampus) in sequential learning (Albouy et al., 2008).

**Figure 1.1**



The figure shows a brief illustration of the direct (excitatory) and the indirect (inhibitory) pathway. Abbreviations: GPi: internal Globus pallidum; GPe: external Globus pallidum; STN: subthalamic nucleus; SN: substantia nigra.

## Cerebellum

The cerebellum is well known for its critical role in sensorimotor integration and movement error correction (Penhune & Steele, 2012). Recent studies have shown that the cerebellum connects not only to the motor cortex, but also to higher-order cognitive areas such as the parietal cortex and prefrontal cortex (Diedrichsen, Balsters, Flavell, Cussans, & Ramnani, 2009; Kelly & Strick, 2003). In animal studies, for example, gene-edited mice with cerebellar function deficits were able to swim towards a given target, but could not optimize their trajectories (Burguiere, Arabo, Jarlier, De Zeeuw, & Rondi-Reig, 2010). Similar observations of impaired movement adjustment were found in human patients with cerebellar lesions (Laforce & Doyon, 2001). In healthy subjects, neurofunctional correlations were observed between the motor cortex and the

cerebellum. For instance, higher activity in the motor cortex was related to decreased activity in the cerebellum during motor learning (Penhune & Steele, 2012). In another study, transcranial magnetic stimulation (TMS) of the cerebellum had a negative effect on motor movement (Miall, Christensen, Cain, & Stanley, 2007) and transcranial direct-current stimulation (tDCS) stimulation to the lateral cerebellum led to improved performance of the performance (subjects can reduce errors faster) during visuomotor learning (Galea, Vazquez, Pasricha, de Xivry, & Celnik, 2011). The above-mentioned studies have shown the critical role of the cerebellum during motor learning.

### **Frontal and Parietal regions**

The planning of a movement takes place in higher motor areas such as the premotor area and the SMA (Nachev, Kennard, & Husain, 2008). These plans are subsequently executed in the primary motor cortex (Dum & Strick, 1996). A well-known finding is that the activity in the SMA can be detected before the activity in the primary motor cortex during voluntary movements (Weilke et al., 2001). In addition, the premotor area and SMA are also part of the direct/indirect pathway. In a primate study, Chen and Wise (Chen & Wise, 1995) recorded neuronal activity in the monkeys' SMA and found an increased activity of these neurons when the animals learned a novel task. In a human study, increased release of dopamine was found in the SMA during motor learning, which corresponded with a reduced dopamine release in GPI. (Garraux, Peigneux, Carson, & Hallett, 2007).

The parietal regions play a unique role in specific aspects of learning, such as spatial imagery (Zhang et al., 2012). They are also involved in the planning of the kinetic parameters of an upcoming movement (Kuang, Morel, & Gail, 2016). Lesions in these areas can lead to spatial neglect (Parton, Malhotra, & Husain, 2004). Frontal-parietal regions are therefore also considered as key areas for motor learning.

### **Hippocampus**

The hippocampus is well known for its critical role in memory formation and spatial navigation (Clark, Broadbent, & Squire, 2005; Jarrard, 1993; Maguire et al., 2000). The memory formation function of the hippocampus was detected in the famous patient H.M. whose bilateral medial temporal lobes were mostly removed to cure his epilepsy. Since then, Mr. H.M. lost his ability to build long-term declarative memory, yet he maintained the function in a motor learning task. Researchers concluded from the

experiments that the hippocampus is a brain region to consolidate the newly learned memory into long-term memory. However, impairment of the hippocampus did not necessarily influence the motor procedure memory.

With modern fMRI technology, researchers found that the activation of the hippocampus was affected by a short-term motor learning task (Albouy et al., 2008; Schendan et al., 2003). In addition, Fernández-Seara and colleagues found highly correlated cerebral flow between the hippocampus and the striatum in a short-term motor sequential learning study (Fernandez-Seara, Aznarez-Sanado, Mengual, Loayza, & Pastor, 2009). These newly published studies have raised novel interest in the hippocampus's role in short-term motor learning.

### **1.3 Major brain neurotransmitters involved in motor learning**

#### **1.3.1 Glutamate is highly involved in learning**

Glutamate, GABA and dopamine are shown to be the primary neurotransmitters for LTP and have prominent roles in the direct/indirect movement pathway in motor learning studies (Kida et al., 2016; Stagg et al., 2014).

Glutamate is the major excitatory neurotransmitter that is ubiquitously distributed throughout the brain. The primary glutamatergic receptors are i) the ionotropic receptors  $\alpha$ -amino-3-hydroxy-5-methyl-4-isoxazolepropionic acid receptor (AMPA) and ii) the N-methyl-D-aspartate receptor (NMDA) as well as iii) the metabotropic glutamate receptors which create slow sustained effects on their target neurons. Glutamatergic neurotransmission is a significant contributor to synaptic LTP and has been repeatedly shown to be crucially associated with learning and memory (Abraham & Mason, 1988; Bliss & Collingridge, 2013).

The role of glutamatergic modulation in learning-induced plasticity has been well established in animal models. For example, motor training can shift the glutamatergic NMDA receptor subunit composition in basal ganglia (Kent, Deng, & McNeill, 2013) and promote the NMDA dependent synaptic plasticity in the primary motor cortex of rats (Kida et al., 2016), while impaired motor performance was observed in mGluR4 gene (metabotropic glutamate receptors 4, a subtype of glutamate receptor that closely correlated with learning, memory, anxiety and perception of pain) knock out mice (Pekhletski et al., 1996). In humans, direct evidence for the role of glutamate in motor



learning and synaptic plasticity is lacking since the study of receptors and neurotransmitters at synapse resolution is not possible. Instead, several studies have focused on the effects of common functional polymorphisms in genes related to synaptic plasticities, such as the well known Val66Met polymorphism in the brain-derived neurotrophic factor (BDNF) gene (Fritsch et al., 2010; McHughen et al., 2010). Its role in motor learning is suggested by evidence that Met carriers showed less efficiency during motor skills acquisition.

### **1.3.2 Role of GABA and dopamine during learning**

GABA is the most prevalent inhibitory neurotransmitter in the brain, which is mostly located in interneurons. The primary GABA receptors are i) GABA<sub>A</sub> receptor, ii) GABA<sub>A-ρ</sub> receptor and iii) GABA<sub>B</sub> receptor. The role of GABA in modulating synaptic changes has been well described in a variety of animal studies (Donato, Rompani, & Caroni, 2013; Trepel & Racine, 2000). For example in rats, GABA<sub>A</sub> antagonists can block the induction of neocortical LTP and slow the development of potentiation. The in vivo measurement of GABA in humans is well established using magnetic resonance spectroscopy (MRS). These studies have consistently shown that motor training can lead to reduced GABA concentration during both short-term (Floyer-Lea, Wylezinska, Kincses, & Matthews, 2006; Levy, Ziemann, Chen, & Cohen, 2002) and long-term learning (Sampaio-Baptista et al., 2015; Stagg et al., 2014). In addition, GABA concentration was correlated with changes in resting-state sensorimotor functional connectivity (Stagg et al., 2014), which could also be related to GABAergic gamma oscillation (Hall et al., 2011).

Another crucial neurotransmitter is dopamine which is involved in the modulation of synaptic strength (LTP and LTD) in the prefrontal cortex and striatum (Gurden, Tassin, & Jay, 1999; Huang, Simpson, Kellendonk, & Kandel, 2004; Molina-Luna et al., 2009; Rioult-Pedotti, Pekanovic, Atiemo, Marshall, & Luft, 2015). Modulations of direct and indirect pathways are highly dependent on the depolarization of dopamine receptor D1 and hyperpolarization of dopamine receptor D2. Dopamine is therefore critically involved in movement control and motor learning.

## **1.4 Motor learning and schizophrenia**

Motor deficits are shared across a broad range of brain disorders, including neural degeneration diseases such as Parkinson's disease or psychiatric diseases such as schizophrenia (Walther & Strik, 2012; Wolff & O'Driscoll, 1999). Motor deficits in schizophrenia include abnormal involuntary movements (Whitty, Owoeye, & Waddington, 2009) which can occur during the entire disease period, especially in aging patients (Quinn et al., 2001).

Schizophrenia is a complex mental disease with high heritability (Meyer-Lindenberg & Weinberger, 2006). The genetic contribution to motor abnormalities in schizophrenia is still unclear. While most of the studies on schizophrenia focused on cognitive aspects, an increasing number of MRI studies has started to investigate the motor abnormalities in schizophrenia using structural (Dazzan et al., 2004; Hirjak, Kubera, et al., 2019; Hirjak et al., 2012; Janssen et al., 2009; Sarro et al., 2013; Thomann et al., 2009) and functional neuroimaging (Hirjak, Rashidi, Kubera, et al., 2019; S. Kodama et al., 2001; Muller, Roder, Schuierer, & Klein, 2002; Rogowska, Gruber, & Yurgelun-Todd, 2004; Schroder et al., 1999; Schroder, Wenz, Schad, Baudendistel, & Knopp, 1995). For example, neurological soft signs and abnormal involuntary movements have been found to be associated with the grey matter volume of the primary motor cortex (M1), basal ganglia and cerebellum (Hirjak, Rashidi, Fritze, et al., 2019; Hirjak, Thomann, et al., 2015; Hirjak, Wolf, et al., 2015; Li et al., 2013). Motor learning tasks are therefore a promising approach to investigate differences in learning-induced neural plasticity between patients with schizophrenia and healthy individuals in the future.

## **1.5 Imaging method and modeling**

### **1.5.1 Brief introduction of MRI, fMRI and MRS**

Magnetic resonance imaging (MRI) technique is one of the most frequently used tools to acquire in-vivo brain images non-invasively. The MRI technique is an application of the nuclear magnetic resonance (NMR) phenomenon. Briefly, by applying an additional weak oscillating magnetic field that has a specific frequency to the atoms under a strong magnetic field, the spin movements of the atoms will be disturbed. The atoms will gradually recover to the original spin movements along the strong magnetic field, but the recovery duration varies in different brain tissues. This phenomenon could

allow us to acquire high dimensional structural brain images. In recent decades, functional MRI (fMRI) was introduced into neuroimaging studies to investigate the brain activity based on the discovery of blood-oxygenation-level-dependent (BOLD) signal. The BOLD signal measures the hemodynamic response – a sluggish signal (a few seconds delay) that is triggered by neural activity. Although fMRI (BOLD) is an indirect measure of brain neural activity (Logothetis, 2002), it is widely applied in neuroimaging studies because it's capability to provide high spatial resolution whole-brain functional images (around 3mm).

Magnetic resonance spectroscopy (MRS) is a technique that has been widely used to obtain the distribution and concentration of brain metabolites such as N-acetyl aspartate (NAA), choline (Cho), creatine (Cr), and glutamate (Glu). These metabolites have different chemical structures which determine the nuclear environment and thereby react slightly different to the magnetic field (chemical shift). Therefore, signals from different metabolites can be detected due to the slightly different resonance frequencies of each metabolite. In addition to chemical shift, the signal is also partly determined by J-coupling, which is an internal indirect interaction of two nuclear spins and can lead to modulation of signal intensity depending on different sequences and parameters such as the echo time (TE) (Blüml, 2013). MRS has been extensively applied to investigate the concentration of glutamate in borderline disorder (Hoerst et al., 2010). In the current project, MRS data were acquired to evaluate the associations between the glutamatergic concentration in the primary motor area and the functional response as well as connectivity during the motor learning process.

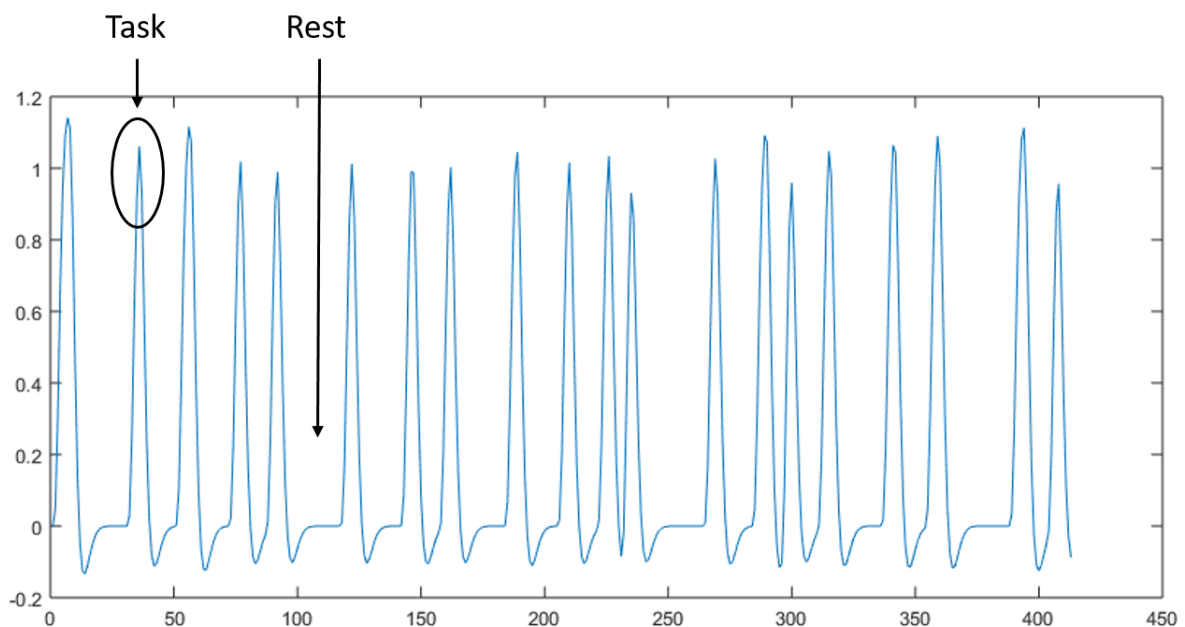
### **1.5.2 Functional Activation**

Functional MRI studies can roughly be divided into resting-state fMRI and task fMRI. During resting-state fMRI, no external task is given to the subjects during the entire scan. Subjects may close their eyes or leave their eyes open and fixate a crosshair on a screen. Resting-state fMRI is designed to investigate the intrinsic spontaneous neural activity. Since no external task is given, the interpretation of the neural mechanisms of resting-state studies is less straightforward compared to task fMRI that challenges a certain type of neural activity with high experimental control. Here, brain activation is studied under specific task conditions (e.g. during finger tapping vs. no finger tapping). There are two types of task designs referred to as 'block design' and 'event-related design'. In block designs, the task conditions are presented in alternating

blocks with durations of up to half a minute (e.g. 30s-blocks of finger tapping, followed by 30s-blocks of no finger tapping). The blocks are repeated several times to allow for a robust estimation of functional activation. The 'event-related design' was introduced to the field at a later time point and allows for the assessment of brain responses to single, short events (e.g alternating between single finger tapings of the left and right hand).

In the current project, the 'block design' was applied. In order to estimate functional activation to task conditions, the raw data needs to be preprocessed and fitted to a statistical model. In the statistical analysis, the task conditions are modeled as boxcar functions that are convolved with the hemodynamic response function (HRF) (Figure 1.2). The resulting functions are then used as regressors of interests together with covariates of non-interests (e.g. head motions) in a general linear model (GLM). This GLM model will be estimated for each voxel to test the model fit, i.e. how well the model fits the time series of the voxel. The outputs of the GLM model are beta images that reflect the distribution of weights (i.e. estimated slope of the GLM model) of certain task conditions.

**Figure 1.2**



The figure shows an example of block design in the motor learning task fMRI study. The horizontal axis indicates the number of scans ( $TR = 1.79$  seconds). The vertical axis indicates the magnitude of the task condition (arbitrary units). The brain activation is a linear regression 'fitness' of the fMRI BOLD signal from the brain to the time series shown.

### 1.5.3 Functional Connectivity

While functional activation is used to estimate the instantaneous response of the brain to external stimuli, functional connectivity is the method of choice to assess the synchronization (correlation) of two given time series (e.g. of two brain areas). Functional connectivity is assessed as Pearson correlation coefficient ( $R$ ) which scales between -1 to 1 and which is defined by the covariance of the two time series ( $X$  and  $Y$ ):

$$R = \frac{cov(X,Y)}{\sigma_X \sigma_Y},$$

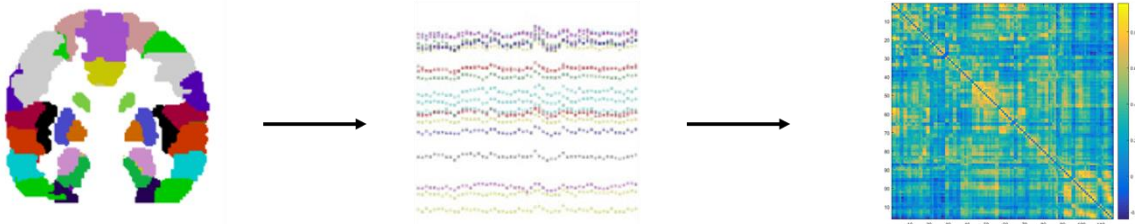
where  $cov(X,Y)$  denotes the covariance of  $X$  and  $Y$ , and  $\sigma_X$  and  $\sigma_Y$  denote the variance of  $X$  or  $Y$  respectively. A negative correlation coefficient  $R$  implies that the two time series are negatively correlated or anticorrelated, while a positive correlation coefficient implies that the two time series are positively correlated. The two time series are not correlated with each other if the correlation coefficient  $R$  is close to 0.

### 1.5.4 Graph theory

In the recent decade, tools from the mathematical field of graph theory have been increasingly applied to brain imaging data to investigate brain function from a network perspective. These network models of brain function are able to account for the high interdependence of brain functions and the precise orchestration of multiple brain areas in the execution of behavior and cognition. Nodes and connections are the fundamental elements to construct a network. To build functional brain networks from brain imaging data, nodes are defined as brain areas and the connections between them are estimated by functional connectivity. For example, one of the most frequently used atlas to define brain nodes is the AAL brain atlas (Tzourio-Mazoyer et al., 2002). Based on this atlas, the average time series from each brain region will be extracted to represent the regional brain activity. Next, pair-wise functional connectivity will be calculated to represent the connections between each pair of nodes resulting in an adjacency matrix  $A_{i,j}$  is constructed, in which each element reflects the connection of nodes  $i$  and  $j$  (Figure 1.3). Based on the adjacency matrix  $A$  of the brain network, a variety of network properties can be calculated that described the network architecture in a biologically meaningful way, such as small worldness, global efficiency, modularity and characteristic path length.

The basic parameters of a graph network include the number of nodes and connections. The latter is often referred to as the network density, which is the relative number of connections present divided by the absolute number of possible connections. Other more advanced measures include nodal degree, clustering coefficient and path length. The nodal degree is simply the number of connections a particular node has. The clustering coefficient is the number of existing triangle connections (closed triplets) around a single node divided by the number of all possible triangles and indicates how well a node is integrated with its neighboring nodes. The path length is a measure of how many connections must be passed to visit any other nodes in the network. The characteristic path length is an indicator of network segregation and is calculated based on the averaged shortest distance between every pair of nodes in the network. One of the most famous and well-established graph theoretical measures is small worldness. Small-worldness is a ratio of (normalized) clustering coefficient and path length and measures how well the global network balances local connectedness while keeping the overall distance short. It is often interpreted as a reflection of how the network could operate at high speed while the cost is relatively low (Braun et al., 2012; Rubinov & Sporns, 2010; Watts & Strogatz, 1998) (Figure 1.3 & 1.4).

**Figure 1.3**



The figure shows the flow chart of network analysis. The brain will firstly be parcellated into a certain number of brain nodes (e.g., AAL = 116 brain areas). Next, the BOLD signals will be extracted from those brain areas and a correlation matrix will be built by computing the pair-wise Pearson correlation coefficient.

**Figure 1.4**

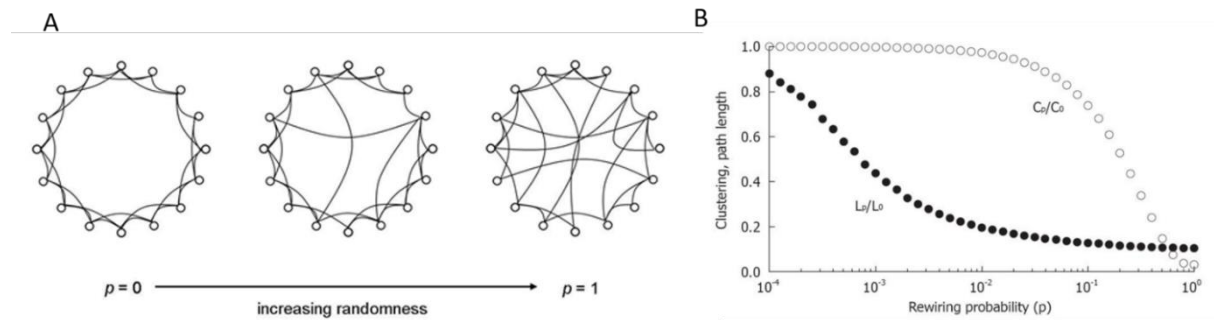


Figure Panel A shows the network changes from highly regular to highly random along with randomness  $p$ . In the regular network ( $p = 0$ ), the connections are fully connected in the neighbor nodes whereas in the random network the connections are totally random. The small-world network sits in between where the neighbor connections are still existing but the long-distance connections are also available. Panel B shows the fraction trade-off between normalized clustering coefficient and path length as fundamental elements of small-world network properties. The largest proportion sit in between rewiring probability  $p = 0$  and 1 which correspond to the network in the middle of Panel A.

## 1.6 Hypotheses

Motor learning studies have been carried out for decades using both animal models and human populations. While these studies have shed light on the genetic, molecular, cellular and circuit processes underlying the different stages of motor learning, a comprehensive overview of how these processes relate to the whole brain, system-level activity and connectivity patterns remains elusive as outlined above. Based on the existing studies, the current project will focus on the following questions:

First, to what extent do graph-theoretical parameters like small worldness, that are well known to highly correlate with cognitive functions, relate to motor learning ability?

Second, what are the brain networks that differentiate good motor learners from bad learners and are these networks modulated by glutamate?

Third, is long-term motor learning associated with structural (grey matter morphology) and functional (neural activity and connectivity) changes in motor learning-related areas, such as the frontal-parietal network and hippocampus?

Based on these questions, the following specific research hypotheses were derived:

- 1) Global brain functional network properties are closely linked to the individual ability to acquire novel motor skills during short-term motor learning.
- 2) The cerebellum and the primary motor cortex are more strongly involved in short-term motor learning while higher-order sensorimotor areas such as premotor area / SMA and basal ganglia are

more strongly involved in long-term motor learning. 3) In line with the involvement of glutamate in synaptic plasticity, the neural activity and connectivity of the motor learning associated networks are modulated by glutamate. 4) Based on the critical role of the hippocampus in other aspects of learning, the morphology, activity or connectivity of the hippocampus is altered by short-term and long-term motor learning. These hypotheses are tested in a multimodal neuroimaging study involving short-term motor learning (training approximately 30 minutes) and long-term motor learning (11 days of continuous training, daily training is approximately 30 minutes). Motor training was performed using the sequential visual isometric pinch task (SVIPT) (Reis et al., 2009) that challenges the control of pinch force according to visually guided targets displayed on the monitor.



## 2 STUDY 1: RESTING-STATE BRAIN NETWORK FEATURES ASSOCIATED WITH SHORT-TERM SKILL LEARNING ABILITY IN HUMANS AND THE INFLUENCE OF N-METHYL-D-ASPARTATE RECEPTOR ANTAGONISM<sup>1</sup>

### 2.1 Abstract

Graph theoretical functional magnetic resonance imaging (fMRI) studies have demonstrated that brain networks reorganize significantly during motor skill acquisition, yet the associations between motor learning ability, brain network features and the underlying biological mechanisms remain unclear. In the current study, we applied a visually guided sequential pinch force learning task and graph theoretical analyses to investigate the associations between short-term motor learning ability and resting-state brain network metrics in 60 healthy subjects. We further probed the test-retest reliability ( $n = 26$ ) and potential effects of the NMDA antagonist ketamine ( $n = 19$ ) in independent healthy volunteers. Our results show that the improvement of motor performance after short-term training was positively correlated with small-worldness ( $p = 0.032$ ) and global efficiency ( $p = 0.025$ ) while negatively correlated with characteristic path length ( $p = 0.014$ ) and transitivity ( $p = 0.025$ ). In addition, using network-based statistic (NBS), we identified a learning ability-associated ( $p = 0.037$ ) and ketamine susceptible ( $p = 0.027$ ) cerebellar-cortical network with fair to good reliability ( $ICC > 0.7$ ) and higher functional connectivity in better learners. Our results provide new evidence for the association of intrinsic brain network features with motor learning and suggest a role of NMDA-related glutamatergic processes in learning-associated subnetworks.

### 2.2 Introduction

The acquisition of new motor skills requires the brain to flexibly reconfigure neural circuits to master a desired performance level (Bassett & Mattar, 2017). Recent studies have demonstrated that different circuits are involved at distinct stages of learning (Dayan & Cohen, 2011; Penhune & Steele, 2012). While the initial learning phase engages a widespread network consisting of primary motor area (M1), supplementary

---

<sup>1</sup> Published paper: Zang, et al., (2018). "Resting-state brain network features associated with short-term skill learning ability in humans and the influence of N-methyl-d-aspartate receptor antagonism." *Network Neuroscience* 2(4): 464-480.

motor area (SMA), basal ganglia (BG), dorsolateral prefrontal cortex (DLPFC), premotor cortex and posterior cerebellum, the following longer-term learning phase relies on a smaller set of brain regions including M1, SMA, BG and the lateral cerebellum (Dayan & Cohen, 2011). In addition, the specific type of motor learning task determines the preferential involvement of brain regions with sequential learning challenging cortical areas while more complex sensorimotor tasks with novel kinematic additionally challenge the BG and cerebellum (Hardwick, Rottschy, Miall, & Eickhoff, 2013).

The interactions between brain regions during motor learning can be studied in the framework of brain networks. By combining network analysis and functional magnetic resonance imaging (fMRI), recent studies have shown that brain network features including flexibility (Bassett et al., 2011), connectivity strength, local path length and nodal efficiency (Heitger et al., 2012; Sami & Miall, 2013) change in response to motor learning and can predict its rate (Bassett et al., 2011). Notably, changes in the brain network architecture cannot only be assessed *during* the process of motor learning using task-based fMRI, but also during rest. While there is some evidence that intrinsic network connectivity measures derived from prior resting-state fMRI (rs-fMRI) predict motor learning abilities (Mawase, Bar-Haim, & Shmuelof, 2017; Wu, Srinivasan, Kaur, & Cramer, 2014), recent studies also suggest that motor learning effects can be detected using rs-fMRI *after* task practice (Albert et al., 2009; Sami & Miall, 2013; Sami et al., 2014). However, while plasticity-related effects of motor learning likely shape the intrinsic configuration of brain circuits the biological mechanisms in humans remain largely unknown.

Plausible molecular mechanisms contributing to motor learning-related network changes include glutamate-dependent processes (Dayan & Cohen, 2011). Supportive evidence is provided by animal studies showing that motor training can shift the glutamatergic N-methyl-D-aspartate (NMDA) receptor subunit composition in BG (Kent et al., 2013) and promote the NMDA dependent synaptic plasticity in the primary motor cortex of rats (Kida et al., 2016), while impaired motor performance was observed in mGluR4 gene knock out mice (Pekhletski et al., 1996). In humans, evidence for the involvement of glutamate-dependent processes during motor learning is less direct. Here, many studies have focused on the effects of a common functional polymorphism (Val66Met) in the brain-derived neurotrophic factor (BDNF) gene (Fritsch et al., 2010; McHughen et al., 2010), a downstream modulator of the molecular cascade supporting

synaptic plasticity linked to motor learning impairments and altered motor cortical activations in the plasticity-impaired Met allele carriers (Fritsch et al., 2010; McHughen et al., 2010; Thomason, Yoo, Glover, & Gotlib, 2009). For the evidence in humans, a study by Tahar et al. further showed that the NMDA receptor antagonist amantadine significantly impairs motor learning in healthy subjects (Hadj Tahar, Blanchet, & Doyon, 2004).

In the current work we aimed to answer two main questions in healthy humans, first whether the brain's resting-state network configuration relates to individual differences in short-term motor learning, and second whether these metrics can be influenced by NMDA receptor antagonism. We first investigated whether resting-state network features relate to individual differences in short-term motor learning ability by combining an established sequential visual isometric pinch force learning task (Reis et al., 2009) with rs-fMRI and graph theoretical analyses. We hypothesized that both global network diagnostics and functional connectivity amongst a circumscribed set of brain visuomotor brain areas would relate to individual motor learning ability (J. Doyon & Benali, 2005; Hikosaka et al., 2002). Secondly, we tested whether ketamine influences the functional connectivity of motor learning-related subnetworks. Here, we hypothesized that NMDA receptor blockade would decrease the connectivity of motor learning-related subnetworks.

## **2.3 Materials and Methods**

### **2.3.1 Participants and motor learning task description**

Sixty healthy right-handed volunteers (mean age  $26.6 \pm 7.5$  years, 33 males) underwent visuomotor training followed by a resting-state fMRI scan (mean training duration:  $26.9 \pm 5.7$  minutes, mean time interval between motor training and fMRI scan:  $45.8 \pm 7.5$  minutes). Exclusion criteria included MRI contraindications, a history of psychiatric and neurological illness, prior head trauma, and current alcohol or drug abuse. None of the subjects had a first-degree relative with a psychiatric disorder or received psychopharmacological treatment. All participants provided written informed consent for a protocol approved by the Ethics Committee of the University of Heidelberg.

### Visuomotor learning task

Behavioral training consisted of a single session with a modified version of an established (Reis et al., 2009) sequential visual isometric pinch force task. Subjects were seated 80 cm in front of a 28-inch monitor depicting a home position and five target gates ( $G_1$ - $G_5$ , Figure 2.1) while holding a force transducer between their right thumb and index finger. The application of pinch force moved a screen cursor from the home position in a right hand direction towards the target gates while relaxation resulted in a leftward cursor movement back towards the home position. The distance of the cursor to the home position increased logarithmically with increasing pinch force in order to make the task more difficult. Subjects were instructed to modulate their pinch force so that the cursor navigated as quickly and accurately as possible along the following sequence: *home- $G_2$ -home- $G_5$ -home- $G_3$ -home- $G_1$ -home- $G_4$* . After getting familiar with the setting, subjects performed 4 training blocks consisting of 35 trials (completed sequences) each. Movement times per trial were measured from movement onset in the home position to stopping at the last gate ( $G_4$ ). Error rates were calculated as ratio of gates per block with over- or undershooting cursor movements (missed gates).

**FIGURE 2.1**

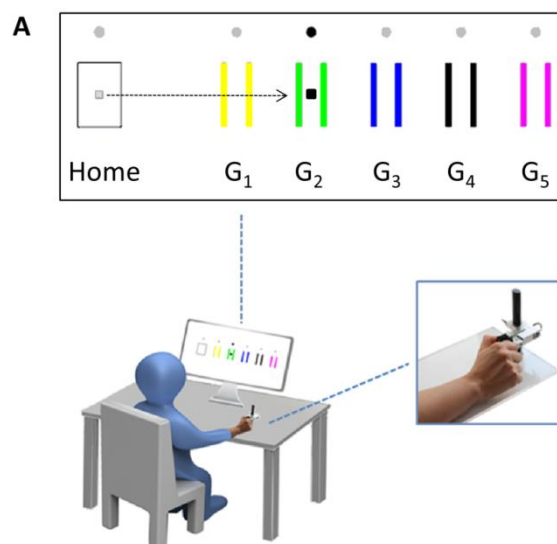


Figure 2.1. Set-up of the sequential visual isometric pinch task (SVIPT, see Methods for details). Subjects were asked to move the cursor into the highlighted targets (i.e.  $G_2$ ) as fast and as accurate as possible. The sequence of targets was 2-5-3-1-4. The manikin illustration is copyright protected (©Petr Ciz – Fotolia.com).

### **Definition of skill learning**

Following prior work with this task (Reis et al., 2009) we calculated individual skill measures for each block using the formula

$$skill\ measure = \ln\left(\frac{1 - error\ rate}{error\ rate(\ln(duration)^{5.424})}\right)$$

where *duration* is the average movement time across the trials of the block, *error rate* is the rate of over- and undershoots across the trials of the block (Reis et al., 2009). Over all training blocks, individual differences in skill learning ability were calculated based on the difference in the skill measure between the last and first training block (skill learning = skill measure<sub>block4</sub> – skill measure<sub>block1</sub>).

### **2.3.2 Data acquisition and analyses**

#### **MRI data acquisition**

Neuroimaging was performed on a 3T MRI scanner (Siemens Trio, Erlangen, Germany) equipped with a 32 channel multi-array head-coil. Details on MRI sequences are given in supplemental materials.

#### **fMRI data processing**

Image processing was performed using standard routines implemented in the Statistical Parametric Mapping software (SPM8, <http://www.fil.ion.ucl.ac.uk/spm/software/spm8/>) and the Data Processing Assistant for Resting-State fMRI toolbox (DPARSF, (C. Yan & Zang, 2010)). All images were realigned to the first image of the time series, corrected for slice timing, spatially normalized to the Montreal Neurological Institute (MNI) EPI template, and spatially smoothed with an 8 mm full-width at half-maximum (FWHM) Gaussian kernel. For each participant, we then extracted the mean time series from 264 brain regions derived from the Automated Anatomical Labeling (AAL 116) brain atlas (Tzourio-Mazoyer et al., 2002) by random parcellation (Zalesky, Fornito, Harding, et al., 2010). From the node time series, we regressed out the time series of white matter and cerebrospinal fluid masks (derived from SPM tissue probability maps thresholded at 90% for CSF and 99% for WM) (Cao et al., 2014) and the six head motion parameters from the

realignment step. The resulting residual time series were temporally filtered using a 0.01 - 0.1 Hz band-pass filter.

### **Quantification of head displacements**

The functional connectivity estimates and network diagnostics derived from resting-state fMRI may be impacted by motion artifacts (Power, Barnes, Snyder, Schlaggar, & Petersen, 2012; Satterthwaite et al., 2013; C. G. Yan et al., 2013). To account for this, we used in-house software to estimate averaged frame-wise displacement (FD) (Power et al., 2012) and included average FD as covariates of non-interest in our analyses.

### **Construction of connectivity matrices**

For the construction of brain networks, we computed pairwise Pearson correlation coefficients between the processed time series of each node, which resulted in a  $264 \times 264$  two-dimensional matrix for each subject. We then thresholded the matrices in 1% intervals over a range of 40 densities from 1% to 40% to generate binary graphs (e.g., in the 1% thresholded matrix only the top 1% of the highest positive correlations are represented by assigning a value of 1 to the internode connections).

### **Calculation and analysis of graph diagnostics**

On the global brain network level, graph features were computed using the Brain Connectivity Toolbox (BCT) (Rubinov & Sporns, 2010). Specifically, for each density, we calculated 7 reliable (Cao et al., 2014) global brain network markers that reflect the integration and segregation of whole brain network and were shown to be in association with cognitive functions (Alavash et al., 2015): Transitivity, characteristic path length, global efficiency, smallworldness, modularity Q (Newman, 2006), assortativity, and mean connectivity coefficient. The detailed descriptions of the 7 markers are given in the supplemental materials.

For association with the degree of skill learning, the network properties were averaged across densities and introduced as dependent variable into separate linear regression models with skill learning as independent variables of interest and age, sex, and averaged FD as covariates of non-interests. Hochberg's stepwise p value adjustment method (Hochberg, 1988) was used to correct raw p values for multiple hypothesis testing.

### **Network-based statistic (NBS)**

We analyzed the connectivity matrices with NBS to identify clusters of node connections associated with skill learning ability. Compared to the mass-univariate testing of independent links, NBS offers higher statistical power by identifying connected components from a set of uncorrected thresholded links that are significantly associated with a variable of interest (Zalesky, Fornito, & Bullmore, 2010) and then uses a randomization approach to evaluate the null hypothesis on the level of connected subclusters (rather than individually for each connection). Following prior procedures (Wang et al., 2013), we defined initial linear regression models for each of the  $(N(N-1))/2 = 34716$  ( $N = 264$ ) possible links in the connectivity matrices. The regression models included skill learning as independent variable of interest and age, sex, and the averaged FD as covariates of non-interest. From the resulting  $p$  matrix, we defined a set of suprathreshold connections by isolating all links with  $t > 3.48$  and  $p < 5 \times 10^{-4}$  and used  $M = 5000$  permutations (Wang, Zuo, & He, 2010) to estimate the null distribution during permutation testing of the identified cluster association.

### **Supplemental analyses**

To further probe the quality of the skill learning-related NBS result, we further a) quantified the test-retest reliability of the mean connectivity of the identified cerebellar-cortical cluster, b) considered the potential role of structural confounds by testing the relationship between skill learning and grey matter volume of the nodes contributing to the cluster, and c) explored the effects of low dose ketamine as NMDA receptor antagonist on skill learning ability and the connectivity of the identified NBS cluster. Additionally, we aimed to probe d) the robustness of our results using a more conservative head motion correction approach and e) the specificity of the association between motor learning ability and global network features by controlling for the mean functional connectivity as covariate of non-interest. Finally, we examined the identified cerebellar-cortical network association to skill learning with respect to potential effects of the choice of the initial cluster-forming significance threshold and parcellation scheme for NBS, respectively, by exploring the outcome of f) two additional cluster-forming significance thresholds ( $p < 0.001$ ,  $p < 0.0001$ ) and g) an alternative whole-brain functional atlas (Rosenberg et al., 2016) containing a comparable number of nodes (268 parcellations) as our AAL-based atlas.

### **Test-retest reliability**

As previous studies have demonstrated that the reliability of functional connectivity estimates is spatially heterogeneous (Mueller et al., 2015), we aimed to establish the robustness of the connectivity estimates in the identified subnetwork before further exploring it in the context of a pharmacological challenge study. To quantify the test-retest reliability of the connectivity phenotype, we reanalyzed the resting-state reliability data reported in (Cao et al., 2014). Following the nomenclature of Fleiss (Fleiss, 1986), we considered an ICC value below 0.4 as *poor*, 0.4-0.75 as *fair to good*, and  $> 0.75$  as *excellent*. Detailed information about fMRI data is given in supplemental materials.

### **Structural correlates**

We analyzed the high resolution structural data with the voxel-based morphometry toolbox (VBM8, <http://dbm.neuro.uni-jena.de/vbm8/>) using default parameters. Detailed descriptions of preprocessing the structural data are provided in supplemental materials. We then extracted the GM volume of the nodes contributing to the identified NBS cluster and entered the sum GM volume as dependent variable in a regression model that included skill learning as independent variable of interest and age and sex as covariates of non-interest (significance level:  $p < 0.05$ ).

### **NMDA receptor challenge**

To quantify the effects of the NMDA receptor antagonist ketamine on the identified cerebellar-cortical subnetwork, we analyzed the ketamine challenge data reported in (Francois et al., 2016; Grimm et al., 2015). In this study, resting-state fMRI data were acquired in 24 healthy individuals (12 female, mean age 25 years, mean body weight 70 kg) undergoing three consecutive fMRI sessions over the course of three weeks. The pharmacological protocol followed a double blind, placebo-controlled, order randomized, three-period cross-over design with single intravenous doses of either saline (placebo condition), ketamine (0.5 mg/kg body weight), or scopolamine (4  $\mu$ g/kg body weight). Drug infusions started  $73.8 \pm 13.8$  minutes prior to the resting state scan and were  $40.02 \pm 6.02$  minutes in duration. The visuomotor learning task started  $15.6 \pm 3.5$  minutes after infusion onset and was completed around the end of the infusion (at  $40.4 \pm 8.61$  minutes). To ensure this, we used the same experimental setup for the



training as in the main study except for a slightly shorter training duration (25 trials for each block, 4 blocks in total). Since we did not test a hypothesis assuming effects of mACh-blockade (scopolamine condition) on the identified subnetwork phenotype, we only analyzed the rs-fMRI data from the ketamine and placebo conditions in the current study. For this, we created a covariate of non-interest coding for the order of ketamine and placebo conditions (ketamine first, placebo first) that was included in the applied repeated-measure ANOVA. For pharmacokinetic analysis, blood samples for quantification of norketamine plasma levels were drawn immediately before and after the MRI scan (see (Francois et al., 2016; Grimm et al., 2015) for details). The time interval between ketamine and placebo infusion was  $9.6 \pm \text{SD } 3.5$  days. One subject was excluded due to side effects under ketamine (Francois et al., 2016); four more subjects were excluded because they had already participated in either the current (3 subjects) or in other visuomotor learning studies (1 subject). In total, 19 subjects were included in further data analyses. The processing of the behavioral data, rs-fMRI data, node definitions, and construction of connectivity matrices followed the protocol described above. To test for drug effects, we extracted the mean connectivity from the links of the cerebellar-cortical subnetwork identified in the NBS analysis (see results section) and used a repeated measures ANOVA with drug as within-subjects factor and age, sex (as factor), body mass index (BMI), the order (as factor) of drug and the differences of averaged frame-wise displacement (placebo vs. ketamine condition) as covariates of non-interest. To directly relate the connectivity indices of the identified subnetwork to the administration of the drug in the ketamine condition, we quantified intravenous norketamine levels by chromatographic analysis from the blood samples taken immediately prior to the MRI scan. For details on the blood sample processing, please refer to (Francois et al., 2016). We used a linear regression model in which the norketamine values were introduced as dependent variable, the mean connectivity estimates from the network links as independent variable of interest and age, sex, body mass index (BMI) and averaged frame-wise displacement as nuisance covariates (significance level:  $p < 0.05$ ). Detailed descriptions about drug administration are provided in supplemental materials.

### ***Controlling for mean individual functional connectivity differences***

As global differences in connectivity strength might directly influence network properties (van den Heuvel et al., 2017), we aimed to replicate our results using the

individual mean functional connectivity average over all connections as an additional covariate of non-interest in our analyses.

### ***Scrubbing to correct for head motion***

Since sharp in-scanner motion can introduce systematic, artificial connectivity (Power et al., 2012), we aimed to replicate our findings using a “scrubbing” approach as described in detail in (Power et al., 2012). In short, all frames of the time series with a frame-wise displacement  $> 0.5$  mm were removed. Two subjects were excluded from this analysis because their number of spikes exceeded 10% of the total time points, leaving a total of 58 subjects.

## **2.4 Results**

### **2.4.1 Main results**

#### **Skill learning ability**

Training improved SVIPT performance as indicated by significant decrease in the trial durations and error rates and a significant increase in the skill measure (Figure 2.2A) across blocks ( $F_{(3,57)}$  values  $> 4.27$ , all  $p$  values  $< 0.009$ ). The analysis of the skill learning measure confirmed a significant increase in skill performance (skill measure block 4-1) at the end of the training (one-sample t-test,  $t_{(59)} = 11.43$ ,  $p = 1.2 \times 10^{-16}$ ).

#### **Relationship to graph-based diagnostics**

At the global brain network level, we observed significant associations between the individual skill learning ability and four of the seven graph diagnostics. While positive correlations were found for smallworldness ( $t_{(55)} = 2.73$ ,  $r = 0.35$ ,  $p_{raw} = 0.008$ ,  $p_{corr} = 0.032$ , Figure 2.2B) and global efficiency ( $t_{(55)} = 2.90$ ,  $r = 0.36$ ,  $p_{raw} = 0.005$ ,  $p_{corr} = 0.025$ , Figure 2.2C), we detected negative associations for characteristic path length ( $t_{(55)} = -3.33$ ,  $r = -0.41$ ,  $p_{raw} = 0.002$ ,  $p_{corr} = 0.014$ , Figure 2.2D) and transitivity ( $t_{(55)} = -2.92$ ,  $r = -0.37$ ,  $p_{raw} = 0.005$ ,  $p_{corr} = 0.025$ , Figure 2.2E). We observed no significant associations between skill learning ability and assortativity and modularity Q of the network (all  $p_{corr}$  values  $> 0.225$ , Table S2.2). In addition, there was no significant correlation between skill learning ability and whole brain mean connectivity ( $r =$

-0.11,  $p_{raw} = 0.41$ , Table S2.2). All calculated graphs displayed small-world network properties ( $\sigma = \gamma/\lambda > 1$ , range 1.02 – 2.69).

**FIGURE 2.2**

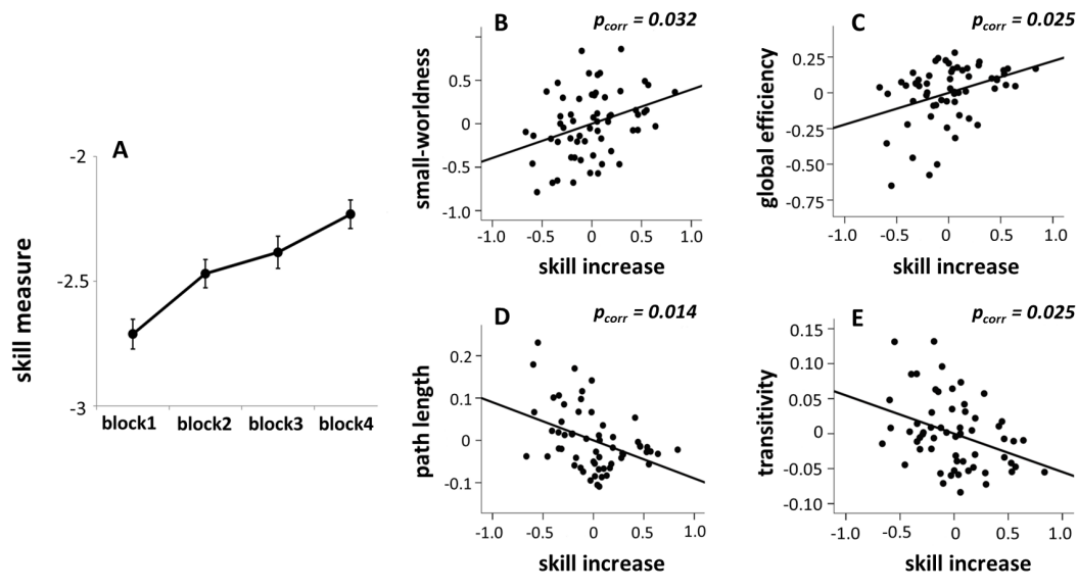


Figure 2.2. Panel A: Skill increase in the sequential visual isometric pinch task (SVIPT) across the training blocks (dots depict the mean values of the skill measure across blocks). Error bars indicate standard errors. Panels B-E: regression plots show significant associations of short-term motor learning ability (block4 – block1) and resting-state fMRI-derived graph diagnostics (adjusted for covariates and constant, see results section for details) after controlling for age, sex and FD.

### Relationship to subnetwork functional connectivity

Although we did not detect a significant association between short-term skill learning ability and the mean correlation estimates of the whole-brain functional connectome ( $r = -0.11$ ,  $p_{raw} = 0.41$ , Table S2.2), significantly associated brain subnetworks likely exist. Consistent with this notion, NBS identified a cluster of links with a significant positive association between skill learning ability and the functional connectivity estimates of the cluster links (uncorrected initial  $p < 5 \times 10^{-4}$ , FWE corrected  $p = 0.037$ , Figure 2.3). The cluster consisted of 69 nodes and 91 links mainly interconnecting the cerebellum, frontal, and parietal lobes. Specifically, most of the links of this cluster connected area 7b and area 8 of the left cerebellum to the cortex, in particular to nodes mapping in proximity to M1, primary sensory cortex, SMA, dorsal premotor cortex, intraparietal sulcus, and the motion sensitive visual processing area V5. A detailed description of all nodes and links of the identified subnetwork is provided in Table S1.

**FIGURE 2.3**

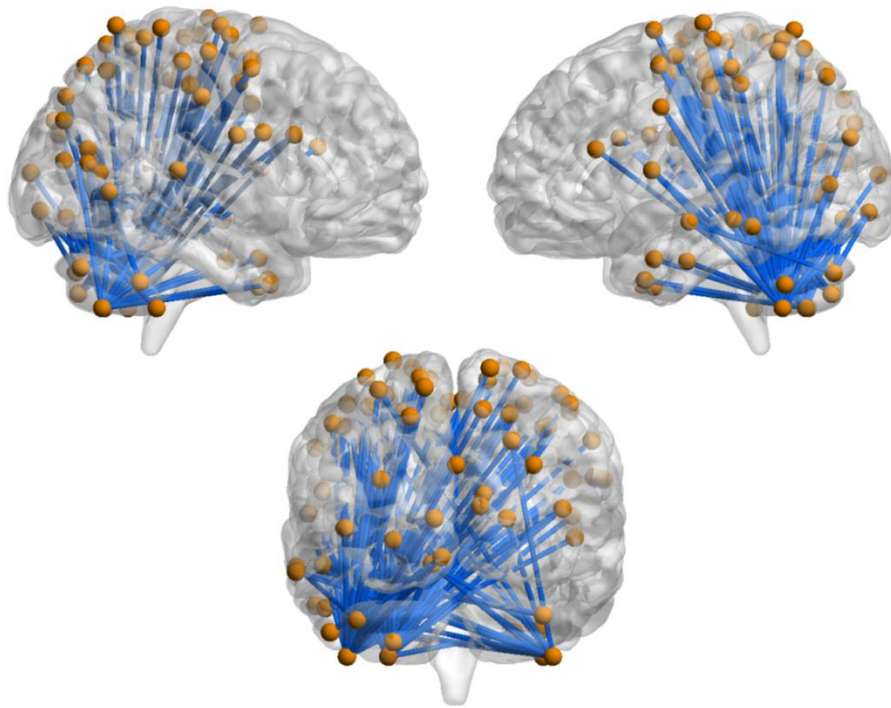


Figure 2.3. Illustration of the NBS-derived cerebellar – cortical functional network associated with short-term skill learning. Spheres represent center-of-gravity coordinates of the NBS-derived regions. Images are visualized using BrainNet Viewer (Xia, Wang, & He, 2013). Detailed information can be found in Table S2.1.

## **2.4.2 Supplemental results**

### ***Test-retest reliability***

The test-retest reliability analysis of the connectivity estimates of the NBS subnetwork yielded an ICC<sub>2,1</sub> of 0.72 and an ICC<sub>3,1</sub> of 0.73, respectively. This indicates an almost excellent robustness of the connectivity estimates of the cluster identified to relate to skill learning ability.

### ***Structural analysis***

The structural analysis did not provide any evidence for an association between the mean grey matter volume of the 69 subnetwork nodes and skill learning ability ( $t_{(56)} = -0.33$ ,  $p = 0.74$ ). Also, we detected no significant correlations between mean grey matter volume of the 69 subnetwork nodes and the mean functional connectivity estimates of the 91 links of the NBS subnetwork ( $t_{(56)} = -0.10$ ,  $p = 0.92$ ) or any of the four whole-brain graph features identified to relate to skill learning ability (all  $|t_{(56)}| <$

1.28,  $p > 0.21$ ). This makes the influence of structural confounds on skill learning ability and its association with the identified NBS subnetwork unlikely.

### **Effects of NMDA receptor challenge**

We detected no significant behavioral differences for skill increase (block 4 - block 1,  $F_{(1,17)} = 0.33$ ,  $p = 0.86$ ), task duration ( $F_{(1,17)} = 1.82$ ,  $p = 0.20$ ) or error rate ( $F_{(1,17)} = 0.48$ ,  $p = 0.50$ ) between the placebo and ketamine conditions (drug order was included as covariate of non-interest). In comparison to placebo, application of ketamine did not result in significant differences in global network measures (all  $F_{(1,12)} < 0.83$ ,  $p > 0.38$ ) or whole brain mean connectivity ( $F_{(1,12)} = 2.04$ ,  $p = 0.18$ ), but significantly decreased the mean functional connectivity of the learning associated cerebellar-cortical network ( $F_{(1,12)} = 6.38$ ,  $p = 0.027$ ). In addition, the mean connectivity of the cerebellar-cortical network was significantly negatively correlated with individual Norketamine concentrations ( $46.1 \pm 21.6$  ng/ml,  $t_{(13)} = -2.40$ ,  $r = -0.55$ ,  $p = 0.032$ , Figure 2.4) in the ketamine condition (age, sex, FD and BMI were controlled as covariates of non-interest). Average frame-wise displacement ( $p = 0.424$ ) and the time interval between drug infusion and resting state scan ( $p = 0.219$ ) were not significantly different between the ketamine and placebo conditions. A trend towards a main effect of drug order was found ( $p = 0.06$ ). The results indicate that the functional connectivity of the NBS-derived cerebellar-cortical network is impacted by ketamine and negatively associated to the concentration of the major active metabolite (i.e., Norketamine).

**FIGURE 2.4**

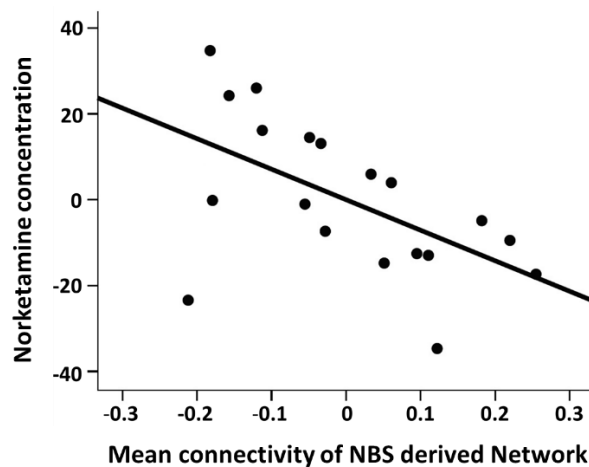


Figure 2.4. Partial correlation plot of negative correlation between blood Norketamine concentration and the mean connectivity of the NBS derived cerebellar – cortical network in the ketamine condition ( $p = 0.032$ ; adjusted for covariates and constant), controlled for age, sex, BMI and FD.

### ***Controlling for individual mean functional connectivity differences***

We replicated the findings that skill increase is significantly positively associated with smallworldness ( $p = 0.008$ ) and global efficiency ( $p = 0.005$ ) and negatively associated with characteristic path length ( $p = 0.002$ ) and transitivity ( $p = 0.006$ ) using the mean functional connectivity as an additional covariate of non-interests. Likewise, we replicated our NBS results using the mean correlation as an additional covariate of non-interest. Specifically, we found both statistically-equivalent (same uncorrected initial threshold, different number of links in network; FWE corrected  $p < 0.001$ , 220 links, ICC > 0.75) and density-equivalent (similar number of links in network, but more strict initial threshold  $p < 0.0001$ ; FWE corrected  $p < 0.001$ , 87 links, ICC > 0.72) cerebellar – cortical subnetworks that were significantly associated with short-term motor learning ability and were modulated by ketamine ( $F_{(1,11)} = 6.97$ ,  $p = 0.023$  for the subnetwork with 220 links;  $F_{(1,11)} = 4.93$ ,  $p = 0.048$  for the subnetwork with 87 links). Age, sex, order, BMI, mean FD and mean connectivity were controlled for as covariates of non-interests. Moreover, a marginal significant negative correlation was found between the mean connection of the statistically-equivalent subnetwork and the Norketamine concentration ( $r = -0.51$ ,  $p = 0.060$ ) while the mean connection of the density-equivalent subnetwork was significantly correlated with the Norketamine concentration ( $r = -0.56$ ,  $p = 0.037$ ).

### ***Scrubbing***

Using a more stringent motion correction approach, we could replicate our previous findings that motor learning is positively correlated with smallworldness ( $r = 0.39$ ,  $p = 0.003$ ), global efficiency ( $r = 0.41$ ,  $p = 0.002$ ) and negatively correlated with transitivity ( $r = -0.39$ ,  $p = 0.003$ ) (Table S2). However, motor learning was no longer correlated with characteristic path length ( $r = -0.24$ ,  $p = 0.074$ , Table S2.2).

In addition, we could replicate our finding of a cerebellar-cortical subnetwork that was correlated with learning rate. In detail, 81 connections linking bilateral cerebellum to visual, sensorimotor, parietal and frontal areas were positively correlated with skill increase (uncorrected initial  $p < 5 \times 10^{-4}$ , FWE corrected  $p = 0.036$ ) while controlling age and sex as covariates of non-interest (FD was no longer controlled as covariate of non-interest since we used FD for scrubbing). This subnetwork also had a fair to good reliability (ICC > 0.73). We then extracted the mean connectivity of the 81 connections

and found a significant main effect of drug ( $F_{(1,13)} = 5.10$ ,  $p = 0.042$ ) controlling for age, sex, order and BMI as covariates of non-interest. The mean connectivity of the 81 connections was also significantly negatively correlated with Norketamine concentrations ( $r = -0.55$ ,  $p = 0.03$ ) when age, sex and BMI were controlled as covariates of non-interest.

### ***Influence of initial threshold definition***

To further explore the robustness of our NBS finding, we repeated our skill learning association analysis using two different initial thresholds for cluster definition, i.e.  $p < 0.001$  (less strict) and  $p < 0.0001$  (more strict). Notably, a less strict initial  $p$  value should result in a larger but more unspecific network, while a stricter initial  $p$  value should provide a more specific, but smaller network. As expected, using an initial threshold of  $p < 0.0001$ , we found a similar, but smaller network of 38 links including the left cerebellum and cortical areas that was significantly correlated with skill learning (FWE  $p_{corr} = 0.012$ ). Moreover, the  $p < 0.001$  initial threshold resulted in a larger, cerebellar-cortical network consisting of 134 links that were significantly correlated with skill learning (FWE  $p_{corr} = 0.048$ ). We conclude from these observations that the reported association of the cerebellar-cortical network with skill learning is observed across a range of initial  $t$  threshold definitions for NBS.

### ***Influence of parcellation choice***

To further probe our AAL-based findings for potential effects of parcellation choice, we repeated our analysis with a recently published functional parcellation atlas including 268 nodes (Rosenberg et al., 2016). Notably, the choice of this particular functional atlas was motivated by the fact that it contains a comparable number of node definitions and covers the cerebellum in adequate detail, which is an important prerequisite given that we employed a motor-learning paradigm challenging subcortical and cerebellar structures. All other data processing and analysis procedures were kept identical to our initial AAL-based analysis. Similar to our AAL-based analysis, we detected a significant positive correlation of skill increase with small-worldness ( $r = 0.28$ ,  $p = 0.031$ ) and global efficiency ( $r = 0.36$ ,  $p = 0.005$ ) and a significant negative correlation of skill increase with transitivity ( $r = -0.38$ ,  $p = 0.002$ ). In addition, the NBS analysis with the Rosenberg atlas resulted in a very similar, but interestingly less reliable ( $ICC_{2,1} = 0.63$ ,  $ICC_{3,1} = 0.64$ ) cerebellar – cortical network with 69 links that

showed a significant positive association with skill learning (FWE corrected  $p = 0.044$ , Figure S2.1). Moreover, comparable to our AAL-based findings, the mean connectivity of this network was significantly negatively correlated with Norketamine concentrations ( $r = -0.62$ ,  $p = 0.014$ ). We conclude from these observations that a) our AAL-based NBS findings do not relate to the choice of this particular parcellation scheme, and b) that the choice of a functional parcellation atlas does not necessarily improve the reliability of the examined connectivity estimates.

## 2.5 Discussion

In the current resting-state fMRI study, we found several global brain network features to be significantly associated with individual motor learning ability. Further, we identified a cerebellar-cortical functional subnetwork that was a) significantly associated with short-term learning ability using a well-established motor learning task (Reis et al., 2009) and b) significantly modulated by NMDA receptor antagonism. We discuss our findings in more detail in the following paragraphs.

Firstly, we demonstrate that short-term motor learning ability is associated with several global network features that characterize a network's capability to process information efficiently (Bullmore & Sporns, 2009; Rubinov & Sporns, 2010). Specifically, global efficiency and small-worldness were positively correlated with motor learning ability, while transitivity and characteristic path length were negatively correlated. Although these learning-associated global network features are highly correlated with each other, they converge on the idea that higher network integration may favor better short-term motor learning ability. This notion is in line with previous studies demonstrating that higher network integration is beneficial for a range of brain functions, including intelligence (van den Heuvel, Stam, Kahn, & Hulshoff Pol, 2009) and working memory (Alavash, Doebler, Holling, Thiel, & Giessing, 2015). Importantly, while previous studies have suggested that motor learning changes resting-state connectivity patterns in terms of local network measures (Sami et al., 2014; Zhang et al., 2012), global resting-state network characteristics of the brain have been shown to be relatively stable (Braun et al., 2012; Cao et al., 2014) and untouched by the effects of motor learning (Heitger et al., 2012; Sami & Miall, 2013). Taken together, this may indicate that those global features of brain networks rather reflect the brain's general capability to master a task independent of training-induced alterations.



Secondly, we identified a highly plausible cerebellum centered network with links between cerebellar, visuospatial, sensorimotor, frontal and temporal regions that were positively associated with an individual's learning ability. We further provided evidence suggesting that the associated subnetwork is relatively reliable and robust against a variety of potential influencing factors including local grey matter volume, age, sex, head motion, individual mean functional connectivity differences, and the choice of the initial cluster-forming significance threshold and parcellation scheme, respectively.

Notably, the identified subnetwork is highly plausible since it connects several key areas involved in the early phase of visuomotor learning, including M1, SMA, premotor cortex, V5, parietal cortex and cerebellum (Bassett et al., 2011; J. Doyon et al., 2002; Hikosaka et al., 2002; Zhang et al., 2012). Among these regions, M1, SMA, premotor and visual cortex in particular have been related to the computational integration of spatial motor demands (Hikosaka et al., 2002) and the handling of on-line visual feedback (Z. Y. Dong et al., 2012) during the acquisition of complex motor skills. Both functions are crucially important in the early learning phase of our complex motor learning paradigm which requires constant visually-guided feedback control and real-time adjustments of executed motor programs. In addition, several parietal regions participated in the cerebellum-centered network, an observation that is in line with the suggested role of these regions in motor imagery learning (Zhang et al., 2012), a key element for planning the upcoming movements' kinetic parameters (Kuang et al., 2016). Moreover, the involvement of bilateral DLPFC is consistent with previous motor learning studies (Bassett et al., 2015; Heitger et al., 2012) and may plausibly relate to the high level of visual attention demands (Barbey et al., 2013 (Barbey, Koenigs, & Grafman, 2013)) and complex sequential memory input in motor learning tasks (Toni & Passingham, 1999), especially during the early learning phase (Bassett et al., 2015). Further, the central role of the cerebellum in our identified sub-circuit is in good agreement with prior PET and fMRI studies. These studies demonstrated a crucial role of the cerebellum as an error detector and parameter modifier of motor reference plans in early learning phases (J. Doyon et al., 2002; Penhune & Steele, 2012). This has been evidenced, for example, by severe impairments in certain aspects of motor learning (e.g. reaction time) due to lack of behavioral adjustment in face of errors in patients with cerebellar lesions (Laforce & Doyon, 2001; M. A. Smith & Shadmehr, 2005). While the observed association between connectivity of the cerebellum-centered subnetwork and motor learning ability could be interpreted as a stronger

intrinsic capability of the network architecture in superior learners, it could also be argued that the association is a consequence of learning-induced motor memory consolidation (Albert et al., 2009; Sami et al., 2014) since the resting-state scan was acquired post training.

Thirdly, consistent with prior system-level ketamine studies in humans (Kraguljac et al., 2016; Niesters et al., 2012), we found that the cerebellum centered network was significantly modulated by NMDA receptor antagonism and its connectivity was negatively correlated with blood-level Norketamine concentrations. Interestingly, the motor learning performance before the scan itself was not affected (Francois et al., 2016; van Loon et al., 2016) by low-dose ketamine infusion. Similar observations were made in object-recognition and reward-anticipation fMRI studies, where authors showed significantly altered BOLD responses but no main effect of drug under low dose (e.g.,  $\leq 0.5$  mg/kg) ketamine administration during task performance. This might indicate that the administered drug dose was sufficient to alter neural functional interactions in the identified cerebellum-centered subnetwork, but below the dose level at which overt interruptions of motor learning behavior become evident. In addition, the absence of a behavioral differences between the drug conditions suggests that the observed connectivity differences are unlikely the consequence of drug-induced changes in motor performance. The detected changes in cerebellar-cortical network connectivity suggest a role for NMDA receptor-dependent glutamatergic neurotransmission that may relate to consolidation processes. This interpretation is consistent with previous reports of a strong dependence of memory consolidation processes (Volianskis et al., 2015), BDNF genotype (Gosselin et al., 2016) and plasticity-related protein synthesis in the motor cortex (Luft, Buitrago, Ringer, Dichgans, & Schulz, 2004). Notably, the fact that we found no modulation of global network measures by ketamine further supports our earlier interpretation of these whole-brain efficiency markers as trait-like reflections of the brain's capability to perform a range of different tasks.

Our study has several limitations worth mentioning. Most importantly, while our finding of learning-related subnetwork connectivity indices is in line with the hypothesis that motor training leads to temporary changes in the functional brain network architecture, the directionality of such an effect cannot be claimed with our cross-sectional data. Even though we acquired resting-state data *after* off-line motor learning, the interpretation of a predisposed suitability of intrinsic brain networks for the challenged

motor performance is equally plausible (Mary et al., 2016). Secondly, while the connectivity within the motor learning associated subnetwork was significantly decreased under NMDA receptor blockade, the interpretation of impaired motor memory consolidation would ultimately require an affected motor performance in a preceding motor task. However, as we did not reassess the motor performance after scanning we must defer such a proof to future studies. Thirdly, previous resting state studies (Albert, Robertson, & Miall, 2009;(Barnes, Bullmore, & Suckling, 2009)) provided evidence for an impact of motor and cognitive tasks on the functional configuration of resting state networks in subsequent MRI scans. This implicates that in the case of drug-dependent differences in task engagement prior to the scan, variant carry-over effects (instead of or in addition to an NMDA receptor-related neural plasticity mechanism) may have influenced our drug challenge results. Notably, we did not detect significant main effects of drug condition on behavioral markers of training performance, which argues against such an interpretation. We nonetheless cannot fully exclude that other drug-induced differences in task engagement may have existed and have been carried over to the following resting state scan. Fourthly, although ketamine modulated our specific cerebellum centered subnetwork, ketamine as a non-competitive NMDA receptor antagonist may also plausibly influence other brain subnetworks.

In conclusion, we demonstrate that global brain network characteristics and specific subnetwork connectivity patterns during resting-state are associated with motor learning *before* scanning. We further show that the identified learning-related subnetwork connectivity estimates are unrelated to the grey matter volume of the nodes, reliable, and susceptible to glutamate challenge. We posit that the observed differential modulation of the examined whole-brain graph theoretical vs. cerebellar-cortical network features by ketamine may reflect distinct qualities of learning-related brain function, for example, individual predisposition for learning new motor skills (global brain network measures) vs. glutamate-dependent processes related to active motor memory consolidation (cerebellar-cortical network connectivity). Taken together, this investigation may offer valuable information on the neural processes related to short-term motor learning in humans and provide a starting point for future studies in a still under-researched area of human neuroscience.

## 2.6 Supplemental Information

### 2.6.1 S-Method

#### MRI data acquisition parameters

Resting-state fMRI was performed using an echo-planar imaging (EPI) sequence with the following parameters: TR = 1790 ms, TE = 28 ms, 34 axial slices per volume, voxel size = 3 x 3 x 3 mm, 1 mm slice gap, 192 x 192 mm field of view, and 76° flip angle, descending acquisition. For the resting-state experiment, we instructed participants to close their eyes, relax, and not engage in any particular mental activity during the scan (task duration: 5 minutes, 167 whole-brain scans). After each scan, we confirmed with the subjects that they had not fallen asleep in the scanner. In addition, we acquired high-resolution T1-weighted 3-dimensional images with a magnetization-prepared rapid gradient echo sequence (3D-MPRAGE) and the following parameters: TR = 2530 ms, TE = 3.8 ms, TI = 1100 ms, 176 slices, 256 x 256 mm field of view, 7° flip angle, and 1 mm<sup>3</sup> spatial resolution.

#### Global graph diagnostics

*Characteristic path length* is the average shortest path length between each pair of nodes in the network, with shorter path lengths indicating faster information flow. *Global efficiency* is the average of the inverse shortest path length and relates to the capacity of the network for information transfer at the global level. *Smallworldness* is the ratio of the normalized clustering coefficient (segregation) and normalized path length (integration) (Bullmore & Sporns, 2009). In the current study, 100 randomized networks were generated to calculate smallworldness. *Modularity Q* is the degree to which the network can be partitioned into non-overlapping modules, with higher values indicating a more developed network community structure with more densely connected local nodes. *Assortativity* reflects how often nodes of a similar degree are connected with each other. And *transitivity* reflects the global clustering coefficient of nodes (Rubinov & Sporns, 2010). The underlying methods and interpretation of these metrics are discussed in more detail elsewhere (Bassett & Bullmore, 2006; Bullmore & Sporns, 2009; Rubinov & Sporns, 2010).

#### Test-retest reliability data

STUDY 1: RESTING-STATE BRAIN NETWORK FEATURES ASSOCIATED WITH SHORT-TERM SKILL LEARNING ABILITY IN HUMANS AND THE INFLUENCE OF N-METHYL-D-ASPARTATE RECEPTOR ANTAGONISM

In this study, 26 healthy volunteers (mean age:  $24.4 \pm 2.8$  years, 15 females) underwent a 5 minute resting-state scan twice within two consecutive weeks (mean interval:  $14.6 \pm 2.1$  days). All 26 volunteers were naive to the current motor learning task. The processing of data, definition of nodes, and construction of connectivity matrices were consistent with the current work. We extracted the mean connectivity estimates from the links identified in the current NBS analysis (see results section) and calculated intra-class correlation coefficients (ICCs) as indices of robustness.

### Structural correlates

Briefly, the processing of images included tissue classification, normalization to MNI space with a diffeomorphic image registration algorithm, correction for image intensity non-uniformity, a thorough cleaning up of gray matter partitions, application of a hidden Markov random field model, transformation of GM density values into volume equivalents, and smoothing with an 8mm FWHM Gaussian kernel.

## 2.6.2 S-Results

Table S2.1

Node	Coordinates	T value	P value	Node	Coordinates	T value	P value
<b>CEREBELLUM.7B.L (-43, -54, -48)</b>							
Frontal.Sup.R <sup>[2]</sup>	32, -11, 67	4.35	$2.92 \times 10^{-5}$	SMA.R <sup>[4]</sup>	5, -19, 58	3.83	$1.64 \times 10^{-4}$
Frontal.Sup.L <sup>[2]</sup>	-27, -8, 60	4.55	$1.52 \times 10^{-5}$	SMA.L <sup>[4]</sup>	-5, -21, 52	3.58	$3.59 \times 10^{-4}$
	-16, 1, 71	4.20	$4.88 \times 10^{-5}$	PreCentral.R <sup>[3]</sup>	59, 3, 26	4.55	$1.52 \times 10^{-5}$
	-20, -5, 53	4.04	$8.28 \times 10^{-5}$		21, -15, 71	4.11	$6.74 \times 10^{-5}$
Frontal.Mid.R <sup>[2]</sup>	49, -2, 53	4.49	$1.83 \times 10^{-5}$		40, -7, 47	3.88	$1.43 \times 10^{-4}$
	30, -2, 56	3.81	$1.74 \times 10^{-4}$	PreCentral.L <sup>[3]</sup>	-24, -20, 74	4.59	$1.33 \times 10^{-5}$
Frontal.Inf.Tri.R <sup>[7]</sup>	50, 16, 25	3.71	$2.41 \times 10^{-4}$		-43, -1, 56	4.38	$2.70 \times 10^{-5}$
Cuneus.R	2, -85, 31	3.53	$4.23 \times 10^{-4}$		-35, -24, 67	4.03	$8.57 \times 10^{-5}$
Rolandic.Oper.L <sup>[5]</sup>	-59, 2, 11	4.18	$5.33 \times 10^{-5}$	PostCentral.R <sup>[3]</sup>	49, -31, 56	5.13	$1.98 \times 10^{-6}$
Parietal.Sup.R <sup>[6]</sup>	-16, -59, 71	4.76	$7.18 \times 10^{-6}$		38, -28, 46	4.08	$7.41 \times 10^{-5}$
	13, -72, 54	4.19	$5.09 \times 10^{-5}$		29, -40, 70	4.05	$8.1 \times 10^{-5}$
	24, -63, 52	4.17	$5.49 \times 10^{-5}$		45, -20, 60	4.04	$8.28 \times 10^{-5}$
	15, -47, 66	4.09	$7.20 \times 10^{-5}$		63, -8, 25	3.66	$2.81 \times 10^{-4}$
Parietal.Sup.L <sup>[6]</sup>	-30, -52, 62	4.64	$1.10 \times 10^{-5}$	PostCentral.L <sup>[3]</sup>	-45, -23, 47	4.29	$3.59 \times 10^{-5}$
	-17, -73, 51	3.51	$4.58 \times 10^{-4}$		-56, -2, 38	4.20	$4.96 \times 10^{-5}$
Parietal.Inf.L	-49, -36, 48	4.28	$3.72 \times 10^{-5}$		-34, -32, 55	4.01	$9.22 \times 10^{-5}$
Paracentral.Lobule.L	-9, -30, 66	3.67	$2.75 \times 10^{-4}$	Occipital.Sup.R <sup>[1]</sup>	25, -80, 41	4.62	$1.16 \times 10^{-5}$
Precuneus.L	-13, -54, 67	4.75	$7.36 \times 10^{-6}$	Occipital.Mid.R	34, -81, 31	4.55	$1.49 \times 10^{-5}$
	-11, -63, 63	4.36	$2.92 \times 10^{-5}$	Occipital.Mid.L	-29, -83, 25	4.08	$7.32 \times 10^{-5}$
Calcarine.R	13, -71, 19	4.00	$9.41 \times 10^{-5}$		-44, -74, 5	3.88	$1.37 \times 10^{-4}$
	23, -66, 9	3.77	$1.98 \times 10^{-4}$	Temporal.Mid.R	46, -71, 13	4.18	$5.28 \times 10^{-5}$
	12, -81, 14	3.49	$4.81 \times 10^{-4}$		51, -62, 1	3.93	$1.19 \times 10^{-4}$
Calcarine.L	-4, -91, -7	3.95	$1.11 \times 10^{-4}$	Lingual.L	-8, -80, -10	4.75	$7.50 \times 10^{-6}$

STUDY 1: RESTING-STATE BRAIN NETWORK FEATURES ASSOCIATED WITH SHORT-TERM SKILL LEARNING ABILITY IN HUMANS AND THE INFLUENCE OF N-METHYL-D-ASPARTATE RECEPTOR ANTAGONISM

	-7, -95, 9	3.61	3.29×10 <sup>-4</sup>	SupraMarginal. R	58, -23, 41	4.13	6.23×10 <sup>-5</sup>
<b>CEREBELLUM.8.L (-26, -64, -48)</b>							
Frontal.Sup.R <sup>[2]</sup>	32, -11, 67	3.84	1.59×10 <sup>-4</sup>	<b>PreCentral.R<sup>[3]</sup></b>	<b>59, 3, 26</b>	<b>4.34</b>	<b>3.05×10<sup>-5</sup></b>
Frontal.Sup.L <sup>[2]</sup>	-27, -8, 60	3.94	1.16×10 <sup>-4</sup>		40, -7, 47	3.56	3.81×10 <sup>-4</sup>
	-20, -5, 53	3.86	1.50×10 <sup>-4</sup>	<b>PreCentral.L<sup>[3]</sup></b>	<b>-43, -1, 56</b>	<b>4.16</b>	<b>5.69×10<sup>-5</sup></b>
	-16, 1, 71	3.50	4.65×10 <sup>-4</sup>	PostCentral.L <sup>[3]</sup>	-56, -2, 38	3.81	1.77×10 <sup>-4</sup>
<b>Frontal.Mid.R<sup>[2]</sup></b>	<b>49, -2, 53</b>	<b>4.40</b>	<b>2.50×10<sup>-5</sup></b>		-34, -32, 55	3.62	3.17×10 <sup>-4</sup>
Calcarine.R	23, -66, 9	3.67	2.71×10 <sup>-4</sup>	<b>Lingual.L</b>	<b>-8, -80, -10</b>	<b>4.11</b>	<b>6.74×10<sup>-5</sup></b>
	13, -71, 19	3.53	4.25×10 <sup>-4</sup>		-24, -71, 0	3.54	4.10×10 <sup>-4</sup>
<b>Temporal.Sup.R</b>	<b>50, -33, 10</b>	<b>4.09</b>	<b>7.07×10<sup>-5</sup></b>	SMA.R <sup>[4]</sup>	5, -19, 58	3.55	3.98×10 <sup>-4</sup>
Temporal.Mid.R	46, -71, 13	3.59	3.48×10 <sup>-4</sup>	SMA.L <sup>[4]</sup>	-1, -2, 57	3.52	4.33×10 <sup>-4</sup>
Temporal.Pole.Mid.R	26, 6, -38	3.50	4.72×10 <sup>-4</sup>	Rolandic.Oper.L <sup>[5]</sup>	-59, 2, 11	3.78	1.94×10 <sup>-4</sup>
<b>CEREBELLUM.8.R (38, -42, -48)</b>							
Lingual.L	-8, -80, -10	3.63	3.07×10 <sup>-4</sup>				
<b>CEREBELLUM.Crus1.R (38, -74, -31)</b>				<b>CEREBELLUM.Crus1.L (-39, -76, -33)</b>			
Temporal.Mid.L	-64, -14, -11	3.95	1.13×10 <sup>-4</sup>	<b>Temporal.Mid.L</b>	<b>-64, -14, -11</b>	<b>4.08</b>	<b>7.39×10<sup>-5</sup></b>
	-53, -33, -10	3.52	4.38×10 <sup>-4</sup>	Lingual.L	-8, -80, -10	3.84	1.58×10 <sup>-4</sup>
				Calcarine.L	-4, -91, -7	3.52	4.31×10 <sup>-4</sup>
<b>CEREBELLUM.Crus1.R (37, -49, -37)</b>				<b>CEREBELLUM.Crus1.L (-50, -55, -38)</b>			
Lingual.L	-8, -80, -10	3.76	2.06×10 <sup>-4</sup>	Lingual.L	-8, -80, -10	3.53	4.28×10 <sup>-4</sup>
Calcarine.R	23, -66, 9	3.53	4.29×10 <sup>-4</sup>				
<b>CEREBELLUM.Crus2.R (42, -65, -48)</b>							
<b>Frontal.Inf.Tri.L<sup>[7]</sup></b>	<b>-53, 26, 20</b>	<b>4.18</b>	<b>5.34×10<sup>-5</sup></b>	<b>Temporal.Inf.L</b>	<b>-52, -13, -28</b>	<b>4.93</b>	<b>3.95×10<sup>-6</sup></b>
PreCentral.L <sup>[3]</sup>	-43, -1, 56	3.76	2.06×10 <sup>-4</sup>		-38, 5, -36	3.90	1.31×10 <sup>-4</sup>
Parietal.Sup.L <sup>[6]</sup>	-30, -52, 62	3.92	1.25×10 <sup>-4</sup>	Fusiform.L	-27, 1, -39	3.58	3.6×10 <sup>-4</sup>
Occipital.Sup.R <sup>[1]</sup>	25, -80, 41	3.50	4.66×10 <sup>-4</sup>	<b>CEREBELLUM.Crus2.L (-24, -75, -72)</b>			
<b>Temporal.Mid.L</b>	<b>-53, -33, -10</b>	<b>4.65</b>	<b>1.05×10<sup>-5</sup></b>	Frontal.Sup.L <sup>[2]</sup>	-20, -5, 53	3.53	4.24×10 <sup>-4</sup>
	<b>-56, 1, -27</b>	<b>4.06</b>	<b>7.92×10<sup>-5</sup></b>	Frontal.Mid.R <sup>[2]</sup>	49, -2, 53	3.84	1.58×10 <sup>-4</sup>
	<b>-64, -41, -13</b>	<b>4.04</b>	<b>8.49×10<sup>-5</sup></b>	<b>Frontal.Inf.Tri.R<sup>[1]</sup></b>	<b>50, 16, 25</b>	<b>4.46</b>	<b>2.03×10<sup>-5</sup></b>
	<b>64, -14, -11</b>	<b>4.03</b>	<b>8.91×10<sup>-5</sup></b>				

Table S2.1. Bolded letters indicate the links with the strongest ( $P < 1 \times 10^{-4}$ ) individual associations with skill learning ability. Map coordinates refer to the center of gravity of the nodes and the standard space defined by the Montreal Neurological Institute, MNI. The corresponding label of the AAL atlas was assigned to each node for orientation. Numbers in square brackets indicate nodes mapping in proximity to: [1] visual motion-sensitive areas V5, [2] dorsal premotor cortex, [3] primary sensory-motor cortex, [4] supplementary motor area, [5] ventral premotor cortex, [6] intraparietal sulcus, [7] dorsolateral prefrontal cortex.

Table S2.2

Network features	Original results		Mean connectivity corrected			Scrubbing
	T values	P_raw	T values	P_raw	T values	P_raw
Smallworldness	2.73	0.008	2.74	0.008	3.13	0.003
Global efficiency	2.90	0.005	2.92	0.005	3.28	0.002
Path length	-3.33	0.002	-3.20	0.002	-1.82	0.074
Modularity Q	1.55	0.126	1.29	0.203	2.32	0.024

STUDY 1: RESTING-STATE BRAIN NETWORK FEATURES ASSOCIATED WITH SHORT-TERM SKILL LEARNING ABILITY IN HUMANS AND THE INFLUENCE OF N-METHYL-D-ASPARTATE RECEPTOR ANTAGONISM

Assortativity	-1.82	0.075	1.89	0.064	-2.21	0.031
Transitivity	-2.92	0.005	-2.84	0.006	-3.13	0.003
Mean connection	-0.84	0.406	/	/	-0.73	0.443

Table S2.2. List of T values and P values on the association between motor learning ability and graph properties for original results, mean correlation corrected results and scrubbing results.

Figure S2.1

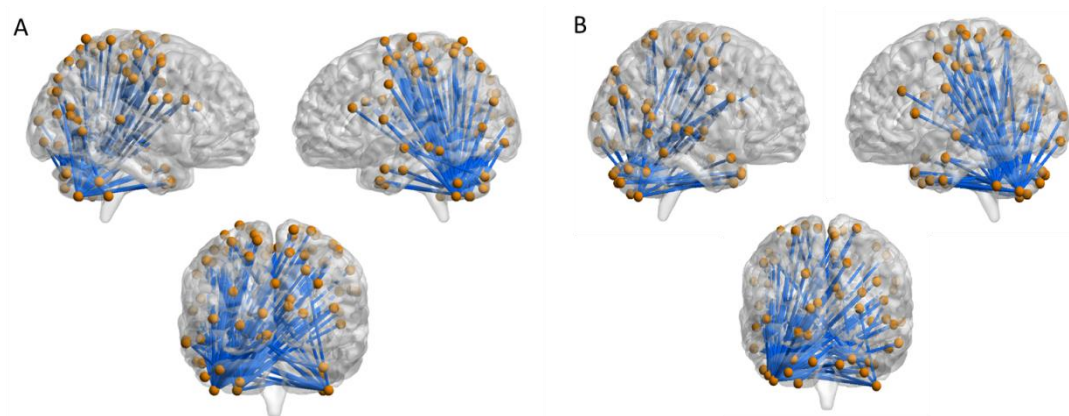


Figure S2.1. Panel A: Learning related cerebellum – cortical network identified based on AAL parcellation. In summary, 91 links were significantly correlated with skill learning (FWE  $p = 0.037$ ) Panel B: Replication of cerebellum – cortical network using functional parcellation. In summary, 69 links were significantly correlated with skill learning (FWE  $p = 0.044$ ). Displayed nodes represent the coordinates of the center of gravity of the sub-regions.

### **3 STUDY 2<sup>2</sup>: MULTI-IMAGING MODALITY IDENTIFIES DYNAMIC GLUTAMATERGIC DEPENDENT NEURAL PLASTICITY IN HUMAN BRAIN DURING LONG-TERM MOTOR LEARNING**

#### **3.1 Abstract**

The process of motor learning is accompanied by neural plasticity in a variety of brain areas. However, most of the motor learning studies applied univariate imaging modality to a limited amount of imaging time points (e.g. pre v.s. post-training), making it difficult to reveal the dynamic process of neural alterations during motor learning and the underlying biological mechanisms in the human brain. Therefore, we used multi-imaging modality including functional and structural magnetic resonance imaging (MRI) as well as magnetic resonance spectroscopy (MRS) to acquire brain multi-imaging data on five-time points along 11 days of sequential motor adaptation training. We obtained a training-induced behavioral improvement, increased activation in frontal-parietal areas as well as increased gray matter volume in the left supplementary motor area (SMA) and the right hippocampus. In addition, we found decreased functional connectivity of a learning rate associated sensorimotor centered subnetwork that covered not only our findings in the functional activity and structural morphological analyses, but also basal ganglia, thalamus, anterior cingulate cortex and temporal regions. The functional connectivity reduction of the sensorimotor centered network was significantly correlated with the glutamate level in the hand knob, suggesting a glutamatergic dependent neural plasticity during motor learning. We believe these results could help demonstrate the importance of multi-imaging modality in revealing neural plasticity in future studies.

#### **3.2 Introduction**

The process of motor learning could be roughly divided into two phases: a short-term learning phase during which novel motor skill is learned within hours or few days and a long-term learning phase where the performance reaches an asymptotic level after months even years of practice (Dayan & Cohen, 2011; Hikosaka et al., 2002; Penhune & Steele, 2012; Ungerleider, Doyon, & Karni, 2002). When the behavioral improvement

---

<sup>2</sup> Presubmission: Zang et al., Multi-Imaging Modality identifies dynamic glutamatergic dependent neural plasticity in human brain during long-term motor learning



achieves a certain level during the learning, a variety category of neural plasticity subserving motor learning was also established in the central nervous system.

From the functional activity perspective, the sensorimotor – cerebellar network is involved more during very early learning phase (e.g., within few hours) where detection of motor mistakes, updating of sensory-motor information and fast adjustment of motor parameters will take place (Penhune & Steele, 2012; Ramnani, 2006; Sami et al., 2014). When learning enters relatively long-term learning phase (e.g. several days to few weeks), functional alterations were obtained in different forms such as increased activation in the primary motor cortex (Floyer-Lea & Matthews, 2005), shifted activation from supplementary motor area (SMA) to basal ganglia (Lehericy et al., 2005) and training-induced autonomy in the visuomotor network (Bassett et al., 2015). Compared with the functional re-organizations, structural changes in the human brain were always observed after a much longer period of training duration. For example, a 3-month juggling training could significantly induce an increase of gray matter volume in the visual area (Draganski et al., 2004). Similarly, Bezzola and colleagues showed increased gray matter volume in the primary motor area and parietal regions after subjects received months of golf training (Bezzola et al., 2011). In addition to the frequently reported visual-sensorimotor areas, cerebellum as well as basal ganglia which directly participate in the majority types of motor learning (i.e. direct / indirect pathway), other areas such as the dorsal lateral prefrontal cortex (DLPFC) (Bassett et al., 2015; Zang et al., 2018) as well as the hippocampus (Albouy et al., 2008; Schendan et al., 2003) were also found in association with motor learning. Specifically, the hippocampus is one of the most interesting brain regions for its critical role in other aspects of learning, such as spatial navigation (Maguire et al., 2000) and episodic memory consolidation (Eichenbaum, 2001; Fernandez et al., 1999). In a study by Albouy and colleagues (Albouy et al., 2008) where they found the activation of the hippocampus in association with basal ganglia was increased over-night (24 hours) in a visual-sequential task and the authors proposed their observations as a motor memory consolidation effect. However, to what extent the hippocampus may involve in the longer term of motor learning remains unclear.

A plausible candidate molecular mechanism that contributes to the re-organization of the brain during motor learning is glutamatergic dependent plasticity (Hasan et al., 2013). Several observations are noteworthy in animal studies that motor training can change the glutamatergic N-methyl-D-aspartate (NMDA) receptor subunit composition

in BG (Kent et al., 2013) and promote the NMDA dependent synaptic plasticity in the primary motor cortex of rats (Kida et al., 2016). Our recent study illustrated an NMDA receptor antagonism influenced short-term (30 minutes) learning related cerebellar – cortical functional network in healthy humans (Zang et al., 2018). It is also worth investigating how glutamate may influence human brain functional as well as structural re-organizations in the longer motor learning process in a more straightforward way. Notably, while most of the motor learning studies used univariate-imaging modality and limited imaging measurements (e.g. two time points) to assess the learning-induced neural plasticity, a study applied multi-imaging modality approach to reveal the dynamic process of learning-induced plasticity in left Brodmann area 44 (Shannon et al., 2016). This study is noteworthy due to the additional implementation of PET measurement that revealed a neuro-biological mechanism (i.e. aerobic glycolysis) to the observed functional changes. Thus, we considered that the combination of more imaging measurements with multi-imaging modality could comprehensively reveal the neural plasticity during motor learning. In the current study, we used a well-established visual guided sequential pinch force (Reis et al., 2009) paradigm to train healthy right-handed participants for 11 consecutive days. The pinch force paradigm challenged not only the ability of motor adaptation that participants learned to adapt their pinch force according to the requests, but also how well participants can remember the given pinching sequence during the task (Reis et al., 2009). Five multi-imaging modality MRI scans including functional and structural MRI as well as magnetic resonance spectroscopy (MRS) (Hoerst et al., 2010) were carried out during the training to study the potential function as well as the structural change of brain throughout 11 days of training. To further investigate the effect of the absence of training, the follow-up MRI scans were carried out 3 months later after the 5<sup>th</sup> scans. We hypothesized that 11 days of motor sequential training would induce brain functional as well as morphological changes in the brain. We in addition aimed to provide further neuro-biological evidence to our targeted observations of neural plasticity and hypothesized that the glutamatergic concentration level may be associated with brain alterations.

### **3.3 Materials and Method**

### **3.3.1 Motor learning task description**

#### ***SVIPT***

Subjects from the training group received a daily single training session outside the scanner from day 1 until day 11. The duration of a single training session was approximately 25 minutes. During the SVIPT training, subjects were holding a force transducer between their right thumb and index finger to modulate their pinch force according to the highlighted 'Gate target' (Figure 3.1). After achieving the highlighted 'Gate target', subjects released their pinch force to allow the cursor return to its 'home position'. The distance of the cursor to the 'home position' increased logarithmically with increasing pinch force in order to make the task more difficult. Subjects were instructed to modulate their pinch force so that the cursor navigated as quickly and accurately as possible along the following sequence: home-G2-home-G5-home-G3-home-G1-home-G4. On each day, subjects performed five training blocks consisting of 35 trials (completed sequences). Movement times per trial were measured from movement onset in the home position to stopping at the last gate (G4).

#### ***SVIPT in fMRI***

Both groups performed the SVIPT during fMRI scans on day 0, day 1, day 4, day 8 and day 11. During the SVIPT, 80 trials were equally and randomly assigned into four conditions, namely, the training condition, the novel condition, the movement-control condition and baseline condition. Each trial's duration was determined by the pace of the participant and may distribute from around 4 seconds up to more than 10 seconds. In the training condition, the order of the 'Gates' was identical to the sequence of the daily training sessions (2-5-3-1-4). In the novel condition, the order of the 'Gates' was randomly generated. In the movement-control condition, subjects were asked to pinch the cursor into 'Gates-3' for 5 times. In the baseline condition, subjects were instructed to only look at the screen without pinching. We considered that the alteration of novel v.s. training contrast could represent the neural plasticity of the motor novelty and automatization process and hence selected it as 'the contrast of interest'.

#### ***MRI data acquisition***

We acquired functional MRI data, high-resolution MP-RAGE structural MRI data as well as MRS. The details of data acquisition are provided in the supplement information (SI).

### 3.3.2 Data analysis

#### ***Estimation of learning rate***

We used a single exponential function to estimate the learning rate of the behavioral training data in the training group (M. Kodama et al., 2018). In detail, the average movement time (MT) in training sessions were modeled using the function  $y = Ae^{\tau t}$ , where  $t$  is the time scale coding day 1 until day 11 ( $t = 1, 2, 3, \dots, 11$ ). Output parameter  $\tau$  represents the exponential drop-off learning rate: more negative  $\tau$  value indicates faster learning process. We used the matlab function 'fit.m' to fit the exponential function with option 'Robust'. One subject was exclude as outlier ( $> 2$  standard deviations).

#### ***Structural data preprocessing and group-level analysis***

Automated image processing was performed using standard procedures implemented in the voxel-based morphometry toolbox (cat12) in SPM12 (<http://www.fil.ion.ucl.ac.uk/spm>). Data preprocessing included tissue classification, correction for image intensity non-uniformity, data denoising, multiplication with the Jacobian determinants of the deformation field to transform gray matter density values into volume equivalents, correction for individual total gray matter volume, normalization to MNI space, and smoothing with an 8 mm full-width-at-half-maximum isotropic Gaussian kernel (Ashburner & Friston, 2000).

For second-level analysis, a group by time interaction effect was tested using the flexible factorial design with a contrast definition that tested for a linear interaction effect in gray matter volume across time. In detail, two regressors were generated for each group separately and were coded for a [-2 -1 0 1 2] weight for each subject's preprocessed structural images on day 0, day 1, day 4, day 8 and day 11. Next, a contrast [1 -1] (training group > control group) was built to represent the positive group by time linear interaction of the five MRI scans (training group v.s. control group by day 0 to day 11). In addition, a pair t-test model was built to estimate the structural change between the last day (day11) and the follow-up measurement. Significance was defined at a threshold of pFWE < 0.05 within predefined regions of interest (ROI, bilateral hippocampus and SMA) derived from the Harvard-Oxford atlas distributed in FSL (S. M. Smith et al., 2004).

### ***fMRI data preprocessing and group-level analysis***

Functional image processing was performed using standard routines implemented in the Statistical Parametric Mapping software (SPM8, <http://www.fil.ion.ucl.ac.uk/spm/software/spm8/>). All images were realigned to the first image of the time series, corrected for slice timing, spatially normalized to the Montreal Neurological Institute (MNI) EPI template, and spatially smoothed with an 8 mm full-width at half-maximum (FWHM) Gaussian kernel.

Both the ‘training condition’ and the ‘novel condition’ consisted of 20 mini blocks. Six head motion parameters from the realignment step were included as nuisance covariates into the model. During model estimation, the data were high-pass filtered with a cutoff of 128 s and an autoregressive model of the first order was applied. The first level contrast images were constructed using the difference between the beta images of the two conditions from a block design general linear model in SPM. Then, the contrast images were selected for the same flexible factorial model described in the structural image analysis section to test for the linear interaction effect between the two groups. A pair t-test model was built to estimate the structural change between the last day (day11) and the follow-up measurement as well. Significance was defined at a threshold of  $p_{FWE} < 0.05$  within a predefined functional activation mask (Figure S3.3) identified from an independent sample (SI) for the same contrast (novel > trained). The group-level interaction model was built to detect the linear group by time interaction effect of the contrast of interest. The paired t-test was also applied to estimate the functional activation change between the last day (day11) and the follow-up measurement.

### ***Correlation matrix construction and network analysis***

For each participant, we extracted the mean time series from a 270 functional sphere ROIs (5 mm) which was based on the Power functional atlas (Power et al., 2011) (Cao et al., 2014). From the node time series, we regressed out the time series of white matter and cerebrospinal fluid masks (derived from SPM tissue probability maps thresholded at 90% for CSF and 99% for WM) ((Cao et al., 2014)) and the six head motion parameters from the realignment step. The resulting residual time series were temporally filtered using a 0.008 Hz high-pass filter. Finally, a 270×270 correlation

matrix was constructed with each element represents the Pearson correlation coefficient.

We analyzed the connectivity matrices with NBS (Zalesky, Fornito, & Bullmore, 2010) to identify clusters connections that showed significant group by time linear interaction effect. Following prior procedures (Wang et al., 2013)), we defined initial linear regression models for each of the  $(N(N-1))/2 = 36315$  ( $N = 270$ ) possible links in the connectivity matrices. The group-level model was built with individual contrast weights  $[-2 \ -1 \ 0 \ 1 \ 2]$  representing the five-time points for the training group and  $[2 \ 1 \ 0 \ -1 \ -2]$  representing the five-time points for the control group in one regressor. Next, a group-level t contrast 1 and -1 was used to estimate the linear interaction effect because previous studies have shown altered functional connectivity during motor learning (Sami et al., 2014; Sampaio-Baptista et al., 2014). From the resulting p matrix, we defined a set of suprathreshold connections by isolating all links with  $t > 3.8$  and  $p < 1 \times 10^{-4}$  and used  $M = 5000$  permutations (Wang et al., 2013) to estimate the null distribution during permutation testing of the identified cluster association.

### **Diffusion Tensor Imaging (DTI)**

DTI data preprocessing was performed with standard routines implemented in the software package FSL(S. M. Smith et al., 2004) including the following steps: correction of the diffusion images for head motion and eddy currents by affine registration to a reference (b0) image, extraction of non-brain tissues and linear diffusion tensor fitting. After the estimation of the diffusion tensor, we performed deterministic whole-brain fiber tracking as implemented in DSI Studio using a modified FACT algorithm (S. M. Smith et al., 2004). For the construction of structural connectivity matrices, we initiated 1,000,000 streamlines for each participant. Streamlines with a length of less than 10 mm were removed. The average fractional anisotropy (FA) of successful streamlines between each pair of nodes defined by the AAL atlas was then used as an estimate of structural connectivity, resulting in a 116 x 116 connectivity matrix for each subject.

### ***MRS data preprocessing and analysis***

We then analyzed the MRS data using LCModel (Provencher, 1993) and GAMMA-simulated basis-sets (Soher, Young, Bernstein, Aygula, & Maudsley, 2007), and

referenced the glutamate metabolite values to the water signal at TE = 30 mms. For later covariation, we quantified the gray matter content of individual MRS voxels relative to white matter and cerebrospinal fluid after segmentation of the T1-weighted structural images and correction for the chemical shift displacement of voxel locations. To test for association between pre-scan SVIPT learning and cortical glutamate, we defined a multiple regression model in SPSS25 with hand knob glutamate concentration as dependent variable.

### ***Correlation analyses***

We performed linear correlation analyses to investigate the association between learning rate ( $\tau$ ) and imaging phenotypes using Pearson correlation coefficient as well as the glutamate concentration level. Correlations with  $p < 0.05$  were considered as significant results.

## **3.4 Results**

### **3.4.1 Subjects and study protocol**

Twenty healthy right-handed subject ( $29.7 \pm 8.5$  years, 8 males) were assigned into the training group and went through 11 consecutive days of SVIPT training and 19 age and sex matched ( $27.87 \pm 8.4$  years, 9 males,  $p$  values  $> 0.48$ ) healthy right-handed subjects were assigned into the control group. All participants provided written informed consent for a protocol approved by the Ethics Committee of the University of Heidelberg. Exclusion criteria included MRI contraindications, a history of psychiatric and neurological illness, prior head trauma, and current alcohol or drug abuse. None of the subjects had a first-degree relative with a psychiatric disorder or received psychopharmacological treatment.

Subjects from the training group received daily trainings from day 1 to day 11 outside of the scanner for approximately 30 minutes. We then acquired functional as well as high-resolution anatomical images of the participants' brain using a 3 Tesla MRI scanner (Siemens Trio, Erlangen, Germany) on day 0 (baseline), day 1, day 4, day 8 and day 11 for both the training and control group. In detail, we firstly acquired a 5-minute resting state scan, followed by a self-paced sequential visual isometric pinch force task (SVIPT) task. Next, a 6-minute structural T1 image, followed by a MRS scan

was taken to measure the glutamate level in the hand knob. *In addition, the same imaging protocol was applied in the 3 months follow-up session (day 90+).* The illustration of the study design is provided in Figure 3.1A. The details of MRI acquisition parameters are provided in the supplemental information (SI). All subjects completed the entire session except for one subject from the training group dropped out for the follow-up measurement due to injury.

**Figure 3.1**

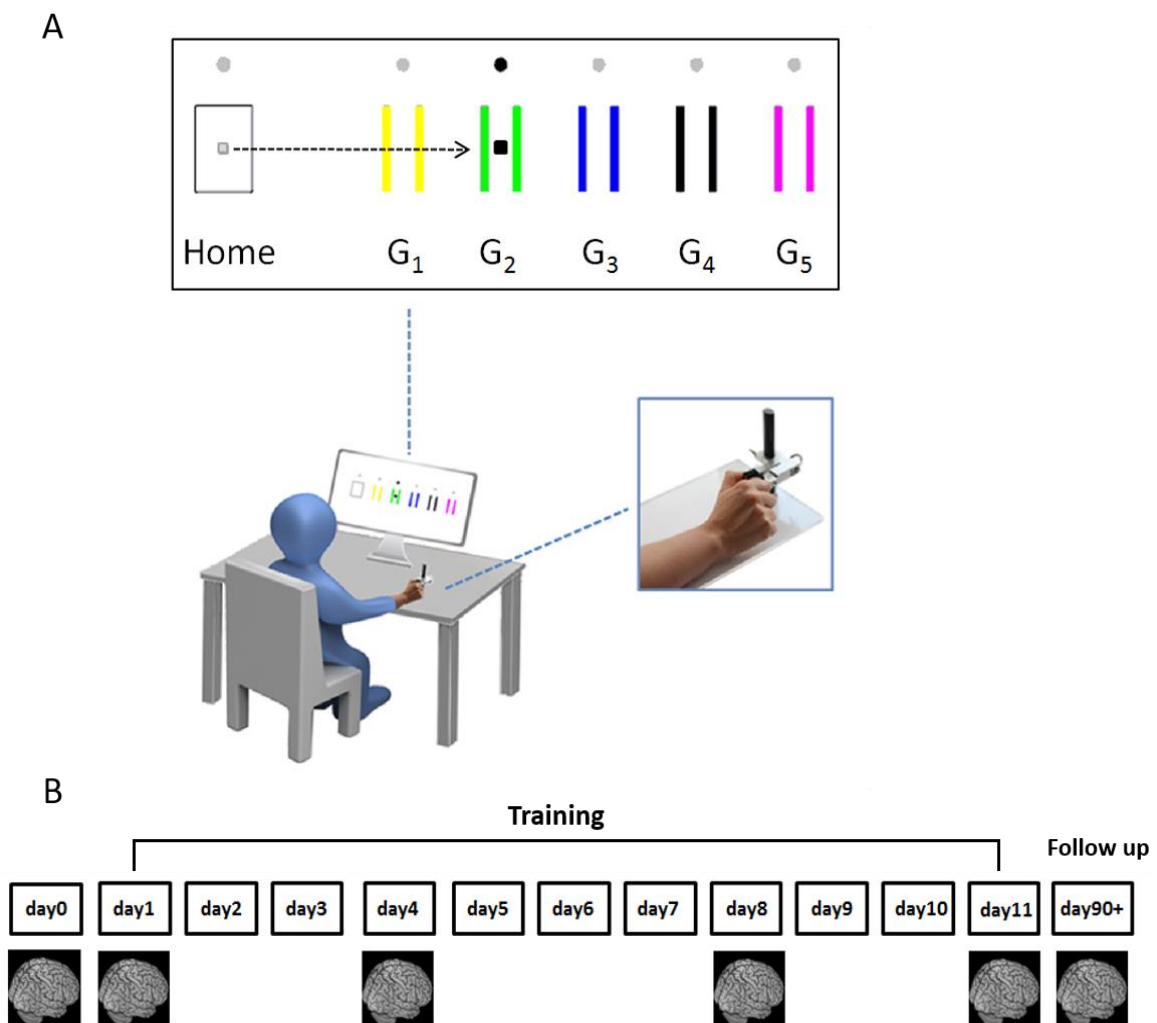


Figure shows the longitudinal study protocol of motor learning task. Panel A shows the motor learning task that has been utilized. Panel B shows the longitudinal design of the study. Subjects received baseline (day0) measurement. The daily training was carried out from day 1 to day 11. Brain imaging data were acquired on day1, day4, day8, day11. After training was stopped for three months, the a follow-up measurement was carried out for subjects who received daily training.



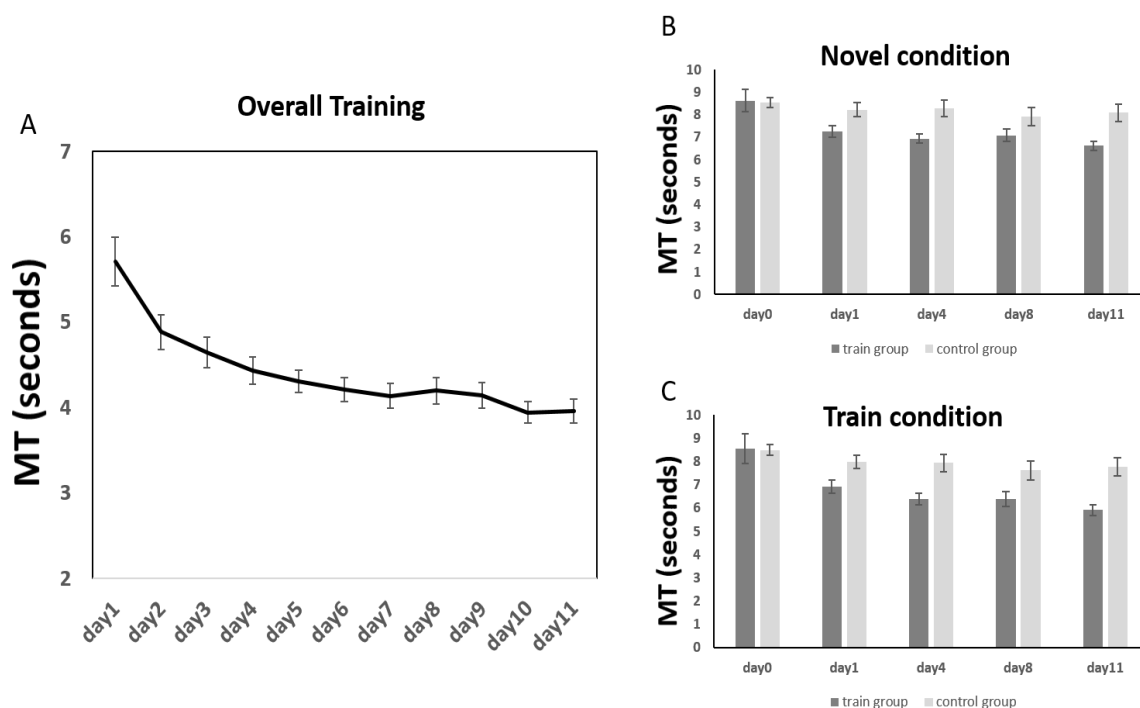
### 3.4.2 Behavioral data

We obtained a significant reduction in movement time (MT) across 11 training days for the training sessions outside the scanner (repeated measures ANOVA:  $F_{(10,190)} = 40.87$ ,  $p < 0.001$ , Figure 3.2A).

For the in-scanner performance, we found significant reduction of MT for both novel condition ( $F_{(4,76)} = 12.91$ ,  $p < 0.001$ ) and training condition ( $F_{(4,76)} = 4.52$ ,  $p < 0.003$ ) in the training group. There was also a significant reduction MT for the training condition ( $F_{(4,72)} = 2.97$ ,  $p < 0.025$ ) in the control group, but no significant effect was found for the novel condition ( $F_{(4,72)} = 1.39$ ,  $p > 0.247$ ). Interestingly, we didn't find any significant changes on MT for neither the novel condition ( $t_{(18)} = 0.81$ ,  $P > 0.93$ ) nor the training condition ( $t_{(18)} = -0.71$ ,  $P > 0.48$ ) between day11 and the follow-up measurement.

In addition, we obtained a significant group by time interaction effect of movement time for novel ( $F_{(4,148)} = 10.86$ ,  $p < 0.001$ , Figure 3.2B) and training ( $F_{(4,148)} = 14.81$ ,  $p < 0.001$ , Figure 3.2C) conditions during fMRI measurement between the two groups. There was no main effect of condition (novel v.s. train) in neither group ( $F_{(1,19)} = 2.20$ ,  $p = 0.16$  for training group;  $F_{(1,18)} = 0.43$ ,  $p = 0.52$  for control group). However, there was a significant time by condition interaction effect in the training group ( $F_{(4,16)} = 3.71$ ,  $p = 0.025$ ) but not in the control group ( $F_{(4,15)} = 2.15$ ,  $p = 0.13$ ).

Figure 3.2



The figure shows the behavioral data from the current motor learning study. Panel A shows the significant reduction of duration during 11 days of training ( $p < 0.001$ ) in the training group. Panel B shows the behavioral group-by-time interaction effect ( $p < 0.001$ ) of the ‘novel condition’ fMRI scan. Panel C shows the behavioral group-by-time interaction effect ( $p < 0.001$ ) of the ‘train condition’ fMRI scan.

### 3.4.3 Brain imaging results

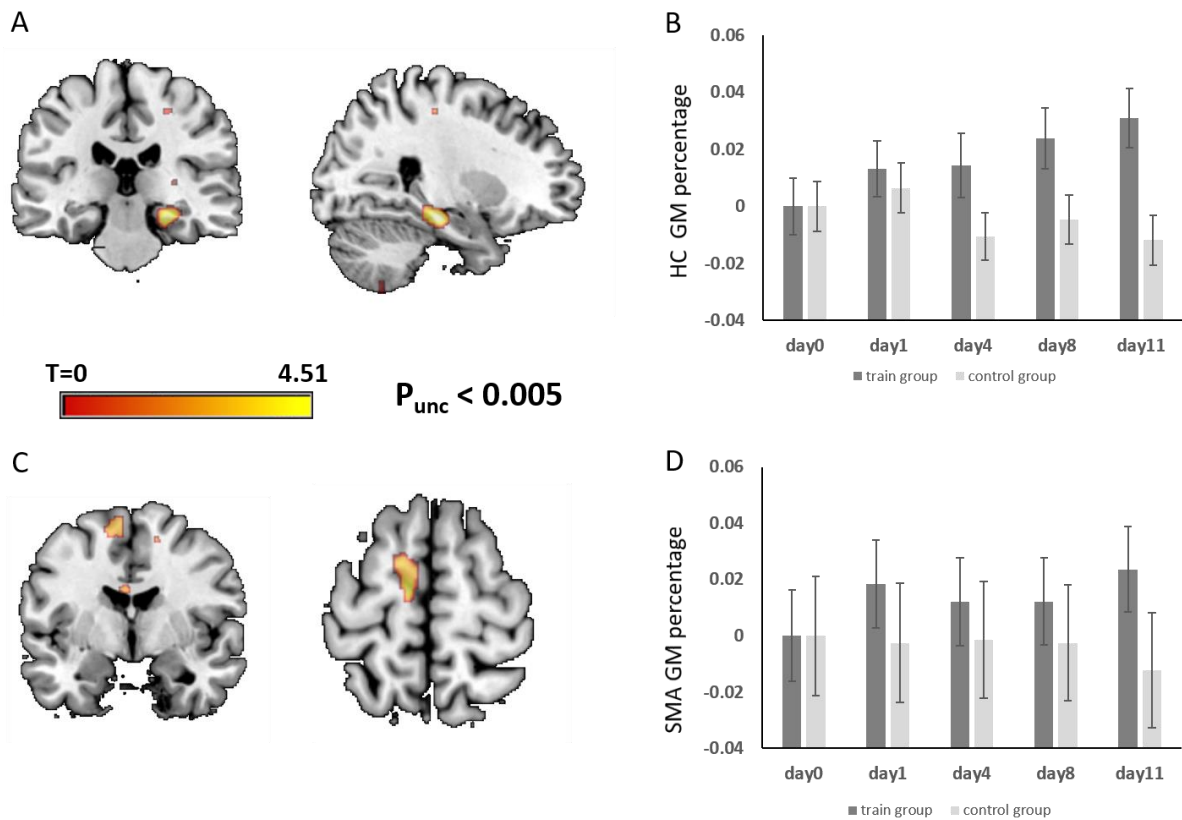
#### ***Structural data***

Being consistent with our hypothesis (following previous accounts of volume increase in hippocampus and SMA), we found a significant linear group by time interaction effect of the gray matter in the right hippocampus ( $t_{(154)} = 4.51$ ,  $P_{SVC} = 0.003$ , peak coordinate = [24 -22 -16], corrected within bilateral hippocampus and SMA mask from the HO atlas Figure 3.3a). The post-hoc analysis **of the peak voxels** further revealed that the gray matter volume of the right hippocampus significantly increased in the training group ( $F_{(4,76)} = 4.52$ ,  $p < 0.003$ ), but not in the control group ( $F_{(4,72)} = 1.9$ ,  $p > 0.12$ ).

In addition, we found a significant interaction effect of gray matter in the left supplementary motor area ( $t_{(154)} = 3.92$ ,  $P_{SVC} = 0.037$ , peak coordinate = [-9 -10 66], Figure 3.3b). The post-hoc analysis further revealed that the gray matter volume of the left supplementary motor area significantly increased in the training group ( $F_{(4,76)} = 5.58$ ,  $p < 0.001$ ), but not in the control group ( $F_{(4,72)} = 1.83$ ,  $p > 0.13$ ). Our structural findings were robust against different choice of preprocessing pipeline (supplemental information SI, Figure S3.1).

Compared with day11, both the hippocampus and SMA showed a decrease of gray matter volume on the follow-up measurement (Figure S3.2).

#### **Figure 3.3**



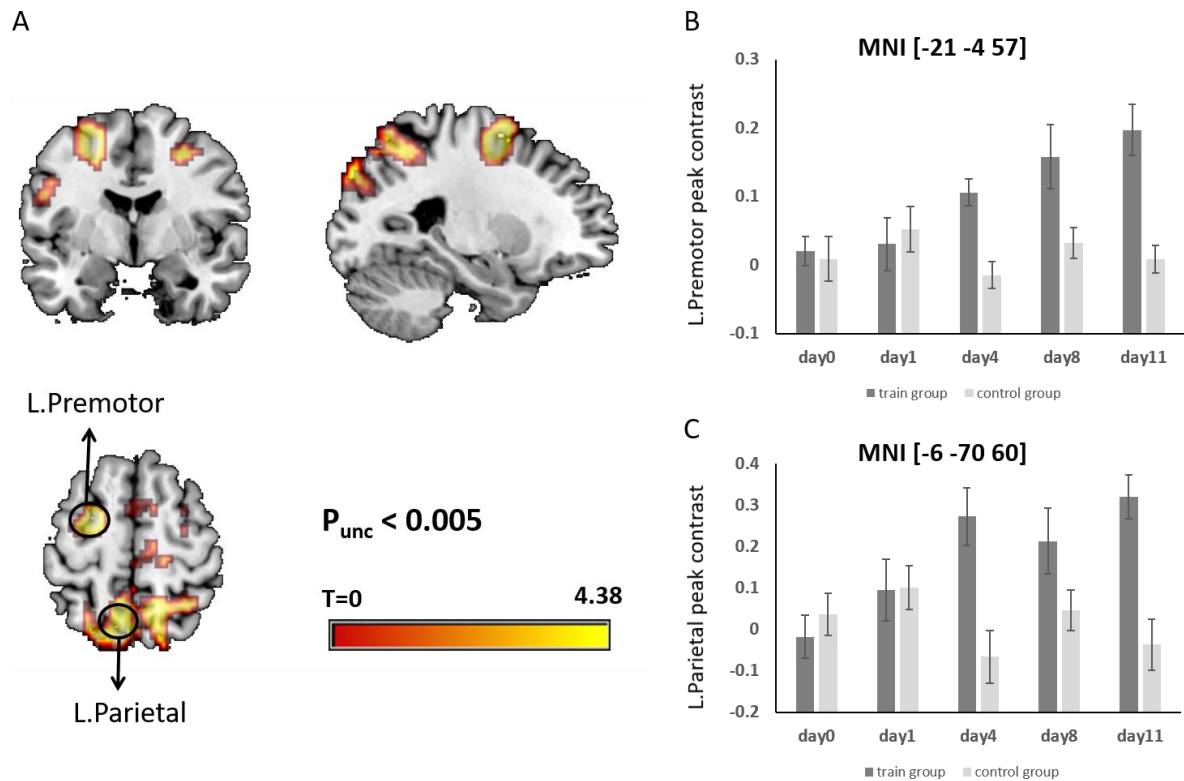
The figure shows the group-by-time interaction of grey matter change during 11 days of training. Panel A&B: Panel A shows the uncorrected  $p < 0.005$  threshold of grey matter volume change in the right hippocampus. Panel B shows the post-hoc percentage of grey matter volume change of the peak voxel (MNI [24 -22 -16]). Panel C&D: Panel C shows the uncorrected  $p < 0.005$  threshold of grey matter volume change in the left SMA. Panel D shows the post-hoc percentage of grey matter volume change of the peak voxel (MNI [-9 -10 66]).

### Activation data

We found significant positive group by time interaction effect in the left premotor cortex ( $t_{(154)} = 4.38$ ,  $P_{SVC} = 0.006$ , peak coordinate = [-21 -4 57], Figure 3.4) and parietal cortex ( $t_{(154)} = 4.11$ ,  $P_{SVC} = 0.047$ , peak coordinate = [-6 -70 60], Figure 3.4) [corrected using an a-priori functional activation map ( $P_{uncorr} < 0.05$ ) from an independent sample with the same contrast (SI, Figure S3.3)]. The post-hoc analyses revealed a significant increase of activation in the left premotor area ( $F_{(4,76)} = 8.41$ ,  $p < 0.001$ ) and left parietal area ( $F_{(4,76)} = 7.02$ ,  $p < 0.001$ ) in the training group but no significant changes in the control group ( $F_{(4,72)} = 1.07$ ,  $p > 0.38$  for premotor area and  $F_{(4,72)} = 1.64$ ,  $p > 0.17$  for parietal area).

As expected, we obtained a decrease of activation when the training was stopped for 3 months (Figure S3.4).

**Figure 3.4**



The figure shows the group-by-time interaction effect on the activation (novel > practice) changes over 11 days of training. Panel A: illustration of  $p < 0.005$  uncorrected threshold of the premotor and parietal areas that showed activation change. Panel B: Post-hoc plots of peak voxel of left premotor area's activation change (MNI [-21 -4 57]). Panel C: Post-hoc plots of peak voxel of left parietal area's activation change (MNI [-6 -70 60]).

### **Network based statistics**

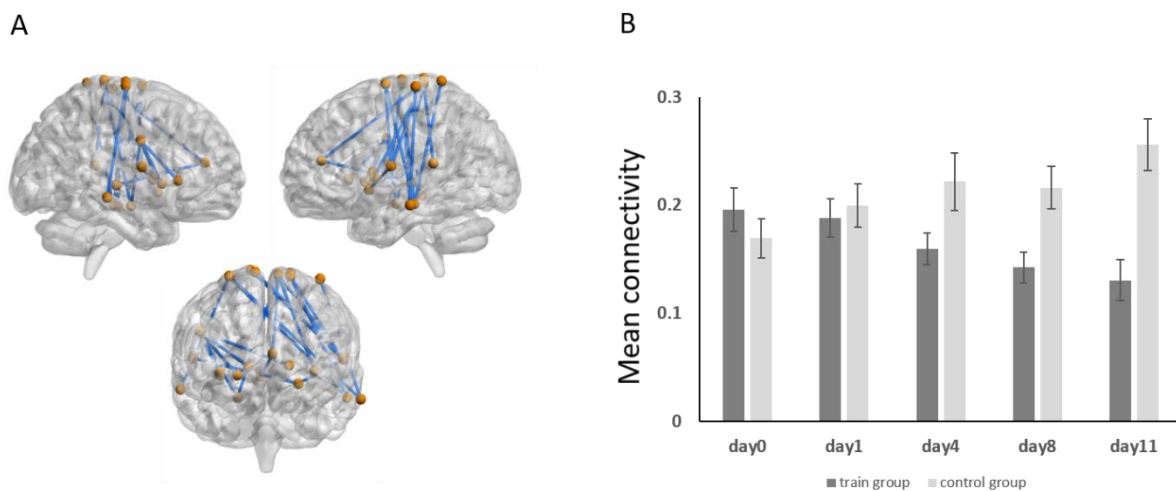
Using Network Based Statistic (Zalesky, Fornito, & Bullmore, 2010) we identified significant group by time interaction effect of the functional connectivity of a sub-network ( $t > 3.8$ , initial  $p < 1 \times 10^{-4}$ , FWE corrected  $p = 0.014$ , Figure 3.5a). The NBS identified sub-network consisting of 23 connections mainly connecting sensorimotor areas to the bilateral basal ganglia, right hippocampus, left anterior cingulate cortex and bilateral temporal areas (Table S3.1), but also spanning to supplementary motor area, parietal area, thalamus and frontal area. Post-hoc analyses revealed a significant decrease of the functional connectivity of the network in the training group ( $F_{(4,76)} = 8.9$ ,  $p < 0.001$ , Figure 3.5b) but a significant increase in the control group ( $F_{(4,72)} = 8.1$ ,  $p < 0.001$ , Figure 5b). *Follow-up measurements showed a marginal significant increase of the identified sensorimotor-centered network when comparing with the last training day (day11) ( $t_{(18)} = 1.84$ ,  $p = 0.083$ ).*

We then extracted the functional connectivity of the NBS identified sub-network from resting state data and found no significant interaction effect ( $F_{(4,148)} = 1.68, p > 0.15$ ), demonstrating that the identified interaction effect is task-specific.

In addition, a significant correlation was obtained between the decreased functional connectivity of the identified sensorimotor-centered network (day 0 v.s. day 11) and the learning rate ( $r = 0.75, p < 0.001$ , Figure 3.6), suggesting that faster learners showed a higher decrease of connectivity.

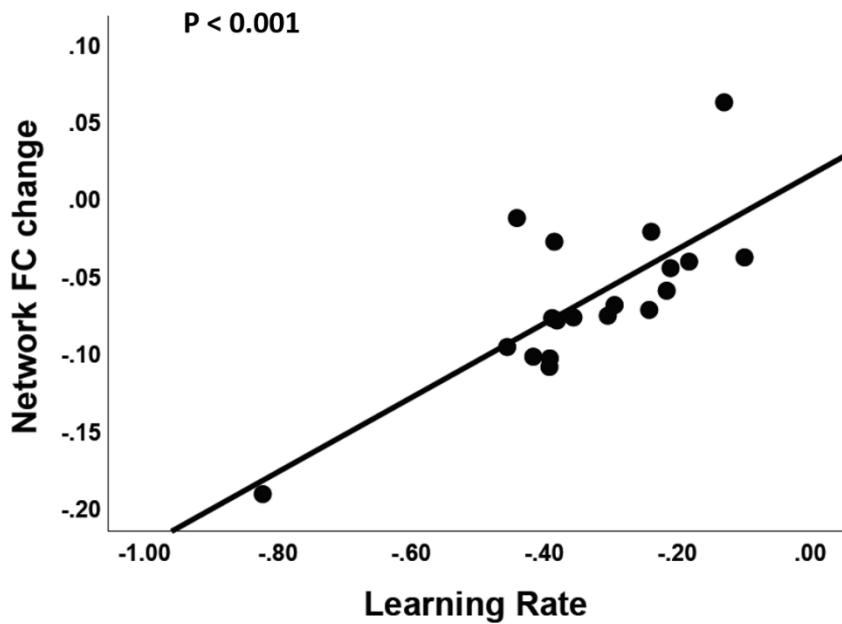
The network was robust against different choice of initial threshold and parcellation (SI, Figure S3.5 & S3.6).

**Figure 3.5**



The figure shows the group-by-time interaction effect of a sensorimotor centered network which extends to the putamen, ACC, hippocampus as well as temporal regions. Panel A shows the spatial distribution of the network ( $p_{FWE} = 0.014$ ). Panel B shows the alteration of the mean connectivity of the identified network in training group and control group during 11 days of training.

**Figure 3.6**



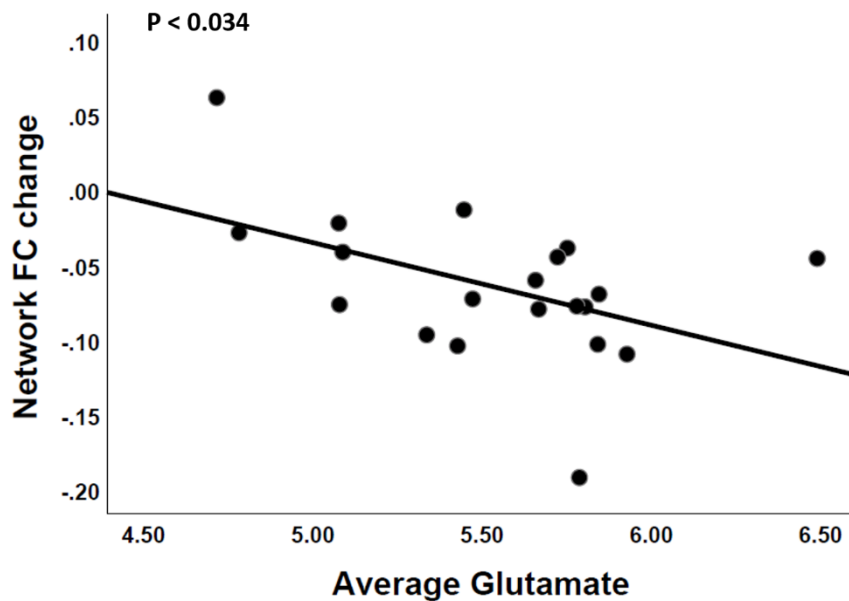
The figure shows the significant positive correlation between the learning rate ( $\tau$ ) and network connectivity change in the training group.

### **MRS**

We did not obtain significant time effect on the glutamate in the training group ( $F_{(4,72)} = 1.67$ ,  $p > 0.17$ ) nor in the control group ( $F_{(4,60)} = 0.8$ ,  $p > 0.53$ ). Neither did we find significant group by time interaction effect on the glutamate concentration level in the hand knob ( $F_{(4,132)} = 1.19$ ,  $p > 0.32$ ).

We found significant correlation between the average glutamate concentration level and the overall functional connectivity change of the sensorimotor-centered network ( $r = -0.48$ ,  $p < 0.034$ , Figure 3.7) in the training group but not in the control group ( $r = 0.13$ ,  $p > 0.61$ ), meaning that more amount of change of the sensorimotor-centered network was associated with higher glutamate level. The correlation is stable over other methodological choice of glutamate level (SI).

**Figure 3.7**



The figure shows the negative correlation ( $p < 0.034$ ) of the average glutamate concentration acquired from the left handknob (average of five MRI measurements) and the alteration of the connectivity of the identified sensorimotor centered network.

### 3.5 Discussion

In the current longitudinal motor learning study, we detected neuroplasticity subserving an 11-day pinch force task. We applied the multi-imaging modality approach with five measurement time points, which allowed us to explore the dynamic process of neuroplasticity during motor learning. As a result, we found significant increased gray matter volume in the right hippocampus and the left SMA in the training group. Functionally, a significant interaction effect was identified in the left frontal-parietal network that showed increased activation in the training group. We further found a significant alteration of the functional connectivity of a sensorimotor centered subnetwork that was associated with the learning rate as well as the glutamate concentration level in the left primary motor cortex. We discuss our findings in more detail in the following paragraphs.

Firstly, we demonstrated a motor learning-induced interaction effect on the gray matter volume in the right hippocampus and the left SMA. The post-hoc analyses revealed a significant increased gray matter volume in the training group but no significant change in the control group, providing evidence that the hippocampus and SMA were involved

in the process of motor sequential learning. The possible underlying cellular mechanisms of the structural alteration might come from the following aspects: 1, gliogenesis (W. K. Dong & Greenough, 2004; Zatorre et al., 2012); 2, vascular changes such as alteration of blood flow (Pereira et al., 2007; Zatorre et al., 2012). Notably, the post-hoc analyses revealed decreased gray matter volume in the hippocampus as well as the SMA on the follow-up measurement when the training was absent for about three months which made the hypothesis of 'neuron growth' unlikely (Zatorre et al., 2012). SMA is a key target region that has been widely reported in a variety of motor studies for its function of planning temporal complex voluntary movements (Gerloff, Corwell, Chen, Hallett, & Cohen, 1997; Weilke et al., 2001). In previous longitudinal motor learning studies, Lehericy and colleagues (Lehericy et al., 2005) obtained an increase activation in pre-SMA and a decreased activation in basal ganglia during a 4-week sequential finger tapping training and proposed the observations as a motor representation shifting. In addition, Sampaio-Baptista and colleagues found that the baseline gray matter volume in SMA could predict long-term motor retention in a 6-week juggling training that challenged the whole body (Sampaio-Baptista et al., 2014). In the current study, we found increased gray matter volume in the left SMA after 11 days of sequential motor adaptation training which provided additional structural evidence of SMA relevance in motor learning. Interestingly, the gray matter volume of the right hippocampus was also increased during the training and the result was very robust against the different choice of structural pre-processing (Thomas et al., 2009). The hippocampus was considered as a key region that contributes critically in spatial navigation (Maguire et al., 2000) as well as in the process of building declarative memory (Eichenbaum, 2001; Fernandez et al., 1999). However, modern functional neuroimaging studies have shown that the activity of the hippocampus was significantly altered during motor sequential learning (Albouy et al., 2008; Schendan et al., 2003) and speculated that it was involved in the process of sleep-dependent motor consolidation process (Albouy et al., 2008). The possible explanations for our observation of increased gray matter volume in the hippocampus may either relate to the effect of motor memory consolidation or visually navigating the motor sequences. Nevertheless, the role of hippocampus during motor learning needs to be further investigated in future studies.

Secondly, in line with the observations from several motor sequential learning studies (Grafton, Hazeltine, & Ivry, 2002; Honda et al., 1998), we identified a significant



increase of activation in the frontal-parietal regions in the training group but not in the control group. The increase of activation observed in the frontal-parietal regions may indicate the recruitment of additional cortical resources along the process of sequential motor learning (Dayan & Cohen, 2011; Poldrack, 2000) such as cerebral blood flow (Xiong et al., 2009). The role of the premotor area in the motor aspects was considered as a processor of higher-order movement (Chouinard & Paus, 2006). Specifically in the current study, we obtained increased activation anterior to the hand knob area, a premotor sub-parcellation that was thought to be involved in linking arbitrary sensory with movements (Brasted & Wise, 2004) or modulated by eye movements (Bruce, Goldberg, Bushnell, & Stanton, 1985). In addition, we observed increased activation in the parietal regions, an area that participated in motor imagery learning (Zhang et al., 2012) and played a critical role as a key element for planning the upcoming movements' kinetic parameters (Kuang et al., 2016). Together, we speculate that the altered functional activity of the identified frontal-parietal regions may indicate increased recruitment of more cortical units supporting the optimization of a set of complex spatial sequential motor parameters and visual-motor information integration during the learning process.

Thirdly, again consistent with prior motor learning studies (J. Doyon & Benali, 2005; Zang et al., 2018), we found significant interaction effect of the functional connectivity of a sensorimotor centered subnetwork between the two groups. The functional connectivity of the sensorimotor-centered subnetwork decreased over time in the training group but increased in the control group. The interaction effect of the functional connectivity of the subnetwork was absent in the post-hoc analysis using resting-state data, demonstrating that the obtained effect was task-specific. The amount of the functional connectivity decrease of the subnetwork was significantly correlated with the learning rate, suggesting that faster learners had stronger functional connectivity plasticity. The subnetwork consisted of not only the connections linking the sensorimotor area to the regions identified in both the structural morphological (i.e. hippocampus and SMA) and functional activity (i.e. frontal-parietal regions) analyses, but also to the thalamus, basal ganglia, anterior cingulate cortex (ACC) as well as temporal regions. A plausible explanation for the overall decreased functional connectivity was the effect of training-induced autonomy (Bassett et al., 2015). In the current study, the pinch force task challenged mainly two aspects of motor learning namely sequential learning and motor adaptation (Reis et al., 2009). Therefore, during

early learning participants were required to adapt their pinch force to different sequences and such behavior required the cooperation of multi-brain areas. During training, participants could gradually master the task and consequently the abundant connection resources were no further needed (Bassett et al., 2015). Specifically, the decrease of the functional connectivity between the hippocampus and sensorimotor cortex further strengthened our morphological observations that the hippocampus acts like a motor memory processor and could help consolidate newly learned sensorimotor memory (Albouy et al., 2008). In addition, the involvement of ACC in the thalamus-ACC-sensorimotor loop may relate to error-monitoring (Lutcke & Frahm, 2008; Seifert, von Cramon, Imperati, Tittgemeyer, & Ullsperger, 2011) which requires a high level of cognitive attention demands. Therefore, decreased functional connectivity among the thalamus-ACC-sensorimotor network may suggest a progressive decrease of attention demand during the task due to training. However, subjects from the control group maintained higher attention demands due to lack of training, which probably drove the arousing of functional connectivity during the task.

Notably, we also detected a significant negative correlation between the amount of functional connectivity decrease of the sensorimotor network and the average glutamate concentration of the hand knob. Participants with higher motor glutamatergic concentration levels were showing a bigger reduction of the sensorimotor centered subnetwork connectivity. This observation provided a plausible biological mechanism of a glutamatergic modulated sensorimotor neural plasticity during motor training. Our speculation was in line with the observation from our previous system-level neuropharmacological studies (Zang et al., 2018) where we showed that ketamine as an NMDA antagonism blocked the functional connectivity of a cerebellar-cortical network after short-term motor learning. Supportive evidence was also provided by animal studies showing that training could promote presynaptic glutamate release (Kida & Mitsushima, 2018; Kida et al., 2016) while motor performance was significantly impaired in mGluR4 gene knock out mice (Pekhletski et al., 1996). Taking together, we interpret our findings as a glutamatergic modulation of motor memory consolidation process (Volianskis et al., 2015).

In conclusion, we demonstrated that an 11-day of motor sequential learning could lead to neural plasticity that identified from multi-neuroimaging modalities. The functional activity of the frontal-parietal cortex was increased during the learning process while the morphological change was obtained in the right hippocampus and the left SMA.

Furthermore, we found decreased functional connectivity of glutamate modulated sensorimotor centered subnetwork that covered areas identified in our functional activation and structural morphology analyses. We posit that the observed changes from multi-imaging modalities may reflect more dynamic neuroplasticity during the motor learning process. Such a study design may help better understand motor learning-induced neuroplasticity in the future.

## 3.6 Supplements

### 3.6.1 Data acquisition parameters

#### ***Structural MRI***

We acquired high-resolution T1-weighted 3-dimensional images with a magnetization-prepared rapid gradient echo sequence (3D-MPRAGE) and the following parameters: TR = 2530 ms, TE = 3.8 ms, TI = 1100 ms, 176 slices, 256 x 256 mm field of view, 7° flip angle, and 1 mm<sup>3</sup> spatial resolution.

#### ***Functional MRI***

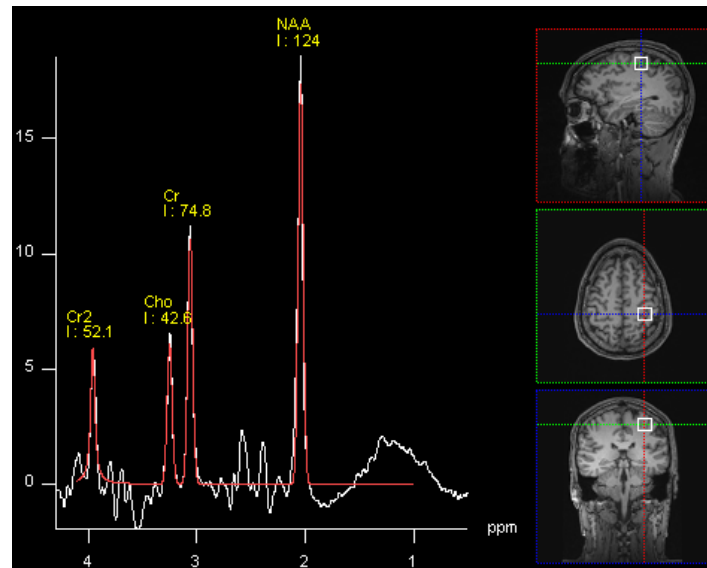
Functional MRI including SVIPT and resting-state fMRI were acquired using an echo-planar imaging (EPI) sequence with the following parameters: TR = 1790 ms, TE = 28 ms, 34 axial slices per volume, voxel size = 3 x 3 x 3 mm, 1 mm slice gap, 192 x 192 mm field of view, and 76° flip angle, descending acquisition. For the SVIPT fMRI, participants were asked to perform the task as quickly and as accurately as possible, resulting in a self-paced task duration. For the resting-state experiment, we instructed participants to open their eyes and fixate on a cross. The resting-state duration was 5 minutes including 167 whole-brain scans.

#### ***Glutamate MRS***

Neuroimaging was performed 6 minutes after completion of the SVIPT training (Structural scan in between) on a 3T MRI scanner (Siemens Trio, Erlangen, Germany) equipped with a 32 channel multi-array head-coil. In vivo proton MRS data were acquired in a 18 mm<sup>3</sup> voxel centered on the contralateral (i.e., left hemisphere) “hand knob”, an omega-shaped anatomical landmark within the precentral gyrus (Figure S3.9) that allows for a reliable identification of the primary motor representation of the trained hand (Yousry et al., 1997). For voxel positioning and tissue segmentation, we acquired T1-weighted 3-dimensional images with a magnetization-prepared rapid gradient echo sequence (spatial resolution: 1 mm<sup>3</sup>). Spectra acquisition and analysis followed previously published procedures (Hoerst et al., 2010). Briefly, this included point-resolved spectroscopy at TE = 80 ms (for optimal separation of glutamate from glutamine) with a transmitter frequency set to the chemical shift value of the gamma methylenecyclopropene protons of the glutamate signal (−2.3 ppm relative to the water

resonance), the acquisition of six fully relaxed and unsuppressed water spectra (TEs 30, 80, 200, 500, 800, and 1100 ms), and eddy current correction.

**Figure S3.1**



The figure shows the MRS data acquisition of one of our subjects in the 'hand knob' area.

### 3.6.2 S-Results

#### *Influence of different choice of co-register image*

The choice of co-register image during the preprocessing of longitudinal structural data may have an influence on the result (Thomas et al., 2009). Thus, we used the averaged raw structural image for co-registration in addition to the baseline image. Other preprocessing parameters as well as group-level modelling were kept identical to our main analysis. Result showed that the interaction effect could be replicated in the right hippocampus ( $P_{\text{svc}} = 0.034$ , [27 -24 -14], Figure S3.2). However, the effect was not significant anymore in the left SMA ( $P_{\text{svc}} = 0.143$ ). Thus, the observations demonstrated that the effect of learning induced structural change in the right hippocampus was very robust against different choice of co-register image during preprocessing.

**Figure S3.2**

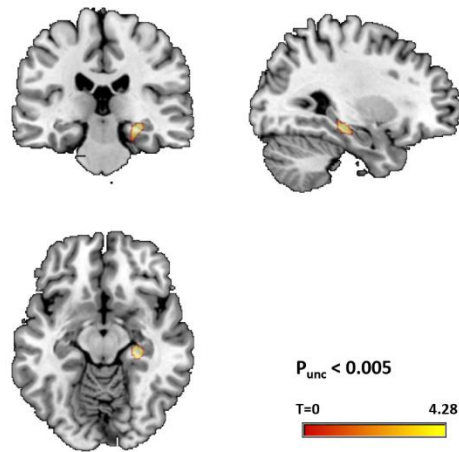


Figure shows the replication of the hippocampus gray matter volume increase using the average raw structural images as co-register template.

### ***Follow-up pair t-test for structural images***

We found significant decrease of gray matter volume in the right hippocampus and left SMA after the training was stopped for 3 months using the pair t-test model in SPM (Figure S3.3).

**Figure S3.3**

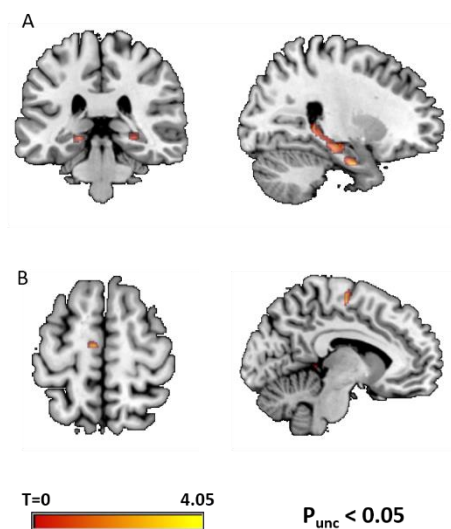


Figure shows a decreased gray matter volume after the training was stopped for 3 months in the training group. Panel A shows the  $p < 0.05$  uncorrected threshold brain map of the hippocampus. Panel B shows the  $p < 0.05$  uncorrected threshold brain map of the SMA.

### **Functional task specific mask identification**

To create a functional activation specific mask for novel > trained contrast, we used 40 healthy right handed subjects (20 males,  $28.13 \pm 8.37$  years old) from an independent sample. The experiment design was similar to the design of our longitudinal study day 1 until day 11. In detail, subjects received training session before they performed the task during SVIPT fMRI session. The data preprocessing and first-level modeling was also identical to the longitudinal study. The functional activation specific mask was identified using a  $P < 0.05$  uncorrected threshold in order to maintain as much as task relevant brain areas as possible (Figure S3.4).

**Figure S3.4**

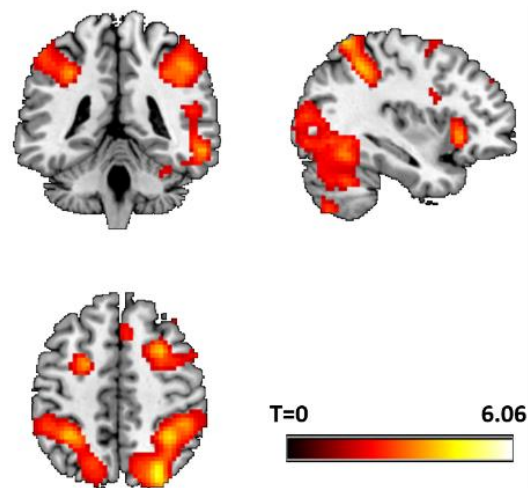


Figure shows the binary functional activation mask defined by a  $P < 0.05$  uncorrected threshold using novel > trained contrast on an independent sample ( $n = 40$ ).

Region	Cluster	T	MNI
R.Precentral	2743	6.06	45 8 30
R.Fontal.Mid		4.4	27 11 54
R.Pallidum		4.28	21 -1 3
R.Occipital.Mid	2649	5.24	33 -70 30
R.Occipital.Sup		5.04	30 -76 42
R.Temporal.Inf		4.9	57 -55 -15
L.Parietal.Inf	2506	4.15	-33 -46 45
L.Parietal.Sup		4.05	-36 -58 63
L.Cerebellum		3.91	-24 -67 -30
L.Frontal.Sup	236	4.06	-21 2 51
L.Frontal.Mid		3.34	-30 5 63
L.Precentral	67	3.3	-42 2 30
L.Frontal.Oper		2.11	-33 5 24
R.Cerebellum	68	3.08	21 -73 -48
L.Frontal.Tri	52	3.08	-48 38 27

R.Frontal.Medial	55	3.06	6 26 45
R.Frontal.Orb	60	2.55	18 32 -18
R.Frontal.Orb		2.48	24 47 -15
R.Frontal.Orb		2.46	39 53 -12
R.Cerebellum	12	2.01	33 -40 -27
R.Cerebellum	11	1.95	33 -58 -30

Figure shows the binary functional activation mask defined by a  $P < 0.05$  uncorrected threshold using novel > trained contrast on an independent sample ( $n = 40$ ).

***Follow-up pair t-test for activation***

We repeated the pair t-test for our activation data and found significant reduction of activation using the pair t-test model in SPM for the novel > trained condition after the training was stopped for 3 months (Figure S3.5).

**Figure S3.5**

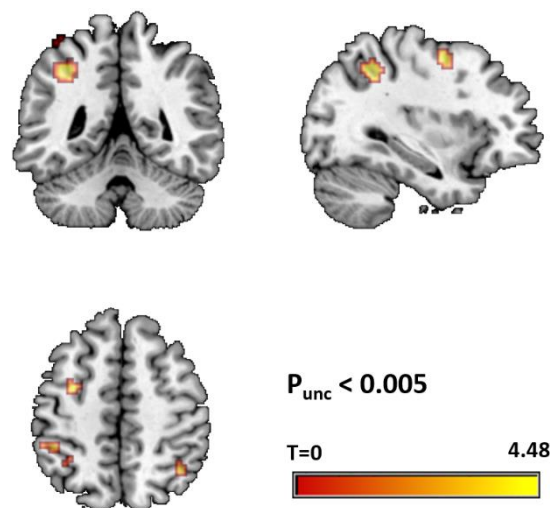


Figure shows significant decrease of activation on the follow-up measurement compared with the last training day (day11).



Table S3.1

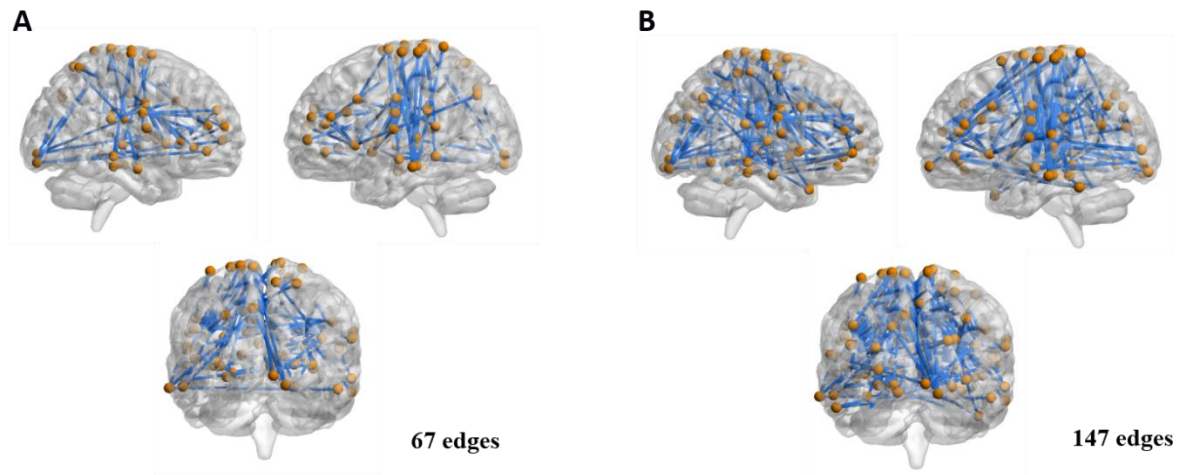
Node	Coordinates	T value	P value	Node	Coordinates	T value	P value
L.Paracentral (-7, -33, -72)				R.Precentral (29, -17, 71)			
L.Putamen	-34, 3, 4	4.03	4.36×10 <sup>-5</sup>	L.Inf.Temporal	-68, -23, -16	4.03	4.36×10 <sup>-5</sup>
L.Rolandic.Oper	-55, -9, 12	4.96	9.08×10 <sup>-7</sup>	R.Mid.Temporal	65, -31, -9	4.03	4.38×10 <sup>-5</sup>
L.Sup.Temporal	-55, -40, 14	4.56	5.09×10 <sup>-6</sup>	L.Mid.Temporal	-58, -26, -15	3.91	6.90×10 <sup>-5</sup>
R.Hippocampus	23, -13, -15	3.86	8.31×10 <sup>-5</sup>				
L.ACC	-3, 42, 16	3.84	8.89×10 <sup>-5</sup>	L.Rolandic.Oper (-55, -9, 12)			
				R.PostCentral	13, -33, 75	4.01	4.68×10 <sup>-5</sup>
R.PostCentral (51, -6, 32)				R.SMA	10, -17, 74	3.95	5.98×10 <sup>-5</sup>
R.Putamen	36, 10, 1	3.92	6.72×10 <sup>-5</sup>	L.Sup.Frontal	-16, -5, 71	4.50	6.76×10 <sup>-6</sup>
R.Insula	36, 22, 3	4.04	4.25×10 <sup>-5</sup>	L.Putamen	-22, 7, -5	4.37	1.13×10 <sup>-5</sup>
L.Pallidum	-15, 4, 8	3.99	5.13×10 <sup>-5</sup>				
R.Pallidum	15, 5, 7	4.02	4.52×10 <sup>-5</sup>	L.Precentral (-38, -27, 69)			
R.Putamen	23, 10, 1	4.02	4.49×10 <sup>-5</sup>	L.Inf.Temporal	-68, -23, -16	4.50	6.76×10 <sup>-6</sup>
R.Hippocampus	23, -13, -15	4.23	2.01×10 <sup>-5</sup>				
				R.Thalamus (6, -24, 0)			
L.Mid.Temporal (-58, -26, -15)				L.ACC	-3, 42, 16	3.89	7.64×10 <sup>-5</sup>
L.Sup.Parietal	-16, -46, 73	4.01	4.70×10 <sup>-5</sup>				
L.Sup.Frontal	-16, -5, 71	4.04	4.28×10 <sup>-5</sup>	L.Putamen (-22, 7, -5)			
				R.Rolandic.Oper	56, -5, 13	3.81	9.92×10 <sup>-5</sup>

NBS network table. The node names are presented according to the location in the AAL brain atlas (Tzourio-Mazoyer et al., 2002).

### ***NBS: Influence of initial threshold***

To further explore the robustness of our NBS derived sensorimotor-centered network, we repeated our analyses using two less strict initial thresholds:  $P < 0.00025$  and  $P < 0.0005$ . Notably, a less strict initial threshold should result in a larger but less specific network. As expected, using  $P < 0.00025$  initial threshold, a similar but larger ( $P_{FWE} = 0.018$ , 67 links) network was identified with more links connecting sensorimotor – visual areas and sensorimotor – frontal areas (Figure S3.6A). Moreover, using  $P < 0.0005$  initial threshold, the identified network was a lot larger ( $P_{FWE} = 0.018$ , 147 links) and unspecific (Figure S3.6B). Those observations suggested that the sensorimotor centered network was robust against different choices of initial thresholds.

### **Figure S3.6**



Panel A: figure shows the sensorimotor network using a initial thresholds:  $P < 0.00025$ . Panel B: figure shows the sensorimotor network using a initial thresholds:  $P < 0.0005$ .

### ***NBS: Influence of parcellation choice***

In order to demonstrate that the identified sensorimotor centered network is robust against other parcellation, we replicated our network findings using the AAL atlas that contains 116 nodes (Tzourio-Mazoyer et al., 2002). The network construction procedures and NBS model estimations were kept identical to our main analysis. The choice of AAL atlas was to demonstrate that our network findings based on a functional atlas could also be replicated using an anatomical atlas. As expected, we found a density-equivalent (20 connections) sensorimotor centered network that was similar to our main finding (uncorrected initial  $p < 2.5 \times 10^{-4}$ , FWE corrected  $p = 0.015$  Figure S3.7A). In addition, the overall functional connectivity change of this AAL-based sensorimotor was also positively correlated with the learning rate ( $r = 0.68$ ,  $p < 0.001$ , Figure S3.7B, one subject was excluded with  $> 2$  standard deviation) and negatively correlated with the average glutamate concentration level ( $r = -0.45$ ,  $p < 0.048$ , Figure S3.7C).

**Figure S3.7**

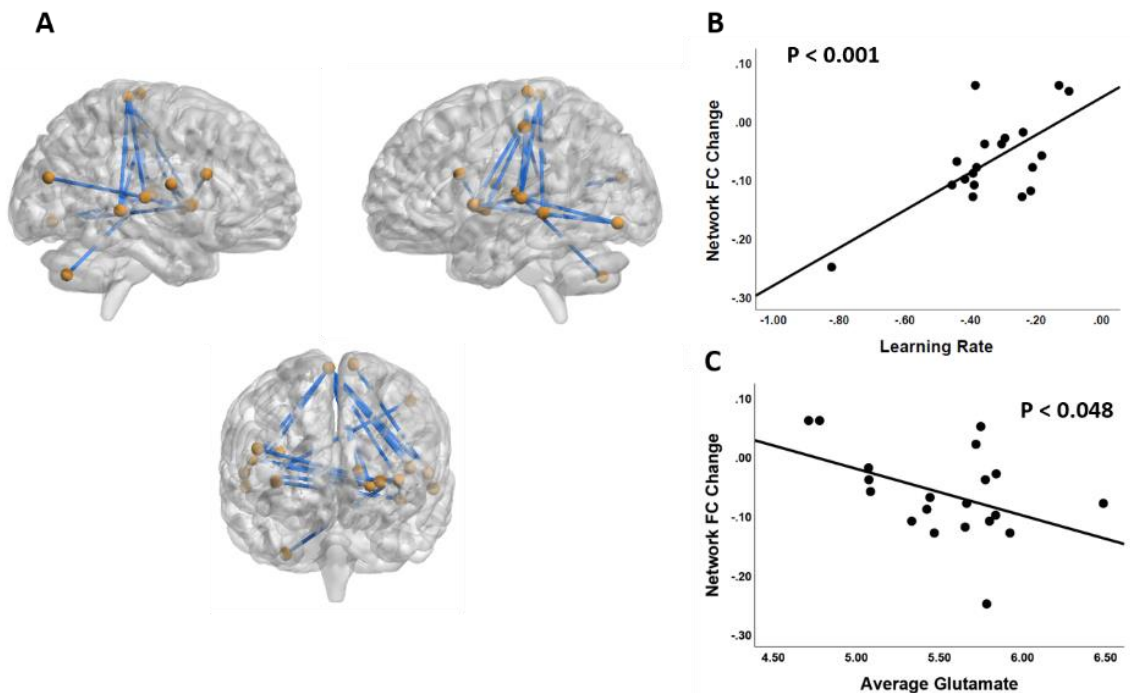


Figure shows the replication of the sensorimotor-centered network using AAL atlas. The connectivity change of this network was also significantly correlated with the learning rate ( $p < 0.001$ ) and the average glutamate level ( $p < 0.05$ ).

### ***MRS: influence of other methodological choices***

We calculated the averaged glutamate / creatine ratio (two subjects were excluded due to extreme low creatine concentration level ( $> 2$  standard deviation)). We replicated our finding that the change of functional connectivity is correlated with the average glutamate / creatine ratio ( $r = -0.52$ ,  $p < 0.026$ ).

To further account for tissue proportion confounds, the averaged glutamate concentrations were corrected for the GM volume within the voxel ( $GM/[GM+WM+CSF]$ ) and the averaged creatine concentrations were corrected for total brain tissue volume ( $[GM+WM]/[GM+WM+CSF]$ ) (Sampaio-Baptista et al., 2015; Stagg et al., 2014). The functional connectivity change of the network was correlated with the corrected averaged glutamate concentration ( $r = -0.49$ ,  $p < 0.027$ ) and glutamate / creatine ratio ( $r = -0.50$ ,  $p < 0.036$ ).

### ***DTI: negative findings***

We used the FA tracking from NBS-AAL replication post-hoc connections (20 links) and found no significant main effect of group ( $F_{1,33} = 2.56$ ,  $P = 0.12$ ) and time ( $F_{4,132}$

= 1.12,  $P = 0.35$ ). The group-by-time interaction is either significant ( $F_{4,132} = 1.15$ ,  $P = 0.34$ , Figure S3.8).

**Figure S3.8**

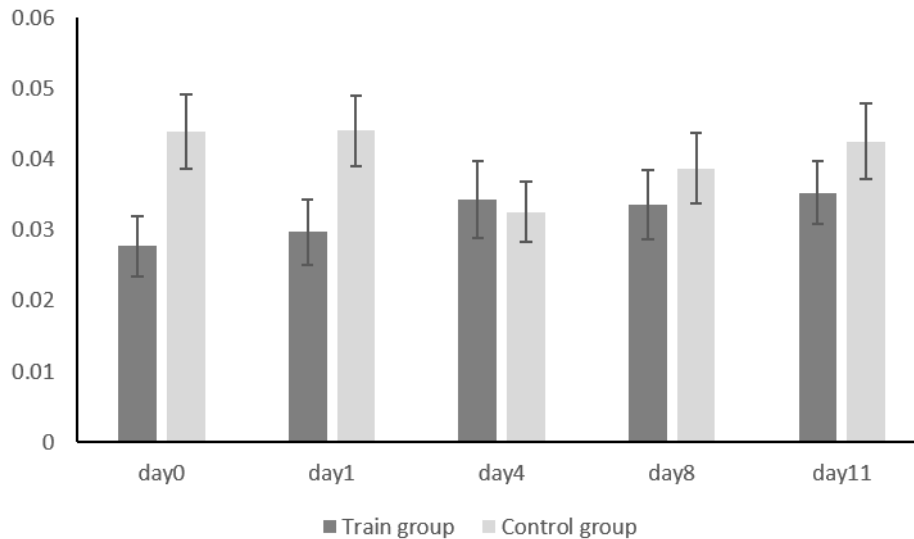


Figure shows post-hoc plots of deterministic fiber trajectory of the sensorimotor centered network defined with AAL atlas (20 links) from day0 to day11 of the train group and control group. Effect of group ( $F_{1,33} = 2.56$ ,  $P = 0.12$ ), time ( $F_{4,132} = 1.12$ ,  $P = 0.35$ ) and group-by-time interaction ( $F_{4,132} = 1.15$ ,  $P = 0.34$ ) are all non significant. Bars represent standard errors.

In addition, we tested the mean diffusivity (MD)(Sagi et al., 2012) from the right hippocampus cluster (extracted using small volume corrected T value as threshold,  $T > 3.65$ , cluster size = 38 voxels) and found significant main effect of group ( $F_{1,33} = 5.98$ ,  $P = 0.02$ ). However, the main effect of time ( $F_{4,132} = 0.22$ ,  $P = 0.64$ ) and group-by-time interaction ( $F_{4,132} = 1.44$ ,  $P = 0.24$ ) are not significant (Figure S3.9).

**Figure S3.9**

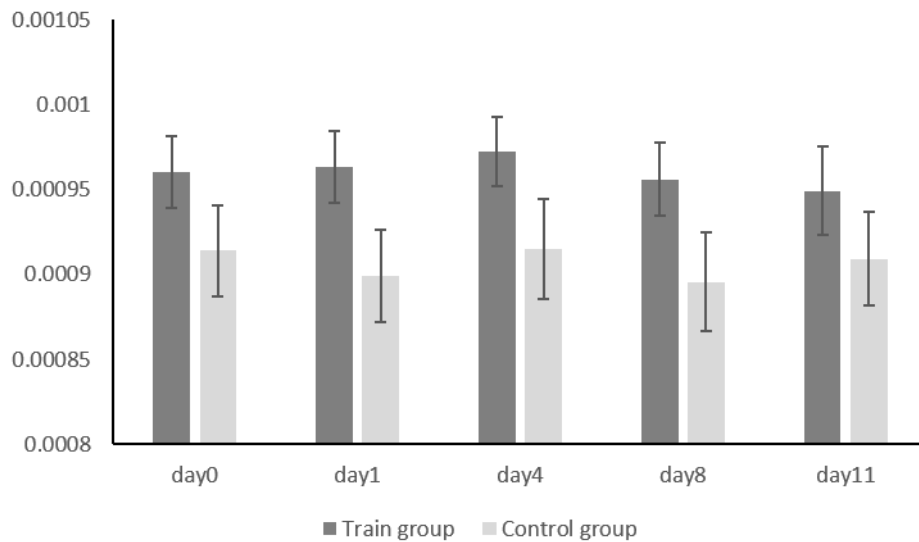


Figure shows posthoc plots of the MD extracted from the right hippocampus cluster that shows significant group-by-time interaction (T threshold > 3.65, cluster size = 38 voxels) of gray matter change along training. There is a significant main effect of group ( $F_{1,33} = 5.98$ ,  $P = 0.02$ ). However, the main effect of time ( $F_{4,132} = 0.22$ ,  $P = 0.64$ ) and group-by-time interaction ( $F_{4,132} = 1.44$ ,  $P = 0.24$ ) are not significant. Bars represent standard errors.

## 4 GENERAL DISCUSSION

### 4.1 Result summary

The primary goal of this thesis was to investigate neural plasticity during short-term and long-term motor learning using multiple neuroimaging modalities. Three primary hypotheses were tested: 1) To investigate the association between short-term motor learning and brain connectivity, including network properties, 2) to identify morphological and functional changes as a result of longer-term motor learning and 3) to investigate the modulation of imaging phenotypes by glutamate. The main hypotheses have been tested in two studies which are briefly summarized below:

The first study focused on short-term motor learning and used resting-state fMRI with a 30 minutes SVIPT training session prior to the scan to investigate the association between brain network properties and short-term motor learning. Training led to a significant improvement of motor performance which was positively correlated with brain network properties relating to efficiency, particularly small-worldness and global efficiency, and negatively correlated with brain network properties relating to network segregation, i.e. characteristic path length and transitivity. When investigating the topography of learning-induced changes of functional connectivity, a cerebellum centered sub-network involving visual, parietal, sensorimotor and temporal areas was detected to be positively correlated with short-term motor learning. Finally, a single dose of Ketamine, an NMDA antagonist, had significant effects on the identified cerebellum-centered network. Functional connectivity within this network was negatively correlated with the Ketamine metabolites (Norketamine) concentration level.

The second study aimed to investigate system-level neural plasticity during long-term motor learning. This study enrolled a 11-day SVIPT longitudinal training protocol in 20 healthy right-handed subjects (training group). An additional sample of 19 subjects, that were matched for age, sex and baseline performance, did not perform any training and served as the control group. Subjects were repeatedly scanned throughout the duration of the study (at five time points during the 11-day period). Subjects of the training group were additionally scanned at a follow-up measurement three months later. The resulting longitudinal data were used to assess dynamic neural plasticity during the whole training session. As expected, we found significant learning-induced

behavioral improvements along 11 days of training in the training groups. Regarding brain function, the activation of the frontal-parietal network increased throughout the training sessions in the training group but remained stationary in the control group, resulting in a significant group-by-time interaction effect. Regarding brain structure, the grey matter volume of the right hippocampus and the left SMA increased significantly in the training group, but not in the control group. A significant group-by-time interaction effect was further identified in the functional connectivity of a sensorimotor-centered network. The network covers the primary sensorimotor area, premotor cortex, parietal cortex, putamen, visual areas, temporal regions and the hippocampus. A post-hoc analysis revealed decreased functional connectivity of this sensorimotor network in the training group, but increased connectivity in the control group. The amount of reduction of the connectivity in the training group was significantly correlated with the behavioral improvement (learning rate) and the glutamatergic concentration level in the left primary cortex (hand knob). Compared to the last training day, the activation of the frontal-parietal network and the gray matter volume of the hippocampus and SMA were reduced at the follow-up. A trend-wise significant increase of functional connectivity of the sensorimotor-centered network was also observed at the follow-up.

The main results could be replicated using different methodological choices and were robust against the selection of another brain atlas. Taken together, the two studies show that the cerebellum is a critical region involved in short-term motor learning while the putamen and hippocampus are involved in motor learning spanning longer time frames. Cortical regions such as the primary sensorimotor, premotor, parietal and visual area are associated with both short-term and long-term learning. The overall findings of the two studies are well in line with the majority of existing motor learning studies (Albouy et al., 2008; Bassett et al., 2015; J. Doyon & Benali, 2005; Sami et al., 2014; Ungerleider et al., 2002).

## **4.2 Behavioral improvements**

Both short-term and long-term training led to a significant improvement in motor performance in the SVIPT. Subjects were able to familiarize themselves with the SVIPT within a short amount of time and showed fast and gradual improvement until reaching a plateau after two weeks of learning. It is also worth noting that during the long-term motor learning phase, subjects who received daily training also showed

better performance during novel sequences than subjects who did not, indicating that their adaptation ability to novel sequence also improved faster. These behavioral results suggest that the SVIPT can be successfully applied to investigate motor learning processes across time frames that range from minutes to weeks.

### **4.3 Short-term learning phase**

The results suggest that the ability to learn a new motor skill relies – to some extent – on the intrinsic properties of the individual’s brain network architecture. A more efficient brain network might therefore enhance the ability to acquire a new motor skill. The investigation of the association between “network efficiency” markers and behavioral improvements during short-term motor learning study is therefore of high relevance. The results of study 1 showed a strong correlation between the ability of novel skill acquisition and brain network features including small-worldness, global efficiency and characteristic path length. Those brain network features are considered to reflect how efficient information can travel through the brain network, and have previously been shown to be correlated with other cognitive aspects such as working memory (Langer, von Bastian, Wirz, Oberauer, & Jancke, 2013) and overall cognition (Douw et al., 2011). The findings obtained in the short-term motor learning study add further evidence to the role of network efficiency for behavioral performance by showing that a more efficient functional brain network architecture also supports the acquisition of novel motor skills. This supports the idea that motor learning requires close and efficient interaction between distant brain regions. In addition, the functional connectivity of a cerebellum-centered network was also correlated with short-term motor learning ability, which is in line with previous studies (J. Doyon et al., 2002; Hikosaka et al., 2002; Tamas Kincses et al., 2008) In a model proposed by Doyon and Unterleider (J. a. U. Doyon, Leslie G., 2002), the cerebellum is considered to participate in the cerebellum-thalamus-striatum-cortical network during fast motor learning. Supportive evidence comes from clinical studies where patients with cerebellum lesions were shown to have difficulties in learning from their previous errors during motor learning (Sanes, Dimitrov, & Hallett, 1990). Those observations point to the fact that the cerebellum is one of the most critical regions for motor learning, especially during the early stage. The parietal area is also critical for motor learning due to its unique role in spatial orientation (Zhang et al., 2012). The current findings of



the cerebellar-cortical network included several connections between the cerebellum and the parietal cortex, suggesting that the connections between those brain regions may contribute to the ability of fast motor learning by coordinating upcoming kinetic parameters in the parietal lobe with parameters of error detection in the cerebellum (Laforce & Doyon, 2001; M. A. Smith & Shadmehr, 2005). As a result, subjects with better coordination of multivariate motor parameters between cerebellum and parietal lobe showed better learning.

Another key region involved in fast motor learning is the primary motor cortex, which was also detected in our first study. Animal studies have consistently shown that the primary motor cortex is associated with fast skill learning (Costa, Cohen, & Nicoletis, 2004) as a result of LTP and LTD (Rioul-Pedotti, Friedman, & Donoghue, 2000; Rioul-Pedotti, Friedman, Hess, & Donoghue, 1998). In human imaging studies, the BOLD activation in the primary motor cortex was shown to be decreased after training (Dayan & Cohen, 2011). It is also worth noting that brain stimulation interventions like tDCS (Reis et al., 2009) or TMS (Pascual-Leone, Grafman, & Hallett, 1994) applied over the primary motor cortex can modulate the off-line motor memory consolidation process. Overall, the first study demonstrated an involvement of the cerebellum-visual-parietal-sensorimotor loop in fast motor learning.

#### **4.4 Long-term learning phase**

No alterations of cerebellum activity or morphology were found in the longitudinal study. Instead, the majority of functional and structural re-organizations took place in the cortical - basal ganglia loop, the frontal-parietal network and the hippocampus. Functional responses of premotor and parietal areas were constantly stronger to novel compared to trained sequences, while the overall activation decreased throughout the 11 training days. This suggests that the change in activation was mainly driven by differences in automatization. Overall, both studies suggest that the premotor and the parietal area as well as the primary sensorimotor cortex are involved in both short-term and long-term motor learning.

#### **4.5 A neurobiological model to interpret the transition from short-term to long-term motor learning**

The applied motor learning task is a visual sequential guided pinch force task that challenges both the “spatial sequence” and “motor adaptation” aspects. During training, subjects need to detect and remember the sequence during the current task block, and additionally update their pinch force according to the position of the cursor displayed on the monitor. These two aspects can be described in terms of the “spatial” and “motor” features as outlined in the motor learning model by Hikosaka and colleagues (Hikosaka et al., 2002). Hikosaka et al considered that the “spatial” component of motor learning relies more on the frontal-parietal network together with associative cerebellum and basal ganglia while the “motor” component of motor learning relies on the sensorimotor cortex and the motor part of the cerebellum and basal ganglia. The observations from the short-term motor learning study indicate that subjects who have an overall better ability to acquire a novel motor skill are equipped with a more efficient brain functional network, driven mainly by connections from the cognitive cerebellum (cerebellum 7b, 8 and crus I) to visual-parietal-motor areas. During short-term motor learning, subjects may need to pay “maximum attention” in order to achieve better performance. Longer-term motor learning instead occurs on a more implicit level and requires less attention. Converging results from functional and structural imaging modalities have shown that the morphology, activity and connectivity of the pre-motor area, SMA, sensorimotor area and putamen were changed during 11 days of training. These longitudinal results are in line with the “motor” component of Hikosaka’s model.

An interesting finding is the increased gray matter volume of the hippocampus, as well as the reduction of the hippocampal functional connectivity with the sensorimotor cortex during the longitudinal motor learning study. The hippocampus is well known for its critical role in “episodic memory” and “spatial navigation” (Maguire et al., 2000). Recent neuroimaging studies in humans identified hippocampal functional changes in a 24-hour oculomotor sequential learning task (Albouy et al., 2008) as well in a 4-day sequential finger tapping reaction time task (Schendan et al., 2003). A longer-term motor learning study conducted by Kodama and colleagues demonstrated a 1-week lasting grey matter increase in the bilateral hippocampus and parahippocampus after a 5-day arm reaching training (M. Kodama et al., 2018). The hippocampal finding in study 2 is therefore very well in line with the above-mentioned studies.

Albouy and colleagues used a visuo-spatial sequential eye-tracking task and found increased hippocampus activation overnight but not within waking hours (5 hours).

In contrast, the activation of ventral putamen increased consistently after 5 hours and 24 hours. These findings were suggested to reflect memory consolidation processes in the hippocampus. The task designs in the study by Albouy et al, Sheden et al and the current project are very similar in their “sequential” nature. The involvement of the hippocampus in all three studies could therefore point to the role of the hippocampus as a “memory consolidation mediator” between the spatial and the motor aspects of Hikosaka’s model. Subjects may rely on their hippocampus to recall the spatial sequential movements during the task. However, the role of the hippocampus during motor sequential learning needs further specification due to the lack of direct evidence from animal studies and conflicting observations in amnesia patients with lesions in the hippocampus. The famous case study of patient H.M., who lost the majority of his medial temporal lobe due to a surgery to cure his severe epilepsy, showed that his ability of acquiring novel motor skill (drawing by looking at the reflection of a mirror) was not significantly reduced, though he could not recall that he had actually participated in the motor learning tasks. Similarly, clinical motor learning studies in amnesia patients with lesions in the medial temporal lobe did not show reduced behavioral motor learning performance (Gabrieli, Corkin, Mickel, & Growdon, 1993). Further experiments are needed to clarify the exact role of the hippocampus in motor learning as well as the conflicting observations between healthy subjects and amnesia patients.

The follow-up measurement after three months revealed reduced activation of the premotor-parietal areas as well as reduced gray matter volume in the SMA and the hippocampus compared to the last training day. Overall, functional and structural changes recovered to the baseline level when training was stopped for three months. A similar trajectory of gray matter volume change was also reported in a previous longitudinal motor learning study that challenged more complicated tasks like juggling (Draganski et al., 2004). For human imaging studies, it is very difficult to explain the underlying mechanism of gray matter volume change. However, this “increase-decrease” pattern of gray matter volume is quite similar to the pattern of gliogenesis that has been observed in animal studies (Zatorre et al., 2012). The decrease of activation in the premotor-parietal area may also indicate the process of “forgetting”. A plausible explanation is the lack of continuous training which might trigger a higher need for neural resources as soon as the task is re-performed.

#### **4.6 Glutamatergic modulation during short-term and long-term motor learning**

Pharmacological interventions and MRS data were used to further investigate potential neurobiological mechanisms of our findings in both the short-term and long-term motor learning studies. Taken together, the functional connectivity of both the cerebellar-centered network identified during the short-term motor learning and the sensorimotor-centered network identified during the long-term motor learning was modulated by glutamate. Specifically, using ketamine (an NMDA receptor antagonist), a decreased functional connectivity of the cerebellar-cortical network after NMDA blockade in the short-term motor learning study was found. In the longitudinal study, the glutamate concentration level did not significantly change in the hand knob area during motor learning. Instead, we observed a significant correlation between glutamate level in the hand knob area and the overall change of the functional connectivity in a network centered on the sensorimotor cortex. This result suggests that glutamate as measured by MRS in the hand knob area provides a trait-like marker of the potential cellular/molecular machinery regulating synaptic plasticity and subserving motor skill acquisition. These results are in line with several animal studies on the pivotal role of glutamate in motor learning which demonstrated that training can promote presynaptic glutamate release (Kida & Mitsushima, 2018; Kida et al., 2016) and that mGluR4 gene knock out mice have impaired motor performance (Pekhletski et al., 1996). In addition, the blockade of glutamate receptor or deletion of glutamatergic gene (Hasan et al., 2013) was shown to lead to impaired LTP and LTD in the motor cortex, prefrontal cortex (Moghaddam, Adams, Verma, & Daly, 1997), the hippocampus (Bannerman et al., 2012) and the striatum (Dang et al., 2006). Interestingly, in the present study, we did not observe impaired motor learning/performance under a low dose of ketamine infusion despite changes in brain function. This is probably due to the fact that the dosage of ketamine was too little to cause behavioral impairments. In addition, the longitudinal study provided direct evidence of glutamate concentration level-dependent functional connectivity plasticity of the sensorimotor centered network. These results suggest that glutamate participates in the modulation of synaptic plasticity processes during long-term motor learning that shape large-scale brain network reorganization and thereby helps optimize motor parameters and sensory experiences (Hasan et al., 2013). Although it is challenging to provide direct evidence of glutamatergic dependent LTP in humans, results from the

current project support this well-known model derived from animal and cellular studies (Bliss & Collingridge, 2013; Bliss & Lomo, 1973; Cooke & Bliss, 2006).

## **4.7 Limitations and Future directions**

### **4.7.1 Limitations of the current project**

The major limitation of our short-term motor learning study is that no “baseline” imaging data were acquired before the training that it is hard to rule out the effect of learning-induced changes that might drive the behavior-network correlation. In addition, the time interval between the ketamine and placebo data was too short to fully rule out any drug carryover effects which might have resulted in drug-by-learning interaction effects.

In the longitudinal study, the glutamate concentration data were acquired using a single significant voxel placed on the hand knob area from each individual brain space. This procedure could potentially cause a slightly shifted position of the hand knob area during spatial normalization and therefore could result in a difference of the coordinate located in the sensorimotor centered network. In fact, the network connections that were significantly correlated with glutamate concentration levels were not only distributed within the primary motor cortex but also to a variety of other motor brain regions, which might be caused by interindividual variations in spatial normalization.

### **4.7.2 Future directions**

Our results build on existing evidence that brain activity, connectivity and structure in multiple regions are associated with various types of motor learning. It is necessary to carry out studies to accurately distinguish the contributions of different regions to different types of motor learning tasks.

Following the successful implementation of the SVIPT protocol, this task could be rolled out in clinical populations with motor deficits. In the psychiatric domain, a target population is patients with schizophrenia and their first-degree relatives. The longitudinal study of sequential motor learning will inform the biological basis of motor symptoms of schizophrenia, the genetic and epigenetic contributions, and whether motor symptoms are rather disease-intrinsic or environmental related.

Last but not least, the role of the hippocampus in motor learning needs further clarification due to conflicting findings between amnesia patient studies and several recent healthy control studies, including this thesis.

## 5 SUMMARY

Motor learning is a fundamental ability and one of the most robust models to study neural plasticity. The majority of human motor learning imaging studies focused on either short-term or long-term learning using one single imaging modality. These studies were thus not able to systematically investigate the dynamic process of motor learning from a multimodal perspective.

The current project combined both short-term and long-term motor learning to comprehensively characterize neural plasticity at multiple phenotypic levels of the brain: functional activation, functional connectivity, grey matter volume, and glutamate concentration. To this end, this project involved a cross-sectional and a longitudinal study with multimodal brain imaging techniques (task fMRI, resting-state fMRI, gray matter structural fMRI, pharmacological fMRI, and MRS).

Short-term motor learning was significantly correlated with brain network features related to network efficiency. It was also associated with a highly reliable cerebellum-centered network which was significantly modulated by the NMDA antagonist ketamine. Long-term motor learning was associated with increased activation in premotor / SMA and parietal regions and with increased gray matter volume of the SMA and the hippocampus. In addition, long-term motor learning was accompanied by a decrease in the functional connectivity of a network centered on the sensorimotor cortex which was related to handknob glutamate concentration levels and which involved regions that were highlighted by our activation and structural analyses. Taken together, this thesis contributes important evidence to the neurofunctional and neurostructural underpinnings of motor learning and points to the critical roles of the cerebellum, the hippocampus and the relevance of glutamate for motor learning in humans.

## 6 REFERENCES

- Abraham, W. C., & Mason, S. E. (1988). Effects of the NMDA receptor/channel antagonists CPP and MK801 on hippocampal field potentials and long-term potentiation in anesthetized rats. *Brain Res*, *462*(1), 40-46.
- Alavash, M., Doebler, P., Holling, H., Thiel, C. M., & Giessing, C. (2015). Is functional integration of resting state brain networks an unspecific biomarker for working memory performance? *Neuroimage*, *108*, 182-193.
- Albert, N. B., Robertson, E. M., & Miall, R. C. (2009). The resting human brain and motor learning. *Curr Biol*, *19*(12), 1023-1027. doi:10.1016/j.cub.2009.04.028
- Albouy, G., Sterpenich, V., Balteau, E., Vandewalle, G., Desseilles, M., Dang-Vu, T., . . . Maquet, P. (2008). Both the hippocampus and striatum are involved in consolidation of motor sequence memory. *Neuron*, *58*(2), 261-272.
- Alexander, G. E., DeLong, M. R., & Strick, P. L. (1986). Parallel organization of functionally segregated circuits linking basal ganglia and cortex. *Annu Rev Neurosci*, *9*, 357-381. doi:10.1146/annurev.ne.09.030186.002041
- Ashburner, J., & Friston, K. J. (2000). Voxel-based morphometry--the methods. *Neuroimage*, *11*(6 Pt 1), 805-821. doi:10.1006/nimg.2000.0582
- Bannerman, D. M., Bus, T., Taylor, A., Sanderson, D. J., Schwarz, I., Jensen, V., . . . Sprengel, R. (2012). Dissecting spatial knowledge from spatial choice by hippocampal NMDA receptor deletion. *Nat Neurosci*, *15*(8), 1153-1159. doi:10.1038/nn.3166
- Barbey, A. K., Koenigs, M., & Grafman, J. (2013). Dorsolateral prefrontal contributions to human working memory. *Cortex*, *49*(5), 1195-1205.
- Barnes, A., Bullmore, E. T., & Suckling, J. (2009). Endogenous human brain dynamics recover slowly following cognitive effort. *PLoS One*, *4*(8), e6626.
- Bassett, D. S., & Bullmore, E. (2006). Small-world brain networks. *Neuroscientist*, *12*(6), 512-523. doi:10.1177/1073858406293182
- Bassett, D. S., & Mattar, M. G. (2017). A Network Neuroscience of Human Learning: Potential to Inform Quantitative Theories of Brain and Behavior. *Trends Cogn Sci*, *21*(4), 250-264. doi:10.1016/j.tics.2017.01.010
- Bassett, D. S., Wymbs, N. F., Porter, M. A., Mucha, P. J., Carlson, J. M., & Grafton, S. T. (2011). Dynamic reconfiguration of human brain networks during learning. *Proc Natl Acad Sci U S A*, *108*(18), 7641-7646. doi:10.1073/pnas.1018985108
- Bassett, D. S., Yang, M., Wymbs, N. F., & Grafton, S. T. (2015). Learning-induced autonomy of sensorimotor systems. *Nat Neurosci*, *18*(5), 744-751. doi:10.1038/nn.3993
- Bezzola, L., Merillat, S., Gaser, C., & Jancke, L. (2011). Training-induced neural plasticity in golf novices. *J Neurosci*, *31*(35), 12444-12448. doi:10.1523/jneurosci.1996-11.2011
- Blüml, S. (2013). *Magnetic Resonance Spectroscopy: Basics*. In: Blüml S., Panigrahy A. (eds) *MR Spectroscopy of Pediatric Brain Disorders*.: Springer, New York, NY.



- Bliss, T. V., & Collingridge, G. L. (2013). Expression of NMDA receptor-dependent LTP in the hippocampus: bridging the divide. *Mol Brain*, 6, 5. doi:10.1186/1756-6606-6-5
- Bliss, T. V., & Lomo, T. (1973). Long-lasting potentiation of synaptic transmission in the dentate area of the anaesthetized rabbit following stimulation of the perforant path. *J Physiol*, 232(2), 331-356.
- Born, R. T., & Bradley, D. C. (2005). Structure and function of visual area MT. *Annu Rev Neurosci*, 28, 157-189. doi:10.1146/annurev.neuro.26.041002.131052
- Brasted, P. J., & Wise, S. P. (2004). Comparison of learning-related neuronal activity in the dorsal premotor cortex and striatum. *Eur J Neurosci*, 19(3), 721-740.
- Braun, U., Plichta, M. M., Esslinger, C., Sauer, C., Haddad, L., Grimm, O., . . . Meyer-Lindenberg, A. (2012). Test-retest reliability of resting-state connectivity network characteristics using fMRI and graph theoretical measures. *Neuroimage*, 59(2), 1404-1412. doi:10.1016/j.neuroimage.2011.08.044
- Bruce, C. J., Goldberg, M. E., Bushnell, M. C., & Stanton, G. B. (1985). Primate frontal eye fields. II. Physiological and anatomical correlates of electrically evoked eye movements. *J Neurophysiol*, 54(3), 714-734. doi:10.1152/jn.1985.54.3.714
- Bullmore, E., & Sporns, O. (2009). Complex brain networks: graph theoretical analysis of structural and functional systems. *Nat Rev Neurosci*, 10(3), 186-198. doi:10.1038/nrn2575
- Burguiere, E., Arabo, A., Jarlier, F., De Zeeuw, C. I., & Rondi-Reig, L. (2010). Role of the cerebellar cortex in conditioned goal-directed behavior. *J Neurosci*, 30(40), 13265-13271. doi:10.1523/jneurosci.2190-10.2010
- Calabresi, P., Picconi, B., Tozzi, A., Ghiglieri, V., & Di Filippo, M. (2014). Direct and indirect pathways of basal ganglia: a critical reappraisal. *Nat Neurosci*, 17(8), 1022-1030. doi:10.1038/nn.3743
- Cao, H., Plichta, M. M., Schafer, A., Haddad, L., Grimm, O., Schneider, M., . . . Tost, H. (2014). Test-retest reliability of fMRI-based graph theoretical properties during working memory, emotion processing, and resting state. *Neuroimage*, 84, 888-900. doi:10.1016/j.neuroimage.2013.09.013
- Chen, L. L., & Wise, S. P. (1995). Supplementary eye field contrasted with the frontal eye field during acquisition of conditional oculomotor associations. *J Neurophysiol*, 73(3), 1122-1134. doi:10.1152/jn.1995.73.3.1122
- Chouinard, P. A., & Paus, T. (2006). The primary motor and premotor areas of the human cerebral cortex. *Neuroscientist*, 12(2), 143-152. doi:10.1177/1073858405284255
- Clark, R. E., Broadbent, N. J., & Squire, L. R. (2005). Hippocampus and remote spatial memory in rats. *Hippocampus*, 15(2), 260-272. doi:10.1002/hipo.20056
- Cooke, S. F., & Bliss, T. V. (2006). Plasticity in the human central nervous system. *Brain*, 129(Pt 7), 1659-1673. doi:10.1093/brain/awl082
- Costa, R. M., Cohen, D., & Nicoletis, M. A. (2004). Differential corticostriatal plasticity during fast and slow motor skill learning in mice. *Curr Biol*, 14(13), 1124-1134. doi:10.1016/j.cub.2004.06.053
- Coyne, D., Marrelec, G., Perlberg, V., Pelegriani-Issac, M., Van de Moortele, P. F., Ugurbil, K., . . . Lehericy, S. (2010). Dynamics of motor-related functional

- integration during motor sequence learning. *Neuroimage*, 49(1), 759-766. doi:10.1016/j.neuroimage.2009.08.048
- Dang, M. T., Yokoi, F., Yin, H. H., Lovinger, D. M., Wang, Y., & Li, Y. (2006). Disrupted motor learning and long-term synaptic plasticity in mice lacking NMDAR1 in the striatum. *Proc Natl Acad Sci U S A*, 103(41), 15254-15259. doi:10.1073/pnas.0601758103
- Dayan, E., & Cohen, L. G. (2011). Neuroplasticity subserving motor skill learning. *Neuron*, 72(3), 443-454. doi:10.1016/j.neuron.2011.10.008
- Dazzan, P., Morgan, K. D., Orr, K. G., Hutchinson, G., Chitnis, X., Suckling, J., . . . Murray, R. M. (2004). The structural brain correlates of neurological soft signs in AESOP first-episode psychoses study. *Brain*, 127(Pt 1), 143-153. doi:10.1093/brain/awh015
- Diedrichsen, J., Balsters, J. H., Flavell, J., Cussans, E., & Ramnani, N. (2009). A probabilistic MR atlas of the human cerebellum. *Neuroimage*, 46(1), 39-46. doi:10.1016/j.neuroimage.2009.01.045
- Ding, L., & Perkel, D. J. (2004). Long-term potentiation in an avian basal ganglia nucleus essential for vocal learning. *J Neurosci*, 24(2), 488-494. doi:10.1523/jneurosci.4358-03.2004
- Donato, F., Rompani, S. B., & Caroni, P. (2013). Parvalbumin-expressing basket-cell network plasticity induced by experience regulates adult learning. *Nature*, 504(7479), 272-276. doi:10.1038/nature12866
- Dong, W. K., & Greenough, W. T. (2004). Plasticity of nonneuronal brain tissue: roles in developmental disorders. *Ment Retard Dev Disabil Res Rev*, 10(2), 85-90. doi:10.1002/mrdd.20016
- Dong, Z. Y., Liu, D. Q., Wang, J., Qing, Z., Zang, Z. X., Yan, C. G., & Zang, Y. F. (2012). Low-frequency fluctuation in continuous real-time feedback of finger force: a new paradigm for sustained attention. *Neurosci Bull*, 28(4), 456-467. doi:10.1007/s12264-012-1254-2
- Douw, L., Schoonheim, M. M., Landi, D., van der Meer, M. L., Geurts, J. J., Reijneveld, J. C., . . . Stam, C. J. (2011). Cognition is related to resting-state small-world network topology: an magnetoencephalographic study. *Neuroscience*, 175, 169-177. doi:10.1016/j.neuroscience.2010.11.039
- Doyon, J., & Benali, H. (2005). Reorganization and plasticity in the adult brain during learning of motor skills. *Curr Opin Neurobiol*, 15(2), 161-167. doi:10.1016/j.conb.2005.03.004
- Doyon, J., Song, A. W., Karni, A., Lalonde, F., Adams, M. M., & Ungerleider, L. G. (2002). Experience-dependent changes in cerebellar contributions to motor sequence learning. *Proc Natl Acad Sci U S A*, 99(2), 1017-1022. doi:10.1073/pnas.022615199
- Doyon, J. a. U., Leslie G. (2002). *Functional anatomy of motor skill learning*. (Vol. Neuropsychology of memory (pp. 225-238). New York, NY, US: The Guilford Press.).
- Draganski, B., Gaser, C., Busch, V., Schuierer, G., Bogdahn, U., & May, A. (2004). Neuroplasticity: changes in grey matter induced by training. *Nature*, 427(6972), 311-312. doi:10.1038/427311a

- Dum, R. P., & Strick, P. L. (1996). Spinal cord terminations of the medial wall motor areas in macaque monkeys. *J Neurosci*, *16*(20), 6513-6525.
- Eichenbaum, H. (2001). The hippocampus and declarative memory: cognitive mechanisms and neural codes. *Behav Brain Res*, *127*(1-2), 199-207.
- Fernandez-Seara, M. A., Aznarez-Sanado, M., Mengual, E., Loayza, F. R., & Pastor, M. A. (2009). Continuous performance of a novel motor sequence leads to highly correlated striatal and hippocampal perfusion increases. *Neuroimage*, *47*(4), 1797-1808. doi:10.1016/j.neuroimage.2009.05.061
- Fernandez, G., Effern, A., Grunwald, T., Pezer, N., Lehnertz, K., Dumpelmann, M., . . . Elger, C. E. (1999). Real-time tracking of memory formation in the human rhinal cortex and hippocampus. *Science*, *285*(5433), 1582-1585.
- Fitts, P. M., & Posner, M. I. (1967). Human performance. *Belmont, CA: Brooks/Cole*.
- Fleiss, J. L. (1986). *The Design and Analysis of Clinical Experiments*. New York: Wiley.
- Floyer-Lea, A., & Matthews, P. M. (2005). Distinguishable brain activation networks for short- and long-term motor skill learning. *J Neurophysiol*, *94*(1), 512-518. doi:10.1152/jn.00717.2004
- Floyer-Lea, A., Wylezinska, M., Kincses, T., & Matthews, P. M. (2006). Rapid modulation of GABA concentration in human sensorimotor cortex during motor learning. *J Neurophysiol*, *95*(3), 1639-1644. doi:10.1152/jn.00346.2005
- Francois, J., Grimm, O., Schwarz, A. J., Schweiger, J., Haller, L., Risterucci, C., . . . Meyer-Lindenberg, A. (2016). Ketamine Suppresses the Ventral Striatal Response to Reward Anticipation: A Cross-Species Translational Neuroimaging Study. *Neuropsychopharmacology*, *41*(5), 1386-1394. doi:10.1038/npp.2015.291
- Fritsch, B., Reis, J., Martinowich, K., Schambra, H. M., Ji, Y., Cohen, L. G., & Lu, B. (2010). Direct current stimulation promotes BDNF-dependent synaptic plasticity: potential implications for motor learning. *Neuron*, *66*(2), 198-204. doi:10.1016/j.neuron.2010.03.035
- Gabrieli, J. D., Corkin, S., Mickel, S. F., & Growdon, J. H. (1993). Intact acquisition and long-term retention of mirror-tracing skill in Alzheimer's disease and in global amnesia. *Behav Neurosci*, *107*(6), 899-910.
- Galea, J. M., Vazquez, A., Pasricha, N., de Xivry, J. J., & Celnik, P. (2011). Dissociating the roles of the cerebellum and motor cortex during adaptive learning: the motor cortex retains what the cerebellum learns. *Cereb Cortex*, *21*(8), 1761-1770. doi:10.1093/cercor/bhq246
- Garraux, G., Peigneux, P., Carson, R. E., & Hallett, M. (2007). Task-related interaction between basal ganglia and cortical dopamine release. *J Neurosci*, *27*(52), 14434-14441. doi:10.1523/jneurosci.1595-07.2007
- Gaser, C., & Schlaug, G. (2003). Brain structures differ between musicians and non-musicians. *J Neurosci*, *23*(27), 9240-9245.
- Gerloff, C., Corwell, B., Chen, R., Hallett, M., & Cohen, L. G. (1997). Stimulation over the human supplementary motor area interferes with the organization of future elements in complex motor sequences. *Brain*, *120* ( Pt 9), 1587-1602.
- Glickstein, M. (2000). How are visual areas of the brain connected to motor areas for the sensory guidance of movement? *Trends Neurosci*, *23*(12), 613-617.

- Gosselin, N., De Beaumont, L., Gagnon, K., Baril, A. A., Mongrain, V., Blais, H., . . . Carrier, J. (2016). BDNF Val66Met Polymorphism Interacts with Sleep Consolidation to Predict Ability to Create New Declarative Memories. *J Neurosci*, *36*(32), 8390-8398. doi:10.1523/jneurosci.4432-15.2016
- Grafton, S. T., Hazeltine, E., & Ivry, R. B. (2002). Motor sequence learning with the nondominant left hand. A PET functional imaging study. *Exp Brain Res*, *146*(3), 369-378. doi:10.1007/s00221-002-1181-y
- Grimm, O., Gass, N., Weber-Fahr, W., Sartorius, A., Schenker, E., Spedding, M., . . . Meyer-Lindenberg, A. (2015). Acute ketamine challenge increases resting state prefrontal-hippocampal connectivity in both humans and rats. *Psychopharmacology (Berl)*, *232*(21-22), 4231-4241. doi:10.1007/s00213-015-4022-y
- Gurden, H., Tassin, J. P., & Jay, T. M. (1999). Integrity of the mesocortical dopaminergic system is necessary for complete expression of in vivo hippocampal-prefrontal cortex long-term potentiation. *Neuroscience*, *94*(4), 1019-1027.
- Hadj Tahar, A., Blanchet, P. J., & Doyon, J. (2004). Motor-learning impairment by amantadine in healthy volunteers. *Neuropsychopharmacology*, *29*(1), 187-194. doi:10.1038/sj.npp.1300317
- Hall, S. D., Stanford, I. M., Yamawaki, N., McAllister, C. J., Ronnqvist, K. C., Woodhall, G. L., & Furlong, P. L. (2011). The role of GABAergic modulation in motor function related neuronal network activity. *Neuroimage*, *56*(3), 1506-1510. doi:10.1016/j.neuroimage.2011.02.025
- Hardwick, R. M., Rottschy, C., Miall, R. C., & Eickhoff, S. B. (2013). A quantitative meta-analysis and review of motor learning in the human brain. *Neuroimage*, *67*, 283-297. doi:10.1016/j.neuroimage.2012.11.020
- Hasan, M. T., Hernandez-Gonzalez, S., Dogbevia, G., Trevino, M., Bertocchi, I., Gruart, A., & Delgado-Garcia, J. M. (2013). Role of motor cortex NMDA receptors in learning-dependent synaptic plasticity of behaving mice. *Nat Commun*, *4*, 2258. doi:10.1038/ncomms3258
- Heitger, M. H., Ronsse, R., Dhollander, T., Dupont, P., Caeyenberghs, K., & Swinnen, S. P. (2012). Motor learning-induced changes in functional brain connectivity as revealed by means of graph-theoretical network analysis. *Neuroimage*, *61*(3), 633-650. doi:10.1016/j.neuroimage.2012.03.067
- Hikosaka, O., Nakamura, K., Sakai, K., & Nakahara, H. (2002). Central mechanisms of motor skill learning. *Curr Opin Neurobiol*, *12*(2), 217-222.
- Hirjak, D., Kubera, K. M., Northoff, G., Fritze, S., Bertolino, A. L., Topor, C. E., . . . Wolf, R. C. (2019). Cortical Contributions to Distinct Symptom Dimensions of Catatonia. *Schizophr Bull*. doi:10.1093/schbul/sby192
- Hirjak, D., Rashidi, M., Fritze, S., Bertolino, A. L., Geiger, L. S., Zang, Z., . . . Wolf, R. C. (2019). Patterns of co-altered brain structure and function underlying neurological soft signs in schizophrenia spectrum disorders. *Hum Brain Mapp*. doi:10.1002/hbm.24755
- Hirjak, D., Rashidi, M., Kubera, K. M., Northoff, G., Fritze, S., Schmitgen, M. M., . . . Wolf, R. C. (2019). Multimodal MRI data fusion reveals distinct patterns of abnormal brain structure and function in catatonia. *Schizophr Bull*, (in press).

- Hirjak, D., Thomann, P. A., Kubera, K. M., Wolf, N. D., Sambataro, F., & Wolf, R. C. (2015). Motor dysfunction within the schizophrenia-spectrum: A dimensional step towards an underappreciated domain. *Schizophr Res*, *169*(1-3), 217-233. doi:10.1016/j.schres.2015.10.022
- Hirjak, D., Wolf, R. C., Kubera, K. M., Stieltjes, B., Maier-Hein, K. H., & Thomann, P. A. (2015). Neurological soft signs in recent-onset schizophrenia: Focus on the cerebellum. *Prog Neuropsychopharmacol Biol Psychiatry*, *60*, 18-25. doi:10.1016/j.pnpbp.2015.01.011
- Hirjak, D., Wolf, R. C., Stieltjes, B., Seidl, U., Schroder, J., & Thomann, P. A. (2012). Neurological soft signs and subcortical brain morphology in recent onset schizophrenia. *J Psychiatr Res*, *46*(4), 533-539. doi:10.1016/j.jpsychires.2012.01.015
- Hochberg, Y. (1988). A sharper Bonferroni procedure for multiple tests of significance. *Biometrika*, *75*, 800-802.
- Hoerst, M., Weber-Fahr, W., Tunc-Skarka, N., Ruf, M., Bohus, M., Schmahl, C., & Ende, G. (2010). Correlation of glutamate levels in the anterior cingulate cortex with self-reported impulsivity in patients with borderline personality disorder and healthy controls. *Arch Gen Psychiatry*, *67*(9), 946-954. doi:10.1001/archgenpsychiatry.2010.93
- Honda, M., Deiber, M. P., Ibanez, V., Pascual-Leone, A., Zhuang, P., & Hallett, M. (1998). Dynamic cortical involvement in implicit and explicit motor sequence learning. A PET study. *Brain*, *121* ( Pt 11), 2159-2173.
- Huang, Y. Y., Simpson, E., Kellendonk, C., & Kandel, E. R. (2004). Genetic evidence for the bidirectional modulation of synaptic plasticity in the prefrontal cortex by D1 receptors. *Proc Natl Acad Sci U S A*, *101*(9), 3236-3241. doi:10.1073/pnas.0308280101
- Iriki, A., Pavlides, C., Keller, A., & Asanuma, H. (1989). Long-term potentiation in the motor cortex. *Science*, *245*(4924), 1385-1387.
- Janssen, J., Diaz-Caneja, A., Reig, S., Bombin, I., Mayoral, M., Parellada, M., . . . Arango, C. (2009). Brain morphology and neurological soft signs in adolescents with first-episode psychosis. *Br J Psychiatry*, *195*(3), 227-233.
- Jarrard, L. E. (1993). On the role of the hippocampus in learning and memory in the rat. *Behav Neural Biol*, *60*(1), 9-26. doi:10.1016/0163-1047(93)90664-4
- Ke, X., Ding, Y., Xu, K., He, H., Wang, D., Deng, X., . . . Fan, N. (2018). The profile of cognitive impairments in chronic ketamine users. *Psychiatry Res*, *266*, 124-131. doi:10.1016/j.psychres.2018.05.050
- Kelly, R. M., & Strick, P. L. (2003). Cerebellar loops with motor cortex and prefrontal cortex of a nonhuman primate. *J Neurosci*, *23*(23), 8432-8444.
- Kent, K., Deng, Q., & McNeill, T. H. (2013). Unilateral skill acquisition induces bilateral NMDA receptor subunit composition shifts in the rat sensorimotor striatum. *Brain Res*, *1517*, 77-86. doi:10.1016/j.brainres.2013.04.021
- Kida, H., & Mitsushima, D. (2018). Mechanisms of motor learning mediated by synaptic plasticity in rat primary motor cortex. *Neurosci Res*, *128*, 14-18. doi:10.1016/j.neures.2017.09.008

- Kida, H., Tsuda, Y., Ito, N., Yamamoto, Y., Owada, Y., Kamiya, Y., & Mitsushima, D. (2016). Motor Training Promotes Both Synaptic and Intrinsic Plasticity of Layer II/III Pyramidal Neurons in the Primary Motor Cortex. *Cereb Cortex*, 26(8), 3494-3507. doi:10.1093/cercor/bhw134
- Kimura, A., Caria, M. A., Melis, F., & Asanuma, H. (1994). Long-term potentiation within the cat motor cortex. *Neuroreport*, 5(17), 2372-2376. doi:10.1097/00001756-199411000-00040
- Kleim, J. A., Barbay, S., Cooper, N. R., Hogg, T. M., Reidel, C. N., Remple, M. S., & Nudo, R. J. (2002). Motor learning-dependent synaptogenesis is localized to functionally reorganized motor cortex. *Neurobiol Learn Mem*, 77(1), 63-77. doi:10.1006/nlme.2000.4004
- Kleim, J. A., Markham, J. A., Vij, K., Freese, J. L., Ballard, D. H., & Greenough, W. T. (2007). Motor learning induces astrocytic hypertrophy in the cerebellar cortex. *Behav Brain Res*, 178(2), 244-249. doi:10.1016/j.bbr.2006.12.022
- Kodama, M., Ono, T., Yamashita, F., Ebata, H., Liu, M., Kasuga, S., & Ushiba, J. (2018). Structural Gray Matter Changes in the Hippocampus and the Primary Motor Cortex on An-Hour-to-One- Day Scale Can Predict Arm-Reaching Performance Improvement. *Front Hum Neurosci*, 12, 209. doi:10.3389/fnhum.2018.00209
- Kodama, S., Fukuzako, H., Fukuzako, T., Kiura, T., Nozoe, S., Hashiguchi, T., . . . Nakajo, M. (2001). Aberrant brain activation following motor skill learning in schizophrenic patients as shown by functional magnetic resonance imaging. *Psychol Med*, 31(6), 1079-1088.
- Kolb, B., Cioe, J., & Comeau, W. (2008). Contrasting effects of motor and visual spatial learning tasks on dendritic arborization and spine density in rats. *Neurobiol Learn Mem*, 90(2), 295-300. doi:10.1016/j.nlm.2008.04.012
- Kraguljac, N. V., Frolich, M. A., Tran, S., White, D. M., Nichols, N., Barton-McArdle, A., . . . Lahti, A. C. (2016). Ketamine modulates hippocampal neurochemistry and functional connectivity: a combined magnetic resonance spectroscopy and resting-state fMRI study in healthy volunteers. *Mol Psychiatry*. doi:10.1038/mp.2016.122
- Kuang, S., Morel, P., & Gail, A. (2016). Planning Movements in Visual and Physical Space in Monkey Posterior Parietal Cortex. *Cereb Cortex*, 26(2), 731-747. doi:10.1093/cercor/bhu312
- Lüscher, C., & Malenka, R. C. (2012). NMDA receptor-dependent long-term potentiation and long-term depression (LTP/LTD). *Cold Spring Harb Perspect Biol*, 4(6). doi:10.1101/cshperspect.a005710
- Laforce, R., Jr., & Doyon, J. (2001). Distinct contribution of the striatum and cerebellum to motor learning. *Brain Cogn*, 45(2), 189-211. doi:10.1006/brcg.2000.1237
- Langer, N., von Bastian, C. C., Wirz, H., Oberauer, K., & Jancke, L. (2013). The effects of working memory training on functional brain network efficiency. *Cortex*, 49(9), 2424-2438. doi:10.1016/j.cortex.2013.01.008
- Lee, H., & Kim, J. J. (1998). Amygdalar NMDA receptors are critical for new fear learning in previously fear-conditioned rats. *J Neurosci*, 18(20), 8444-8454.
- Lehericy, S., Benali, H., Van de Moortele, P. F., Pelegriani-Issac, M., Waechter, T., Ugurbil, K., & Doyon, J. (2005). Distinct basal ganglia territories are engaged in

- early and advanced motor sequence learning. *Proc Natl Acad Sci U S A*, 102(35), 12566-12571. doi:10.1073/pnas.0502762102
- Lev-Ram, V., Wong, S. T., Storm, D. R., & Tsien, R. Y. (2002). A new form of cerebellar long-term potentiation is postsynaptic and depends on nitric oxide but not cAMP. *Proc Natl Acad Sci U S A*, 99(12), 8389-8393. doi:10.1073/pnas.122206399
- Levy, L. M., Ziemann, U., Chen, R., & Cohen, L. G. (2002). Rapid modulation of GABA in sensorimotor cortex induced by acute deafferentation. *Ann Neurol*, 52(6), 755-761. doi:10.1002/ana.10372
- Li, C. T., Chou, K. H., Su, T. P., Huang, C. C., Chen, M. H., Bai, Y. M., & Lin, C. P. (2013). Gray matter abnormalities in schizophrenia patients with tardive dyskinesia: a magnetic resonance imaging voxel-based morphometry study. *PLoS One*, 8(8), e71034. doi:10.1371/journal.pone.0071034
- Logothetis, N. K. (2002). The neural basis of the blood-oxygen-level-dependent functional magnetic resonance imaging signal. *Philos Trans R Soc Lond B Biol Sci*, 357(1424), 1003-1037. doi:10.1098/rstb.2002.1114
- Luft, A. R., Buitrago, M. M., Ringer, T., Dichgans, J., & Schulz, J. B. (2004). Motor skill learning depends on protein synthesis in motor cortex after training. *J Neurosci*, 24(29), 6515-6520. doi:10.1523/JNEUROSCI.1034-04.2004
- Lutcke, H., & Frahm, J. (2008). Lateralized anterior cingulate function during error processing and conflict monitoring as revealed by high-resolution fMRI. *Cereb Cortex*, 18(3), 508-515. doi:10.1093/cercor/bhm090
- Maguire, E. A., Gadian, D. G., Johnsrude, I. S., Good, C. D., Ashburner, J., Frackowiak, R. S., & Frith, C. D. (2000). Navigation-related structural change in the hippocampi of taxi drivers. *Proc Natl Acad Sci U S A*, 97(8), 4398-4403. doi:10.1073/pnas.070039597
- Mary, A., Wens, V., Op de Beeck, M., Leproult, R., De Tiege, X., & Peigneux, P. (2016). Resting-state Functional Connectivity is an Age-dependent Predictor of Motor Learning Abilities. *Cereb Cortex*. doi:10.1093/cercor/bhw286
- Mawase, F., Bar-Haim, S., & Shmuelof, L. (2017). Formation of Long-Term Locomotor Memories Is Associated with Functional Connectivity Changes in the Cerebellar–Thalamic–Cortical Network. *Journal of Neuroscience*, 37(2), 349-361.
- McHughen, S. A., Rodriguez, P. F., Kleim, J. A., Kleim, E. D., Marchal Crespo, L., Procaccio, V., & Cramer, S. C. (2010). BDNF val66met polymorphism influences motor system function in the human brain. *Cereb Cortex*, 20(5), 1254-1262. doi:10.1093/cercor/bhp189
- Meyer-Lindenberg, A., & Weinberger, D. R. (2006). Intermediate phenotypes and genetic mechanisms of psychiatric disorders. *Nat Rev Neurosci*, 7(10), 818-827. doi:10.1038/nrn1993
- Miall, R. C., Christensen, L. O., Cain, O., & Stanley, J. (2007). Disruption of state estimation in the human lateral cerebellum. *PLoS Biol*, 5(11), e316. doi:10.1371/journal.pbio.0050316
- Moghaddam, B., Adams, B., Verma, A., & Daly, D. (1997). Activation of glutamatergic neurotransmission by ketamine: a novel step in the pathway from NMDA receptor blockade to dopaminergic and cognitive disruptions associated with the prefrontal cortex. *J Neurosci*, 17(8), 2921-2927.

- Molina-Luna, K., Pekanovic, A., Rohrich, S., Hertler, B., Schubring-Giese, M., Rioult-Pedotti, M. S., & Luft, A. R. (2009). Dopamine in motor cortex is necessary for skill learning and synaptic plasticity. *PLoS One*, 4(9), e7082. doi:10.1371/journal.pone.0007082
- Mueller, S., Wang, D., Fox, M. D., Pan, R., Lu, J., Li, K., . . . Liu, H. (2015). Reliability correction for functional connectivity: Theory and implementation. *Hum Brain Mapp*, 36(11), 4664-4680. doi:10.1002/hbm.22947
- Muller, J. L., Roder, C. H., Schuierer, G., & Klein, H. (2002). Motor-induced brain activation in cortical, subcortical and cerebellar regions in schizophrenic inpatients. A whole brain fMRI fingertapping study. *Prog Neuropsychopharmacol Biol Psychiatry*, 26(3), 421-426.
- Nachev, P., Kennard, C., & Husain, M. (2008). Functional role of the supplementary and pre-supplementary motor areas. *Nat Rev Neurosci*, 9(11), 856-869. doi:10.1038/nrn2478
- Newman, M. E. (2006). Modularity and community structure in networks. *Proc Natl Acad Sci U S A*, 103(23), 8577-8582. doi:10.1073/pnas.0601602103
- Niesters, M., Khalili-Mahani, N., Martini, C., Aarts, L., van Gerven, J., van Buchem, M. A., . . . Rombouts, S. (2012). Effect of subanesthetic ketamine on intrinsic functional brain connectivity: a placebo-controlled functional magnetic resonance imaging study in healthy male volunteers. *Anesthesiology*, 117(4), 868-877. doi:10.1097/ALN.0b013e31826a0db3
- Parton, A., Malhotra, P., & Husain, M. (2004). Hemispatial neglect. *Journal of Neurology, Neurosurgery & Psychiatry*, 75(1), 13-21.
- Pascual-Leone, A., Grafman, J., & Hallett, M. (1994). Modulation of cortical motor output maps during development of implicit and explicit knowledge. *Science*, 263(5151), 1287-1289.
- Pekhletski, R., Gerlai, R., Overstreet, L. S., Huang, X. P., Agopyan, N., Slater, N. T., . . . Hampson, D. R. (1996). Impaired cerebellar synaptic plasticity and motor performance in mice lacking the mGluR4 subtype of metabotropic glutamate receptor. *J Neurosci*, 16(20), 6364-6373.
- Penhune, V. B., & Steele, C. J. (2012). Parallel contributions of cerebellar, striatal and M1 mechanisms to motor sequence learning. *Behav Brain Res*, 226(2), 579-591.
- Pereira, A. C., Huddleston, D. E., Brickman, A. M., Sosunov, A. A., Hen, R., McKhann, G. M., . . . Small, S. A. (2007). An in vivo correlate of exercise-induced neurogenesis in the adult dentate gyrus. *Proc Natl Acad Sci U S A*, 104(13), 5638-5643.
- Poldrack, R. A. (2000). Imaging brain plasticity: conceptual and methodological issues—a theoretical review. *Neuroimage*, 12(1), 1-13. doi:10.1006/nimg.2000.0596
- Power, J. D., Barnes, K. A., Snyder, A. Z., Schlaggar, B. L., & Petersen, S. E. (2012). Spurious but systematic correlations in functional connectivity MRI networks arise from subject motion. *Neuroimage*, 59(3), 2142-2154. doi:10.1016/j.neuroimage.2011.10.018
- Power, J. D., Cohen, A. L., Nelson, S. M., Wig, G. S., Barnes, K. A., Church, J. A., . . . Petersen, S. E. (2011). Functional network organization of the human brain. *Neuron*, 72(4), 665-678. doi:10.1016/j.neuron.2011.09.006



- Provencher, S. W. (1993). Estimation of metabolite concentrations from localized in vivo proton NMR spectra. *Magn Reson Med*, *30*(6), 672-679.
- Quinn, J., Meagher, D., Murphy, P., Kinsella, A., Mullaney, J., & Waddington, J. L. (2001). Vulnerability to involuntary movements over a lifetime trajectory of schizophrenia approaches 100%, in association with executive (frontal) dysfunction. *Schizophr Res*, *49*(1-2), 79-87.
- Raichle, M. E., MacLeod, A. M., Snyder, A. Z., Powers, W. J., Gusnard, D. A., & Shulman, G. L. (2001). A default mode of brain function. *Proceedings of the National Academy of Sciences*, *98*(2), 676-682. doi:10.1073/pnas.98.2.676
- Ramnani, N. (2006). The primate cortico-cerebellar system: anatomy and function. *Nat Rev Neurosci*, *7*(7), 511-522. doi:10.1038/nrn1953
- Reis, J., Schambra, H. M., Cohen, L. G., Buch, E. R., Fritsch, B., Zarahn, E., . . . Krakauer, J. W. (2009). Noninvasive cortical stimulation enhances motor skill acquisition over multiple days through an effect on consolidation. *Proc Natl Acad Sci U S A*, *106*(5), 1590-1595. doi:10.1073/pnas.0805413106
- Rhyu, I. J., Bytheway, J. A., Kohler, S. J., Lange, H., Lee, K. J., Boklewski, J., . . . Cameron, J. L. (2010). Effects of aerobic exercise training on cognitive function and cortical vascularity in monkeys. *Neuroscience*, *167*(4), 1239-1248. doi:10.1016/j.neuroscience.2010.03.003
- Rioult-Pedotti, M. S., Friedman, D., & Donoghue, J. P. (2000). Learning-induced LTP in neocortex. *Science*, *290*(5491), 533-536.
- Rioult-Pedotti, M. S., Friedman, D., Hess, G., & Donoghue, J. P. (1998). Strengthening of horizontal cortical connections following skill learning. *Nat Neurosci*, *1*(3), 230-234. doi:10.1038/678
- Rioult-Pedotti, M. S., Pektanovic, A., Atiemo, C. O., Marshall, J., & Luft, A. R. (2015). Dopamine Promotes Motor Cortex Plasticity and Motor Skill Learning via PLC Activation. *PLoS One*, *10*(5), e0124986. doi:10.1371/journal.pone.0124986
- Rogowska, J., Gruber, S. A., & Yurgelun-Todd, D. A. (2004). Functional magnetic resonance imaging in schizophrenia: cortical response to motor stimulation. *Psychiatry Res*, *130*(3), 227-243. doi:10.1016/j.psychres.2003.12.004
- Rosenberg, M. D., Finn, E. S., Scheinost, D., Papademetris, X., Shen, X., Constable, R. T., & Chun, M. M. (2016). A neuromarker of sustained attention from whole-brain functional connectivity. *Nat Neurosci*, *19*(1), 165-171. doi:10.1038/nn.4179
- Rubinov, M., & Sporns, O. (2010). Complex network measures of brain connectivity: uses and interpretations. *Neuroimage*, *52*(3), 1059-1069. doi:10.1016/j.neuroimage.2009.10.003
- Sagi, Y., Tavor, I., Hofstetter, S., Tzur-Moryosef, S., Blumenfeld-Katzir, T., & Assaf, Y. (2012). Learning in the fast lane: new insights into neuroplasticity. *Neuron*, *73*(6), 1195-1203. doi:10.1016/j.neuron.2012.01.025
- Sami, S., & Miall, R. C. (2013). Graph network analysis of immediate motor-learning induced changes in resting state BOLD. *Front Hum Neurosci*, *7*, 166. doi:10.3389/fnhum.2013.00166
- Sami, S., Robertson, E. M., & Miall, R. C. (2014). The time course of task-specific memory consolidation effects in resting state networks. *J Neurosci*, *34*(11), 3982-3992. doi:10.1523/JNEUROSCI.4341-13.2014

- Sampaio-Baptista, C., Filippini, N., Stagg, C. J., Near, J., Scholz, J., & Johansen-Berg, H. (2015). Changes in functional connectivity and GABA levels with long-term motor learning. *Neuroimage*, *106*, 15-20. doi:10.1016/j.neuroimage.2014.11.032
- Sampaio-Baptista, C., Scholz, J., Jenkinson, M., Thomas, A. G., Filippini, N., Smit, G., . . . Johansen-Berg, H. (2014). Gray matter volume is associated with rate of subsequent skill learning after a long term training intervention. *Neuroimage*, *96*, 158-166. doi:10.1016/j.neuroimage.2014.03.056
- Sanes, J. N., Dimitrov, B., & Hallett, M. (1990). Motor learning in patients with cerebellar dysfunction. *Brain*, *113* ( Pt 1), 103-120.
- Sarro, S., Pomarol-Clotet, E., Canales-Rodriguez, E. J., Salvador, R., Gomar, J. J., Ortiz-Gil, J., . . . McKenna, P. J. (2013). Structural brain changes associated with tardive dyskinesia in schizophrenia. *Br J Psychiatry*, *203*(1), 51-57. doi:10.1192/bjp.bp.112.114538
- Satterthwaite, T. D., Elliott, M. A., Gerraty, R. T., Ruparel, K., Loughhead, J., Calkins, M. E., . . . Wolf, D. H. (2013). An improved framework for confound regression and filtering for control of motion artifact in the preprocessing of resting-state functional connectivity data. *Neuroimage*, *64*, 240-256. doi:10.1016/j.neuroimage.2012.08.052
- Schendan, H. E., Searl, M. M., Melrose, R. J., & Stern, C. E. (2003). An fMRI study of the role of the medial temporal lobe in implicit and explicit sequence learning. *Neuron*, *37*(6), 1013-1025.
- Schroder, J., Essig, M., Baudendistel, K., Jahn, T., Gerdson, I., Stockert, A., . . . Knopp, M. V. (1999). Motor dysfunction and sensorimotor cortex activation changes in schizophrenia: A study with functional magnetic resonance imaging. *Neuroimage*, *9*(1), 81-87. doi:10.1006/nimg.1998.0387
- Schroder, J., Wenz, F., Schad, L. R., Baudendistel, K., & Knopp, M. V. (1995). Sensorimotor cortex and supplementary motor area changes in schizophrenia. A study with functional magnetic resonance imaging. *Br J Psychiatry*, *167*(2), 197-201.
- Seifert, S., von Cramon, D. Y., Imperati, D., Tittgemeyer, M., & Ullsperger, M. (2011). Thalamocingulate interactions in performance monitoring. *J Neurosci*, *31*(9), 3375-3383. doi:10.1523/jneurosci.6242-10.2011
- Shannon, B. J., Vaishnavi, S. N., Vlassenko, A. G., Shimony, J. S., Rutlin, J., & Raichle, M. E. (2016). Brain aerobic glycolysis and motor adaptation learning. *Proc Natl Acad Sci U S A*, *113*(26), E3782-3791. doi:10.1073/pnas.1604977113
- Smith, M. A., & Shadmehr, R. (2005). Intact ability to learn internal models of arm dynamics in Huntington's disease but not cerebellar degeneration. *J Neurophysiol*, *93*(5), 2809-2821. doi:10.1152/jn.00943.2004
- Smith, S. M., Jenkinson, M., Woolrich, M. W., Beckmann, C. F., Behrens, T. E., Johansen-Berg, H., . . . Matthews, P. M. (2004). Advances in functional and structural MR image analysis and implementation as FSL. *Neuroimage*, *23* Suppl 1, S208-219. doi:10.1016/j.neuroimage.2004.07.051
- Soher, B. J., Young, K., Bernstein, A., Aygula, Z., & Maudsley, A. A. (2007). GAVA: spectral simulation for in vivo MRS applications. *J Magn Reson*, *185*(2), 291-299. doi:10.1016/j.jmr.2007.01.005

- Stagg, C. J., Bachtiar, V., Amadi, U., Gudberg, C. A., Ilie, A. S., Sampaio-Baptista, C., . . . Johansen-Berg, H. (2014). Local GABA concentration is related to network-level resting functional connectivity. *Elife*, 3, e01465. doi:10.7554/eLife.01465
- Stillman, C. M., Gordon, E. M., Simon, J. R., Vaidya, C. J., Howard, D. V., & Howard, J. H., Jr. (2013). Caudate resting connectivity predicts implicit probabilistic sequence learning. *Brain Connect*, 3(6), 601-610. doi:10.1089/brain.2013.0169
- Tamas Kincses, Z., Johansen-Berg, H., Tomassini, V., Bosnell, R., Matthews, P. M., & Beckmann, C. F. (2008). Model-free characterization of brain functional networks for motor sequence learning using fMRI. *Neuroimage*, 39(4), 1950-1958. doi:10.1016/j.neuroimage.2007.09.070
- Taubert, M., Lohmann, G., Margulies, D. S., Villringer, A., & Ragert, P. (2011). Long-term effects of motor training on resting-state networks and underlying brain structure. *Neuroimage*, 57(4), 1492-1498. doi:10.1016/j.neuroimage.2011.05.078
- Thomann, P. A., Wustenberg, T., Santos, V. D., Bachmann, S., Essig, M., & Schroder, J. (2009). Neurological soft signs and brain morphology in first-episode schizophrenia. *Psychol Med*, 39(3), 371-379.
- Thomas, A. G., Marrett, S., Saad, Z. S., Ruff, D. A., Martin, A., & Bandettini, P. A. (2009). Functional but not structural changes associated with learning: an exploration of longitudinal voxel-based morphometry (VBM). *Neuroimage*, 48(1), 117-125. doi:10.1016/j.neuroimage.2009.05.097
- Thomason, M. E., Yoo, D. J., Glover, G. H., & Gotlib, I. H. (2009). BDNF genotype modulates resting functional connectivity in children. *Front Hum Neurosci*, 3, 55. doi:10.3389/neuro.09.055.2009
- Toni, I., & Passingham, R. E. (1999). Prefrontal-basal ganglia pathways are involved in the learning of arbitrary visuomotor associations: a PET study. *Exp Brain Res*, 127(1), 19-32.
- Trepel, C., & Racine, R. J. (2000). GABAergic modulation of neocortical long-term potentiation in the freely moving rat. *Synapse*, 35(2), 120-128. doi:10.1002/(sici)1098-2396(200002)35:2<120::Aid-syn4>3.0.Co;2-6
- Tzourio-Mazoyer, N., Landeau, B., Papathanassiou, D., Crivello, F., Etard, O., Delcroix, N., . . . Joliot, M. (2002). Automated anatomical labeling of activations in SPM using a macroscopic anatomical parcellation of the MNI MRI single-subject brain. *Neuroimage*, 15(1), 273-289. doi:10.1006/nimg.2001.0978
- Ungerleider, L. G., Doyon, J., & Karni, A. (2002). Imaging brain plasticity during motor skill learning. *Neurobiol Learn Mem*, 78(3), 553-564.
- van den Heuvel, M. P., de Lange, S. C., Zalesky, A., Seguin, C., Yeo, B. T. T., & Schmidt, R. (2017). Proportional thresholding in resting-state fMRI functional connectivity networks and consequences for patient-control connectome studies: Issues and recommendations. *Neuroimage*, 152, 437-449. doi:10.1016/j.neuroimage.2017.02.005
- van den Heuvel, M. P., Stam, C. J., Kahn, R. S., & Hulshoff Pol, H. E. (2009). Efficiency of functional brain networks and intellectual performance. *J Neurosci*, 29(23), 7619-7624. doi:10.1523/jneurosci.1443-09.2009
- van Loon, A. M., Fahrenfort, J. J., van der Velde, B., Lirk, P. B., Vulink, N. C., Hollmann, M. W., . . . Lamme, V. A. (2016). NMDA Receptor Antagonist Ketamine Distorts

- Object Recognition by Reducing Feedback to Early Visual Cortex. *Cereb Cortex*, 26(5), 1986-1996. doi:10.1093/cercor/bhv018
- Volianskis, A., France, G., Jensen, M. S., Bortolotto, Z. A., Jane, D. E., & Collingridge, G. L. (2015). Long-term potentiation and the role of N-methyl-D-aspartate receptors. *Brain Res*, 1621, 5-16. doi:10.1016/j.brainres.2015.01.016
- Walther, S., & Strik, W. (2012). Motor Symptoms and Schizophrenia. *Neuropsychobiology*, 66(2), 77-92. doi:10.1159/000339456
- Wang, J., Zuo, X., Dai, Z., Xia, M., Zhao, Z., Zhao, X., . . . He, Y. (2013). Disrupted functional brain connectome in individuals at risk for Alzheimer's disease. *Biol Psychiatry*, 73(5), 472-481. doi:10.1016/j.biopsych.2012.03.026
- Wang, J., Zuo, X., & He, Y. (2010). Graph-based network analysis of resting-state functional MRI. *Front Syst Neurosci*, 4, 16. doi:10.3389/fnsys.2010.00016
- Watts, D. J., & Strogatz, S. H. (1998). Collective dynamics of 'small-world' networks. *Nature*, 393(6684), 440-442. doi:10.1038/30918
- Weilke, F., Spiegel, S., Boecker, H., von Einsiedel, H. G., Conrad, B., Schwaiger, M., & Erhard, P. (2001). Time-resolved fMRI of activation patterns in M1 and SMA during complex voluntary movement. *J Neurophysiol*, 85(5), 1858-1863. doi:10.1152/jn.2001.85.5.1858
- Whitty, P. F., Owoeye, O., & Waddington, J. L. (2009). Neurological signs and involuntary movements in schizophrenia: intrinsic to and informative on systems pathobiology. *Schizophr Bull*, 35(2), 415-424. doi:10.1093/schbul/sbn126
- Wolff, A. L., & O'Driscoll, G. A. (1999). Motor deficits and schizophrenia: the evidence from neuroleptic-naïve patients and populations at risk. *Journal of psychiatry & neuroscience : JPN*, 24(4), 304-314.
- Wu, J., Srinivasan, R., Kaur, A., & Cramer, S. C. (2014). Resting-state cortical connectivity predicts motor skill acquisition. *Neuroimage*, 91, 84-90. doi:10.1016/j.neuroimage.2014.01.026
- Xia, M., Wang, J., & He, Y. (2013). BrainNet Viewer: a network visualization tool for human brain connectomics. *PLoS One*, 8(7), e68910. doi:10.1371/journal.pone.0068910
- Xiong, J., Ma, L., Wang, B., Narayana, S., Duff, E. P., Egan, G. F., & Fox, P. T. (2009). Long-term motor training induced changes in regional cerebral blood flow in both task and resting states. *Neuroimage*, 45(1), 75-82. doi:10.1016/j.neuroimage.2008.11.016
- Xu, L., Anwyl, R., & Rowan, M. J. (1998). Spatial exploration induces a persistent reversal of long-term potentiation in rat hippocampus. *Nature*, 394(6696), 891-894. doi:10.1038/29783
- Yan, C., & Zang, Y. (2010). DPARSF: A MATLAB Toolbox for "Pipeline" Data Analysis of Resting-State fMRI. *Front Syst Neurosci*, 4, 13. doi:10.3389/fnsys.2010.00013
- Yan, C. G., Cheung, B., Kelly, C., Colcombe, S., Craddock, R. C., Di Martino, A., . . . Milham, M. P. (2013). A comprehensive assessment of regional variation in the impact of head micromovements on functional connectomics. *Neuroimage*, 76, 183-201. doi:10.1016/j.neuroimage.2013.03.004

- Yang, G., Pan, F., & Gan, W. B. (2009). Stably maintained dendritic spines are associated with lifelong memories. *Nature*, *462*(7275), 920-924. doi:10.1038/nature08577
- Yousry, T. A., Schmid, U. D., Alkadhi, H., Schmidt, D., Peraud, A., Buettner, A., & Winkler, P. (1997). Localization of the motor hand area to a knob on the precentral gyrus. A new landmark. *Brain*, *120* ( Pt 1), 141-157.
- Zalesky, A., Fornito, A., & Bullmore, E. T. (2010). Network-based statistic: identifying differences in brain networks. *Neuroimage*, *53*(4), 1197-1207. doi:10.1016/j.neuroimage.2010.06.041
- Zalesky, A., Fornito, A., Harding, I. H., Cocchi, L., Yucel, M., Pantelis, C., & Bullmore, E. T. (2010). Whole-brain anatomical networks: does the choice of nodes matter? *Neuroimage*, *50*(3), 970-983. doi:10.1016/j.neuroimage.2009.12.027
- Zang, Z., Geiger, L. S., Braun, U., Cao, H., Zangl, M., Schäfer, A., . . . Tost, H. (2018). Resting-state brain network features associated with short-term skill learning ability in humans and the influence of N-methyl-d-aspartate receptor antagonism. *Network Neuroscience*, *2*(4), 464-480. doi:10.1162/netn\_a\_00045
- Zatorre, R. J., Fields, R. D., & Johansen-Berg, H. (2012). Plasticity in gray and white: neuroimaging changes in brain structure during learning. *Nat Neurosci*, *15*(4), 528-536. doi:10.1038/nn.3045
- Zhang, H., Xu, L., Zhang, R., Hui, M., Long, Z., Zhao, X., & Yao, L. (2012). Parallel alterations of functional connectivity during execution and imagination after motor imagery learning. *PLoS One*, *7*(5), e36052. doi:10.1371/journal.pone.0036052

## 7 PUBLICATIONS

- Zang, Z., U. Braun, L. S. Geiger, T. Wuestenberg, A. Harneit, J. Reis, M. Ruf, A. Schaefer, I. Wolf, G. Ende, A. Meyer-Lindenberg and H. Tost. (Pre-submission). Multi-Imaging Modalities Identify Dynamic Glutamatergic Dependent Neural Plasticity in Human Brain During Long-term Motor Learning.
- Bilek, E., Zang, Z., Wolf, I., Henrich, F., Moessnang, C., Braun, U., . . . Tost, H. (2019). Neural network-based alterations during repetitive heat pain stimulation in major depression. *European Neuropsychopharmacology*, 29(9), 1033 – 1040.
- Harneit, A., Braun, U., Geiger, L. S., Zang, Z., Hakobjan, M., van Donkelaar, M. M., . . . Erk, S. (2019). MAOA-VNTR genotype affects structural and functional connectivity in distributed brain networks. *Human brain mapping*, 40, 5202-5212.
- Cao, H., Harneit, A., Walter, H., Erk, S., Braun, U., Moessnang, C. ... Zang, Z., ... Heinz, A. (2018). The 5-HTTLPR polymorphism affects network-based functional connectivity in the visual-limbic system in healthy adults. *Neuropsychopharmacology*, 43(2), 406 – 441.
- Geiger, L. S., Moessnang, C., Schäfer, A., Zang, Z., Zangl, M., Cao, H., . . . Tost, H. (2018). Novelty modulates human striatal activation and prefrontal–striatal effective connectivity during working memory encoding. *Brain Structure and Function*, 223(7), 3121 – 3132.
- Zang, Z., Geiger, L. S., Braun, U., Cao, H., Zangl, M., Schäfer, A., . . . Schweiger, J. I. (2018). Resting-state brain network features associated with short-term skill learning ability in humans and the influence of N-methyl-d-aspartate receptor antagonism. *Network Neuroscience*, 2(4), 464 – 480.
- Becker, R., Braun, U., Schwarz, A., Gass, N., Schweiger, J., Weber-Fahr, W.... Zang Z., ... Risterucci, C. (2016). Species-conserved reconfigurations of brain network topology induced by ketamine. *Translational psychiatry*, 6(4), e786.
- Francois, J., Grimm, O., Schwarz, A. J., Schweiger, J., Haller, L., Risterucci, C.... Zang, Z., ... Gilmour, G. (2016). Ketamine suppresses the ventral striatal response to reward anticipation: a cross-species translational neuroimaging study. *Neuropsychopharmacology*, 41(5), 1386 – 1394
- Grimm, O., Gass, N., Weber-Fahr, W., Sartorius, A., Schenker, E., Spedding, M. ...Zang, Z. (2015). Acute ketamine challenge increases resting state prefrontal-hippocampal connectivity in both humans and rats. *Psychopharmacology (Berl)*, 232(21-22), 4231 – 4241.

## 8 CURRICULUM VITAE

### PERSONALIEN

Name und Vorname: Zang, Zhenxiang

Geburtsdatum: 16. Apr. 1989

Geburtsort: HEBEI, CHINA

Familienstand: Single

Vater: Zang, Yufeng

Mutter: Wang, Peizhi

### SCHOOL EDUCATION

(2002) – (2008) Zhong Guan Cun middle & high school, Beijing

(06.Jun.2008) High school

### UNIVERSITY EDUCATION

(2008) – (2012) Informatics and Computation Science, Department of Mathematics, Beijing JiaoTong University.

20.June.2012 Bachelor of Science

(2013) – (2014) Medical Physics with distinction in Radiotherapy and Biomedical Optics, Medical Faculty Mannheim.

(28.Aug.2014) Master of Science, Note: Gut

## 9 ACKNOWLEDGMENT

Firstly, I would like to thank my parents who always give me the best supports that I need to finish my ph.D project. Secondly, I thank my supervisor Prof. Heike Tost who provides an open and also helpful research environment in the lab. Last but not least, I especially would like to thank Dr. Carolin Moessnang, Dr. Urs Braun and Ms. Lena Geiger for their valuable help in not only scientific aspects, but also during daily life through-out my ph.D project. Dr. Carolin Moessnang helped a lot in the manuscript revision process. I appreciate Ms. Lena Geiger as one of the best German friends and colleagues whom I have collected our whole datasets during the last 5-6 years. Dr. Urs Braun as my behind-the-scene primary supervisor always shares his knowledge and experience in neuroscience with me, which is extremely important for my entire ph.D project.